AGU PUBLICATIONS

Reviews of Geophysics

REVIEW ARTICLE
10.1002/2015RG000487

Key Points:
- Wave-turbulence interactions in the SABL are poorly understood
- New observational strategies are required
- Numerical parameterization of wave effects is limited

Correspondence to:
J. Sun,
jsun@ucar.edu

Citation:
Sun, J., et al. (2015), Review of wave-turbulence interactions in the stable atmospheric boundary layer, *Rev. Geophys.*, *53*, 956–993, doi:10.1002/2015RG000487.

Received 20 MAR 2015
Accepted 12 JUL 2015
Accepted article online 17 JUL 2015
Published online 4 SEP 2015

Review of wave-turbulence interactions in the stable atmospheric boundary layer

Jielun Sun[1], Carmen J. Nappo[2], Larry Mahrt[3], Danijel Belušić[4], Branko Grisogono[5], David R. Stauffer[6], Manuel Pulido[7], Chantal Staquet[8], Qingfang Jiang[9], Annick Pouquet[10], Carlos Yagüe[11], Boris Galperin[12], Ronald B. Smith[13], John J. Finnigan[14], Shane D. Mayor[15], Gunilla Svensson[16], Andrey A. Grachev[17], and William D. Neff[17]

[1]National Center for Atmospheric Research, Boulder, Colorado, USA, [2]CJN Research Meteorology, Knoxville, Tennessee, USA, [3]NorthWest Research Associates, Corvallis, Oregon, USA, [4]School of Earth, Atmosphere and Environment, Monash University, Melbourne, Victoria, Australia, [5]Department of Geophysics, University of Zagreb, Zagreb, Croatia, [6]Department of Meteorology, Pennsylvania State University, University Park, Pennsylvania, USA, [7]Department of Physics, FACENA, Universidad Nacional del Nordeste and IMIT, UMI-IFAECI/CNRS, CONICET, Corrientes, Argentina, [8]Laboratoire des Ecoulements Géophysiques et Industriels, Grenoble, France, [9]Naval Research Laboratory, Monterey, California, USA, [10]National Center for Atmospheric Research and Laboratory for Atmospheric and Space Physics, University of Colorado Boulder, Boulder, Colorado, USA, [11]Department of Geophysics and Meteorology, Universidad Complutense de Madrid, Madrid, Spain, [12]Physical Oceanography, College of Marine Science, University of South Florida, St. Petersburg, Florida, USA, [13]Department of Geology and Geophysics, Yale University, New Haven, Connecticut, USA, [14]CSIRO Marine and Atmospheric Research, Canberra, ACT, Australia, [15]Department of Geological and Environmental Sciences, California State University, Chico, California, USA, [16]Department of Meteorology, Stockholm University, Stockholm, Sweden, [17]NOAA Earth System Research Laboratory/Cooperative Institute for Research in Environmental Sciences, University of Colorado Boulder, Boulder, Colorado, USA**

Abstract Flow in a stably stratified environment is characterized by anisotropic and intermittent turbulence and wavelike motions of varying amplitudes and periods. Understanding turbulence intermittency and wave-turbulence interactions in a stably stratified flow remains a challenging issue in geosciences including planetary atmospheres and oceans. The stable atmospheric boundary layer (SABL) commonly occurs when the ground surface is cooled by longwave radiation emission such as at night over land surfaces, or even daytime over snow and ice surfaces, and when warm air is advected over cold surfaces. Intermittent turbulence intensification in the SABL impacts human activities and weather variability, yet it cannot be generated in state-of-the-art numerical forecast models. This failure is mainly due to a lack of understanding of the physical mechanisms for seemingly random turbulence generation in a stably stratified flow, in which wave-turbulence interaction is a potential mechanism for turbulence intermittency. A workshop on wave-turbulence interactions in the SABL addressed the current understanding and challenges of wave-turbulence interactions and the role of wavelike motions in contributing to anisotropic and intermittent turbulence from the perspectives of theory, observations, and numerical parameterization. There have been a number of reviews on waves, and a few on turbulence in stably stratified flows, but not much on wave-turbulence interactions. This review focuses on the nocturnal SABL; however, the discussions here on intermittent turbulence and wave-turbulence interactions in stably stratified flows underscore important issues in stably stratified geophysical dynamics in general.

1. Introduction

Turbulence intermittency is a common phenomenon in stably stratified geophysical fluids, such as the stable atmospheric boundary layer (SABL), the upper atmosphere [e.g., *Fritts and Alexander*, 2003], the oceans [e.g., *Seuront et al.*, 1996], in clouds [e.g., *Siebert et al.*, 2010], and even the solar wind [e.g., *Sorriso-Valvo et al.*, 1999; *Pagel and Balogh*, 2001; *Strumik and Macek*, 2008]; however, it is poorly understood. The depth of the SABL usually varies from O(10 m) to O(100 m). Intermittency of turbulence describes turbulence variability [*Frisch*, 1995; *Ditlevsen*, 2004]. Most often the variability refers to turbulence intensity such as temporal and spatial appearance of turbulence patches, which is also called global intermittency [*Mahrt*, 1989; *Vindel et al.*, 2008]. Sometimes the variability refers to intermittent appearance of turbulence eddies of various sizes, which is also

called small-scale intermittency. The latter can be described by classical turbulence similarity theories, but not the former, which is the focus of this review.

Accurate numerical prediction of intermittent turbulent events in the SABL is critically important for atmospheric momentum, energy, and pollutant transport even though the SABL is often considered to be "quiescent" and less critical for operational atmospheric models compared with high-impact weather associated with strong winds and heavy precipitation. Fog and frost formation is strongly dependent on accurate predictions of intermittent heat transport near the surface. High concentrations of pollutants can be trapped near the ground surface and vented out only through intermittent turbulent events in the SABL [e.g., *Deng et al.*, 2004; *Stauffer et al.*, 2009] in contrast to the daytime atmospheric boundary layer (ABL) when positive buoyancy from the heated ground drives continuous turbulent transport. Most numerical models fail to capture intermittent turbulent events in the light-wind SABL and encounter the so-called runaway cooling problem [e.g., *Beljaars*, 2011]. To avoid the runaway cooling problem, turbulent mixing in numerical models is commonly enhanced intentionally without any physical basis, leading to a warm temperature bias. Intermittent turbulence is not unique to the SABL; for example, it has been reported in the ocean and galactic interstellar medium [*Gibson*, 1991; *Ruzmaikin et al.*, 1995].

The nature of these intermittent mixing events in the SABL is not well understood, but they seem to be generated by various nonturbulent submeso motions, which fall between the largest turbulence eddy scale (~O(100 m)) and the smallest meso-gamma scale (~2 km) [*Mahrt*, 2009]. Submeso motions may have various structures, such as steps, ramps, pulses, waves, or complex signatures that cannot be approximated by a simple shape [*Mahrt*, 2010a; *Belušić and Mahrt*, 2012; *Kang et al.*, 2014]. These submeso motions may intermittently create sufficient shear to produce local patches of turbulence in the SABL [e.g., *Baklanov et al.*, 2011; *Mahrt et al.*, 2012]. The inability of numerical models to generate these submeso motions may be one of the reasons for the runaway cooling problem even in state-of-the-art numerical models [*Beare et al.*, 2006; *Cuxart et al.*, 2007; *Svensson et al.*, 2011; *Jimenez et al.*, 2012; *Holtslag et al.*, 2013].

Among all the submeso motions, wavelike motions are ubiquitous in the SABL [*Belušić and Mahrt*, 2012]. Observations of these quasiperiodic motions suggest that they are associated with waves. In this review, we classify these waves into two general types according to their generation mechanisms following the terminology used by *Carpenter et al.* [2013]: buoyancy-generated *buoyancy waves*, such as *internal gravity waves* (IGWs) (section 2.2.1), and transverse vorticity-generated *vorticity waves* (section 2.2.2), such as Kelvin-Helmholtz (K-H) billows. Both types of waves, or combinations of them, appear periodically in time and space, and both have periodic vorticity in the crosswind direction, i.e., transverse vorticity.

Turbulence intensification associated with wave evolution can be closely related to intermittent turbulence [*Finnigan*, 1999]. Interactions between waves and turbulence are poorly understood in the SABL even though the role of dynamic instabilities in turbulence generation has been theoretically investigated for decades, especially for monochromatic IGWs [e.g., *Staquet and Sommeria*, 2002]. Propagating IGWs can at times effectively redistribute a large amount of energy and momentum to modify local atmospheric conditions and break down into spatially and temporally varying turbulence in the SABL [*Einaudi et al.*, 1978; *Sun et al.*, 2015]. Vorticity waves are a result of vorticity growth and lead to turbulence embedded in each transverse vorticity roll, which appears as intermittent turbulence in space and time.

To emphasize nonlinear interactions between wave-turbulence interactions in the upper atmosphere, *McIntyre* [2008] depicted that "there is no turbulence without waves." Here we also recognize that waves and turbulence are often correlated; i.e., one can lead to the other. An extensive knowledge of waves may guide us to understand intermittent turbulence associated with wave-turbulence interactions although waves may be only a fraction of submeso motions in the SABL that initiate intermittent turbulence in an otherwise calm flow. Understanding turbulent intermittency requires understanding of not only how wave motions lead to turbulence, which is often a focus in the literature, but also how turbulence affects waves and their environment [e.g., *Thorpe*, 1987].

In this review, we focus on waves as submeso motions and review our current understanding of interactions between waves and turbulence. To address theoretical, observational, and numerical issues related to wave-turbulence interactions, a workshop, wave-turbulence interactions in the stable boundary layer (WINABL) [*Nappo et al.*, 2014], was organized by the National Center for Atmospheric Research (NCAR). This review is based mainly on the workshop discussions and the relevant literature. The latest theoretical

understanding of wave motions, turbulence, and wave-turbulence interactions relevant to intermittent turbulence in the SABL is investigated in section 2. Observations of wave-turbulence interactions with state-of-the-art observational technology are examined in section 3. Current parameterizations of waves and wave-turbulence interactions in numerical models are discussed in section 4. Challenging issues in each area are listed at the end of each section. Section 5 is a summary.

2. Review of Theories of Waves and Turbulence and Their Interactions in the SABL

There is a large body of theoretical analyses of waves in general and in the atmosphere and oceans in particular [e.g., *Whitham*, 1974; *Gossard and Hooke*, 1975; *Lighthill*, 1978; *Gill*, 1982; *Baines*, 1995; *Miropol'sky*, 2001; *Drazin*, 2002; *Bühler*, 2009; *Sutherland*, 2010; *Nappo*, 2012]. *Einaudi et al.* [1978] reviewed work on tropospheric gravity waves to that date. The review by *Fritts and Alexander* [2003] summarized advances in wave theories developed since the 1970s. Our emphasis here is on wave motions relevant to understanding wave-turbulence interactions in the SABL, where the surface may play a significant role in wave and turbulence generation and wave-turbulence interactions.

2.1. Linear Wave Theory and Nonlinearity

Most of our understanding of waves is based on linear wave theory, which has been described in various textbooks [e.g., *Gossard and Hooke*, 1975; *Nappo*, 2012]. We list a few basic results of linear wave theory here because they form a foundation for nonlinear wave theories and are often used for identifying waves in the atmosphere. The linear theory is based on a first-order perturbation of a slowly changing background inviscid flow. Accordingly, second-order terms such as products of the perturbations in the conservation of momentum, heat, and mass are assumed to be negligible. The equation for linear waves is the Taylor-Goldstein (T-G) equation. Its two-dimensional (2-D) form is

$$\frac{\mathrm{d}^2\tilde{w}}{\mathrm{d}z^2} + m^2\tilde{w} = 0, \tag{1}$$

where

$$m^2 = \frac{N^2k^2}{(\omega - Uk)^2} + \frac{\mathrm{d}^2U}{\mathrm{d}z^2}\frac{k}{(\omega - Uk)} - \frac{k}{H_s(\omega - Uk)}\frac{\mathrm{d}U}{\mathrm{d}z} - \frac{1}{4H_s^2} - k^2. \tag{2}$$

In the above equations, $\tilde{w}$ is the wave perturbation of the vertical velocity (w) as a function of height (z); $N = [(g/\theta_0)\partial\theta/\partial z]^{1/2}$ is the Brunt-Väisälä or buoyancy frequency, where θ and θ_0 are the potential temperatures at z and at the surface, respectively, and g is the gravity constant; U is the mean background wind speed; $H_s = RT/g$ is the scale height, where R and T are the universal gas constant for dry air and the mean atmospheric temperature; k, m, and ω are the horizontal and the vertical wave numbers and the wave frequency, respectively. Assuming constant wind and stratification, and $z \ll H_s$, $w(x, z, t)$ can be expressed as

$$\begin{aligned} w(x, z, t) &= \tilde{w}(z)e^{i(kx-\omega t)} \\ &= [Ae^{imz} + Be^{-imz}]e^{i(kx-\omega t)}, \end{aligned} \tag{3}$$

where A and B are unknown coefficients and t is the time. For real m, w varies sinusoidally with z; the corresponding wave is defined as an internal gravity wave, i.e., IGW. IGWs transport energy and horizontal momentum vertically and horizontally [e.g., *McIntyre*, 1981] because $\tilde{w}$ and $\tilde{u}$ are 180° out of phase. For a complex m, the wave amplitude decays exponentially with z; the wave is called an *evanescent gravity wave*. This wave does not transport energy and momentum because $\tilde{w}$ and $\tilde{u}$ are 90° out of phase. Equation (2) describes the relation between the wave frequency and wave number and is called the *dispersion relation*. The most familiar dispersion relation is a simplified version of (2), with $\mathrm{d}^2U/\mathrm{d}z^2 = 0$ and $z \ll H_s$, i.e.,

$$(\omega - Uk)^2 = \frac{N^2k^2}{k^2 + m^2}. \tag{4}$$

The assumption of linearity allows examination of the fundamental physics of wave propagation and conditions that lead to wave instability when ω becomes complex. Because the amplitude of a linear IGW is assumed to be vanishingly small, wave-wave interactions are precluded except in the case of mountain waves, for which the amplitude is determined by the topography as a boundary condition. Linear wave theory ignores turbulence and irreversible interactions between background flows and waves. Nonetheless, comparison

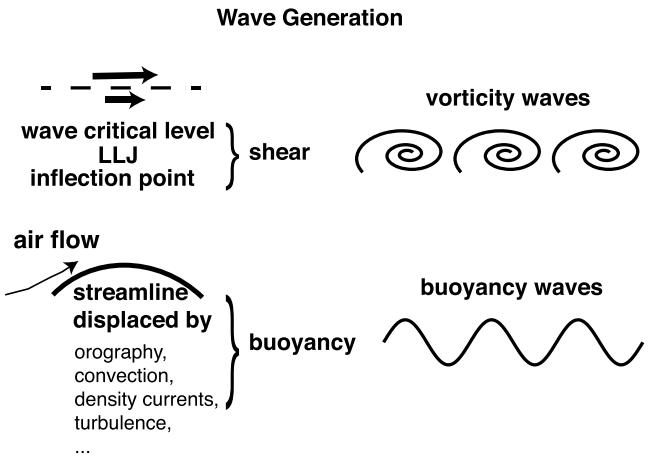

Figure 1. Schematic of wave generation and wave types.

between the linear inviscid theory and observed large-amplitude waves suggests that linear wave theory approximately captures the important physics of wave characteristics such as wave periods, wavelengths, phase velocity [*Einaudi and Finnigan*, 1993], and variances of vertical wave motion and temperature [*Lilly and Lester*, 1974]. The applicability of linear wave theory can be extended to observed nonlinear atmospheric waves if near-real-time profiles of wind and temperature are available [*Dörnbrack and Nappo*, 1997]. Linear wave theory is also valid for observed oceanic waves [e.g., *Bulatov and Vladimirov*, 2010]. However, it fails to accurately predict wave growth rates and amplitudes of mountain waves even for waves with small wave slopes [e.g., *Smith*, 1976].

Nonlinearity becomes important when wave amplitudes become significant with respect to the background flow, resulting in a wave amplitude dependence of the wave dispersion relation [e.g., *Zakharov et al.*, 1992]. Finite amplitudes also affect the symmetry between wave crests and troughs, wave breaking, and turbulence. Although nonlinear wave mechanics are not always dominant during wave development, commonly observed waves usually have amplitudes large enough such that nonlinearity is not negligible. Nonlinearity is central to wave-wave, wave-turbulence, wave-vortex, and vortex-vortex interactions [e.g., *Lelong and Riley*, 1991; *Bühler*, 2010].

The common tools used to investigate nonlinearity are asymptotic approaches for weak nonlinearity [e.g., *Zakharov et al.*, 1992], stochastic theories [e.g., *Sukoriansky and Galperin*, 2005; *Sukoriansky et al.*, 2005; *Galperin and Sukoriansky*, 2010], numerical methods, and laboratory experiments. One of the widely used asymptotic approaches is the WKB (Wentzel-Kramers-Brillouin) theory for describing wave-wave or wave-mean flow interactions [e.g., *Bretherton*, 1966; *Grisogono*, 1994a; *Sutherland*, 2010]. The WKB theory at its lowest order is referred to as linear ray tracing theory [*Lighthill*, 1978].

2.2. Wave Generation Mechanisms in the SABL

Wave generation mechanisms have been widely reported in the literature [e.g., *Chimonas*, 2002; *Nappo*, 2012]. In this review, we are mainly interested in waves that contribute to intermittent turbulence in the SABL; therefore, we do not consider the low-frequency inertia-gravity waves from geostrophic adjustment [e.g., *Blumen*, 1972; *Fritts and Luo*, 1992; *Fritts and Alexander*, 2003], atmospheric jets and fronts [e.g., *Mastrantonio et al.*, 1976; *Chimonas and Grant*, 1984; *Plougonven and Zhang*, 2014], or the spontaneous loss of balanced motions [e.g., *Vanneste*, 2013], but we do consider higher-frequency waves resulting from these processes.

Based on the T-G equation, wave generation is related to two dominant background factors: buoyancy (the first term on the right side of (2)) and vorticity (the third term on the right side of (2) is related to the background vorticity, and the second term is to the vertical variation of vorticity). We first describe each factor and commonly observed phenomena associated with each one in forming different kinds of waves as schematically summarized in Figure 1. Then we describe their combined effects on wave generation.

2.2.1. Buoyancy Waves Generated by Displacement of Streamlines

In the absence of vorticity or shear, wave motions are generated by buoyancy. Propagating buoyancy waves are IGWs and can be initiated by a vertical displacement of flow streamlines in a stratified laminar fluid. The displacement may result from interactions between background flows and either physical obstacles, such as topography, or disturbed density interfaces caused by bulging cold pools, density currents, or convective systems (Figure 1). Through this displacement of streamlines, the energy of IGWs is initially transferred to potential energy of the stably stratified density field, and the buoyancy force acts as a restoring force to generate a periodic energy exchange between potential and kinetic energy, resulting in wind speed oscillations. In addition, temperature oscillates 90°out of phase with w; thus, buoyancy waves do not transport heat but do

transport momentum. Wave reflection by either temperature or wind ducts can trap buoyancy waves within a layer, and they may oscillate for many cycles [e.g., *Chimonas and Hines*, 1986].

Mountain waves refer to all standing waves generated by flow over terrain [e.g., *Long*, 1953; *Klemp and Lilly*, 1975, 1978; *Smith*, 1989]. They often have only a few cycles and propagate upwind at the local wind speed to maintain a fixed spatial relationship to the wave-generating topography. Based on linear theory, surface obstacles and topographical features are expected to generate propagating waves when the advective time required for the flow with a flow speed U to pass over the surface feature with a length scale L is longer than the buoyancy time scale ($L/U > 1/N$) [e.g., *Brown et al.*, 2003]. In linear theory, a steady IGW that propagates in a nondissipative medium conserves its wave momentum flux [*Eliassen and Palm*, 1960].

Large-amplitude nonlinear waves, such as *solitons* (isolated bumps) or *solitary waves* (a train or packet of waves that propagates with a unique wave envelope) [*Jeffrey*, 1989], are likely to be generated through strong convergence between the background flow and density currents generated from sea/land breezes, convective storms, or strong slope flows [e.g., *Christie et al.*, 1978; *Smith*, 1988; *Christie*, 1989; *Rottman and Einaudi*, 1993; *Rees and Rottman*, 1994; *Rees et al.*, 1998; *Sun et al.*, 2004; *Helfrich and Melville*, 2006; *Koch et al.*, 2008]. A solitary wave packet propagates without dispersing and losing its envelope as does a monochromatic wave because of the exactly counteracting nonlinear terms in the equations of motion. In other words, the solitary wave envelope is self-enforced through nonlinear steepening compensating for wave dispersion. The unique energy balance can survive interactions between solitary waves passing through each other. As a result, a solitary wave can travel a long distance without losing its wave envelope in a turbulent atmosphere. Solitary waves demonstrate that nonlinear waves can be stable while the amplitude of each wave within the wave packet varies rapidly with time. Solitary waves can be investigated via numerical models by imposing initial disturbances in the flow. Various theories have been developed for atmospheric solitary waves with different upper boundary conditions [*Rottman and Einaudi*, 1993; *Rottman and Grimshaw*, 2002].

2.2.2. Vorticity Waves Generated by Instabilities

Theoretically, waves can also exist when buoyancy, N, is negligible. Under this situation, wave instability is responsible for the wave growth, which requires the imaginary part of ω, i.e., $\omega_i \neq 0$. The fast growth of an initial wave disturbance can quickly exceed the applicability of linear theory. Rapid growth of a small disturbance can develop to a periodic vortex sheet (vertically confined periodic transverse vortices) and to periodic large transverse rolls [e.g., *Drazin*, 2002].

In contrast to IGWs, once a wave vorticity disturbance starts to grow, nonlinearity and viscosity are assumed. As a result of turbulence generated by shear instability and the overturning of a stably stratified flow, sensible heat flux is nonzero for vorticity waves. Vorticity wave growth as a result of wave momentum flux convergence is at the expense of background flows, which is implicitly assumed in the wave instability theory. Wave momentum divergence, for example, as a result of wave breaking [e.g., *Nastrom and Eaton*, 1993] can force background flows to form vortical modes (horizontal pancake motions) [*Riley and Lindborg*, 2008].

The T-G equation approximately describes the motion prior to the onset of wave instabilities. Therefore, only the conditions required for exponentially growing modes of a wave disturbance, not the subsequent evolution of large-amplitude wave motions in the presence of turbulence, can be investigated through wave instability [*Case*, 1960a, 1960b]. Wave formation is not guaranteed to occur via wave instability although the most unstable wave mode has been observed to grow [*Einaudi and Finnigan*, 1993].

Based on the dispersion relation, the condition for a nonzero ω_i is determined by background atmospheric conditions. The dispersion relation is dominated by either the vertical variation of the vorticity, $\mathrm{d}^2U/\mathrm{d}z^2$, leading to *Rayleigh waves* with cat's eye streamline patterns near a critical wave level (section 2.3.3), or by the vorticity $\mathrm{d}U/\mathrm{d}z$ if $\mathrm{d}^2U/\mathrm{d}z^2$ is negligible, leading to *inflection point waves* [e.g., *Rayleigh*, 1945; *Gossard and Hooke*, 1975] (section 2.2.2.1). The two well-known wave instabilities in an inviscid flow are the inflection point instability and the K-H instability when both shear and buoyancy are relevant for wave generation.

2.2.2.1. Inflection Point Instability

With $\mathrm{d}^2U/\mathrm{d}z^2 = 0$, $N = 0$, and $1/H_s^2 \sim 0$, the dispersion relation (2) becomes

$$\frac{\omega}{k} = U - \frac{1}{H_s(m^2 + k^2)} \frac{\mathrm{d}U}{\mathrm{d}z}. \tag{5}$$

With inflection point instability, the growth rate of a wave perturbation is proportional to the horizontal wave number, so that shortest waves grow fastest and the wave growth does not peak at any wave number. The

inflection point instability has also been extended in 3-D beyond its original definition to include cases with $N \neq 0$, e.g., for flow over canopy top [e.g., *Hu et al.*, 2002; *Finnigan et al.*, 2009; *Belcher et al.*, 2012]. Inflection point instability is commonly included in shear instability as shear is the active force in generating waves.

2.2.2.2. Kelvin-Helmholtz Modes and Shear Instability

The K-H modes follow directly from the Helmholtz profile, which consists of two half-spaces *A* below *B* with a constant density (ρ) and a fluid speed (u) in each space, i.e., ρ_B and u_B in the top half and ρ_A and u_A in the bottom half [e.g., *Nappo*, 2012]. Based on the dynamic and kinematic conditions at the interface between *A* and *B*, i.e., continuous pressure and continuous vertical mass flux, respectively, the balance of the disturbed interface results in

$$\frac{\omega}{k} = \frac{\rho_A u_A + \rho_B u_B}{\rho_A + \rho_B} \pm \left[\frac{g}{k} \frac{(\rho_A - \rho_B)}{(\rho_A + \rho_B)} - \frac{\rho_A \rho_B (u_B - u_A)^2}{(\rho_A + \rho_B)^2} \right]^{1/2}. \tag{6}$$

If ω is real, (6) can be considered as a dispersion relation of evanescent gravity waves propagating at the interface and are called K-H waves. Strictly speaking, K-H waves are interfacial waves associated with the wind speed and density jumps. In a continuously stratified layer, IGWs can be generated, which are also called K-H waves in the literature. However, IGWs and evanescent gravity waves are significantly different in terms of momentum and energy transfer [*Einaudi et al.*, 1978].

If ω is complex, the periodic disturbance grows exponentially with time, which is called K-H instability. Initially, the interface has a vortex sheet with infinite wind shear when the velocity profile is discontinuous. As vortices grow, the interface appears wavelike as turbulence quickly acts to expand the vortex sheet into a shear layer. The disturbance grows nonlinearly into vortex rolls, which are also referred to as K-H *billows* as nonlinear waves saturate [e.g., *Smyth and Peltier*, 1991; *Fritts et al.*, 1996, 2011, 2012].

2.2.2.3. Wave Instabilities in Continuous Shear and Stably Stratified Flows

Unstable modes of the T-G equation with a wave disturbance, and wind and density profiles other than the Helmholtz profile, have often been considered in the wave generation literature [e.g., *Mastrantonio et al.*, 1976]. Inflection-free wind profiles with stratified shear flows, for example, abrupt density variations, may also lead to instability [*Chimonas*, 1974; *Fua et al.*, 1976; *Churilov*, 2005, 2008]. In a layer of depth h with a constant N and uniform wind shear between two zero-shear and zero-density gradient flow layers, an unstable mode exists if $0 < Ri < 0.25$ [e.g., *Miles and Howard*, 1964], where $Ri = (g/\theta_0)(\partial\theta/\partial z)/(\partial U/\partial z)^2$ is the gradient Richardson number. The above result implies that the shear instability dominates the static or convective stability (buoyancy-related stability) when $0 < Ri < 0.25$ or the critical Ri for wave instability is $Ri_{cr} = 0.25$. Using Ri_{cr}, the wavelength of the maximum unstable mode is about 7.5 h [*Turner*, 1973]. Similarly, in a stably stratified flow where shear reaches a maximum, i.e., $d^2U/dz^2 = 0$, the shear instability also overcomes the stable stratification, but the wave growth rate is affected by the stratification. Theoretically, the wave growth may not always be suppressed by stable stratification [*Howard and Maslowe*, 1973].

Nonlinear development of primary waves can also generate secondary instability, leading to thin vortex sheets on top of primary waves [e.g., *Chimonas and Grant*, 1984; *Sutherland et al.*, 1994; *Mashayek and Peltier*, 2012; *Fritts et al.*, 2013]. In the atmosphere, the wave growth rate can be affected by turbulent viscosity and stratification [e.g., *Brown*, 1972]. As a result of turbulence associated with wave instability, the Ri criterion is often used for diagnosing turbulence in general (more in section 2.3.6).

2.2.3. Wave-Wave Interactions

Most investigations of wave-wave interactions in the literature focus on inviscid small-amplitude wave activities associated with nonlinearity. *McComas and Bretherton* [1977] categorized the resonant wave interactions of small wave amplitudes into three classes of nonlinear interacting resonant triads: induced diffusion, elastic scattering, and parametric subharmonic instability (PSI). Among these classes, PSI has drawn special attention in the literature as it explains wave energy transfer from long to short waves [*Mied*, 1976; *Poulin et al.*, 2003; *Koudella and Staquet*, 2006; *Joubaud et al.*, 2012]. For sufficiently small amplitude waves, resonant interactions are much more efficient at transferring energy among the waves of the triad than off-resonant interactions. However, most wave-wave interactions in the atmosphere are off resonant. In addition, the PSI process may take a long time to develop and may be interrupted by highly nonstationary airflow in the SABL. With long-lasting fossil turbulence in the background flow [*Gibson*, 1999], actual occurrence of PSI in the real atmosphere is questionable. In contrast, this process is suspected to play an important role in small-scale energy transfer and mixing in the oceans [*MacKinnon et al.*, 2013].

Interactions of nonlinear waves in an inviscid flow can also lead to waves with a wide range of frequencies and wave numbers, and their spectra resemble turbulence spectra; i.e., they display inertial ranges with specific laws [e.g., *Staquet and Sommeria*, 2002]. The application of nonequilibrium statistical mechanics to random nonlinear waves in a weakly nonlinear regime is sometimes called *wave turbulence* [e.g., *Dewan*, 1979; *Larraza*, 1993; *Nazarenko*, 2011].

2.3. Wave-Turbulence Interactions

Many theoretical investigations of wave-turbulence interactions have focused on conditions for waves breaking down into turbulence [e.g., *Koch et al.*, 2005] but not many on impacts of nonlinear processes associated with wave-turbulence interactions on the evolution of wave motions. Consequently, a *wave saturation theory* is needed to explain the formation of waves of finite amplitudes; i.e., nonlinearity and turbulence are expected to slow wave growth [e.g., *Fritts*, 1989; *Walterscheid and Schubert*, 1990; *Weinstock*, 1990].

Turbulence can be related to both buoyancy and vorticity waves. IGWs can increase/decrease local shear stability and thus enhance/reduce existing turbulence. Wave instability leads to exponential wave growth and vortex rolls, within which turbulence is embedded. In addition, waves can also be generated by turbulent motions such as "bursts" of turbulent jets that break into a stably stratified region, which was investigated in laboratory experiments [e.g., *Dohan and Sutherland*, 2003], and numerically investigated in downslope katabatic flows from "shooting" to "tranquil" toward the foot of the slope [e.g., *Renfrew*, 2004; *Largeron et al.*, 2013]. Interactions between turbulence and IGWs near the surface can also force apparent air and temperature oscillations at the wave frequency above the IGW layer, leading to *turbulence-forced oscillations* (TFOs) [*Sun et al.*, 2015] (more in section 3.1.1). As a result of nonlinearity, wave-turbulence interactions can effect heat transfer at wave frequencies and modify primary wave amplitudes [e.g., *Fua and Einaudi*, 1984; *Einaudi and Finnigan*, 1993].

In this section, we first discuss general characteristics of turbulence in a stably stratified flow (section 2.3.1) and how waves lead to turbulence (sections 2.3.2 and 2.3.3). We then briefly describe some theoretical investigations of wave-turbulence interactions (section 2.3.4). Because this review focuses on the SABL, we illustrate the role of the surface on wave-turbulence interactions (section 2.3.5). As wave instability is critical for generating turbulence in many numerical models, we discuss the generality of Ri_{cr} (section 2.3.6). As a result of the rapid increase in computing capabilities and the wide availability of numerical models, we also briefly review some of numerical tools used in investigating wave-turbulence interactions (section 2.3.7).

2.3.1. Turbulence in Stably Stratified Flows

Turbulence in a stably stratified flow is a broad subject [*Fernando and Hunt*, 1996; *Galperin and Sukoriansky*, 2010; *Sukoriansky and Galperin*, 2013]. The turbulence viscosity, which is much larger than the molecular viscosity in the atmosphere, has strong impacts on atmospheric waves although its influence in the interior of the oceans may be relatively small [*Liu et al.*, 2012]. No matter how stable the SABL is, there seems to be always some turbulence [*Mahrt and Vickers*, 2006]. Theoretically, shear-generated turbulence, including directional shear [*Shutts*, 1998; *Teixeira and Miranda*, 2009; *Mahrt et al.*, 2013], loses turbulence kinetic energy (TKE) through either viscous dissipation or vertical redistribution of temperature through the buoyancy flux. The buoyancy production term, which is proportional to the buoyancy flux, generates the buoyancy fluctuation called turbulence potential energy (TPE) by *Zilitinkevich et al.* [2007, 2013]. By considering the sum of TKE and TPE as the total turbulence energy (TTE = TKE + TPE), *Zilitinkevich et al.* [2007] clearly emphasized the important driving mechanism for the dynamics of a stably stratified flow and the role of heat transfer in redistributing instead of destroying the turbulence energy. As turbulence evolves in the stratified flow, the pressure strain terms in the component variance equations transfer energy preferentially from σ_w to σ_u and σ_v (where σ represents the standard deviation and the subscripts represent the three wind components) so that the eddies increasingly flatten into 2-D horizontal pancake vortices [e.g., *Etling*, 1993; *Sukoriansky et al.*, 2005; *Lindborg*, 2006; *Riley and Lindborg*, 2008; *Galperin and Sukoriansky*, 2010].

The recent discovery of the *zigzag instability* [*Billant and Chomaz*, 2000; *Lindborg*, 2006; *Billant et al.*, 2010], which results in vertically twisted and bent pairs of counterrotating and corotating vertical vortexes in strongly stratified fluids, suggests that the choice of the vertical length scale is determined by fluid dynamics, i.e., the buoyancy length scale $l_b = U/N$ [*Billant and Chomaz*, 2001]. This result on the length scale clearly demonstrates that turbulence in a stably stratified fluid is not the traditional 2-D turbulence. The zigzag instability has been associated with low Reynolds number flows ($Re = UL/\nu$, where L and ν are the characteristic length scale and the kinematic viscosity, respectively), and its significance has been pursued both experimentally and

numerically [e.g., *Lindborg*, 2006; *Waite and Smolarkiewicz*, 2008]. In addition to l_b, the length scale $l_w = \sigma_w/N$ is often used to represent the turbulent mixing length in the stably stratified atmosphere where turbulent eddies are not directly interacting with the surface (*z*-less turbulence) [e.g., *Hopfinger*, 1987; *Rehmann and Koseff*, 2004; *Lindborg*, 2006]. *Riley and Lindborg* [2008] investigated stratified turbulence in the oceans and demonstrated that turbulence eddies becoming isotropic through the energy transfer from TKE to TPE via overturning occur only at scales smaller than the *Ozmidov scale* ($l_o = \sqrt{\epsilon/N^3}$, where ϵ is the eddy dissipation). Because distinguishing cause and effect between turbulent mixing and *N* can be difficult, all the length scales defined through *N* may just reflect the eddy scale of the balanced state instead of the eddy scale being determined by *N* [e.g., *Ostrovsky and Troitskaya*, 1987; *Herring and Métais*, 1989; *Riley and Lindborg*, 2008; *Mahrt et al.*, 2013]. Recently, J. Sun et al. (The role of large-coherent-eddy transport in the atmospheric surface layer based on CASES-99 observations, submitted to *Boundary Layer Meteorology*, 2015) found that turbulence in the SABL observed at level *z* above the surface is generated on scales between the Kolmogorov scale [*Garratt*, 1992] and a scale comparable to *z*.

2.3.2. Wave Breaking Into Turbulence

Wave breaking is one of the most common paths to turbulence generation. Wave breaking can be triggered by self-acceleration due to interactions between waves and wave-induced mean flow through shear and static instabilities [e.g., *Munk*, 1981; *Sutherland*, 2010] or PSI [*Clark and Sutherland*, 2010; *Pairaud et al.*, 2010]. The intuitive picture of wave breaking is that an unstable wave generated by shear instability grows exponentially with time until nonlinear processes take over when wave crests overtake wave troughs, the atmosphere becomes locally statically unstable with denser fluid overlying less dense fluid [*Hines*, 1988], and turbulence is then generated by convective instability. Nonlinearity can both lead to wave breaking by changing the vertical density gradient and also delay or prevent wave breaking [*Hirt*, 1981]. Wave overturning first appears in reduced convective stability regions; convective instability is the first step leading to wave breaking and turbulence generation [*Koudella and Staquet*, 2006]. The critical wave steepness at which the wave breaking occurs may be wave number dependent [*Troy and Koseff*, 2005]. Dissipating waves through wave breaking can lead to mean motions such as quasi-horizontal (or vortical) motions, which is important for atmospheric circulations (more in section 2.3.3).

In addition to convective instability, shear instability can also lead to wave breaking and turbulence generation occurring in K-H billows even if the flow is not convectively overturning especially for waves with small vertical wave numbers [*Sutherland*, 2010, Figure 4.18b]. Wind shear can be locally enhanced in large-amplitude IGWs and triggers small-scale vortices, leading to local turbulence. Turbulence generated by shear instability in an unconfined stably stratified flow domain may be contained within a thin layer and be less intense compared with turbulence generated by large-amplitude wave breaking through convective instability. However, these small vortices can be advected by the background flow and last longer than turbulence generated by convective wave breaking, which explains commonly observed thin turbulent layers in stably stratified flows [*Fritts et al.*, 2003, 2009, 2013].

Wave breaking in the interior of a flow without any dissipation only redistributes the potential vorticity (PV) field without modifying the total PV [*Haynes and McIntyre*, 1987, 1990; *McIntyre and Norton*, 1990], which is not the case near the surface in the SABL where PV can be generated. The theory of wave steepening and breaking is thoroughly reviewed by *Staquet and Sommeria* [2002], *Staquet* [2004], and *Achatz* [2007].

2.3.3. Wave Critical Levels

The T-G equation (1) can become singular at a *critical level*, z_{cl}, where $U(z_{cl}) = c$ and *c* is the wave phase speed in the direction of wind velocity. Most investigations of wave critical levels in the literature focus on their impact on wave generation and property changes such as wave dissipation/breaking [e.g., *Geller et al.*, 1975; *Nappo and Chimonas*, 1992; *Moustaoui et al.*, 2004; *Lane and Sharman*, 2008; *Pulido and Rodas*, 2008], mean flow acceleration through wave momentum flux deposition when IGWs break near critical levels [e.g., *Jones and Houghton*, 1971; *Hirt*, 1981; *Weinstock*, 1982; *Nappo and Chimonas*, 1992], IGW reflection from critical levels [e.g., *Jones*, 1968; *Hirt*, 1981], wave energy leakage across critical levels [e.g., *Booker and Bretherton*, 1967; *Jones and Houghton*, 1971; *Teixeira et al.*, 2008], and three-dimensional wave instability near critical levels [*Winters and D'Asaro*, 1994]. A background shear flow can supply energy to waves through instabilities and can extract energy from waves through wave momentum deposition at wave critical levels [e.g., *West*, 1981]. Wave reflection between wave critical levels and the surface can lead to ducted waves [e.g., *Lindzen and Tung*, 1976; *Monserrat and Thorpe*, 1996]. Reflected downward waves from wave critical levels can have more energy

than upward moving incident waves in a stably stratified shear flow if $0 < Ri(z = z_{cl}) < 0.25$ [*Jones*, 1968], a process known as *overreflection*.

A critical wave level provides a potential location for turbulence generation and wave-turbulence interactions in the SABL. Due to the limitations of linear wave theory for wave critical levels [e.g., *Dörnbrack and Nappo*, 1997], a vast body of literature considering wave critical levels has focused on modification of the linear assumptions used in wave critical levels, which include nonlinearity [*Haberman*, 1973; *Fritts*, 1979; *Churilov and Shukhman*, 1996], viscosity and heat conduction [e.g., *Hazel*, 1967; *Yanowitch*, 1967; *Fritts and Geller*, 1976], and wind direction shear [e.g., *Doyle and Jiang*, 2006]. Overall, predicted impacts of wave critical levels on turbulence generation depend on the assumed background environment and the dynamic complexity considered in the analysis. Uncertainties in the effects of wave critical levels on wave generation, dissipation, breaking, and absorption still exist even in very sophisticated wave investigations. A finite-amplitude wave packet of various wavelengths can be energy diffusive compared to a single wave, so that the singularity at a critical wave level does not appear as dramatic for transient IGW packets as for a monochromatic IGW [*Pulido and Rodas*, 2008].

2.3.4. Theoretical Investigation of Wave-Turbulence Interactions

For slowly varying waves with an approximately constant wave period and a sufficient number of cycles, a net transfer of energy between waves and turbulence can be investigated through decomposing atmospheric variables into a time-averaged mean flow and wavelike and turbulent components [*Fua et al.*, 1982; *Einaudi et al.*, 1984; *Finnigan et al.*, 1984; *Finnigan*, 1988; *Einaudi and Finnigan*, 1993; *Finnigan and Shaw*, 2008]. They devised a triple decomposition to statistically understand the energy and momentum balances in a coexisting wave-turbulence system and used phase averaging to extract wave motions of constant frequency and slowly varying wave amplitude from a turbulent background flow in studying wave-turbulence interactions. The triple decomposition demonstrates that wave-turbulence interactions are achieved through the work done against the strain rates of the wave motion by fluctuations in turbulent stress. Because of the required conditions for the triple decomposition of the fixed-wave frequency, turbulence cannot modify the wave frequency; thus, the wave-turbulence energy exchange at a particular phase of the wave evolution cannot be investigated by this technique directly.

Other aspects of wave-turbulence interactions have also been investigated. Examples include the damping effect of near-surface turbulence on vertical variations of wave momentum fluxes generated by topography [*Grisogono*, 1994a, 1995], effect of nondissipating waves on turbulent mixing in the SABL [*Zilitinkevich et al.*, 2009], the initial stage of wave-induced turbulence when the background flow is approximately unaffected [*Fua et al.*, 1982], and influences of the vertical variation of turbulent mixing represented by eddy coefficients on wave phase velocities, growth rates, and vertical structures of waves [*Fua and Einaudi*, 1984]. In addition, turbulence damping of IGWs as a function of wave numbers has been investigated in laboratories [*Ostrovsky et al.*, 1996].

To investigate wave-turbulence interactions, various simplified turbulence parameterizations, such as Rayleigh friction (the friction term parameterized as a linear function of wind speed), constant viscosity, and quasi-linear theory, have been explored [e.g., *Chimonas*, 1972]. These simplified approaches may capture aspects of wave-turbulence interaction processes, in general, but are limited by their unrealistic description of the atmosphere.

2.3.5. Influences of the Surface on Wave-Turbulence Interactions

The role of the surface on wave motions is traditionally investigated through its generation of unstable modes under various wind shear and stratification conditions in an inviscid flow near the surface [e.g., *Jones*, 1968; *Davis and Peltier*, 1976; *Lalas and Einaudi*, 1976; *Lindzen and Rosenthal*, 1976, 1983; *Rosenthal and Lindzen*, 1983a, 1983b; *Romanova and Yakushkin*, 1995]. The destabilizing effect of the surface on long IGWs was investigated theoretically by *Lalas et al.* [1976] and was observed by *Greene and Hooke* [1979]. With varying density stratification above the surface, resonance between neutral modes supports local standing IGWs between a critical level and the surface (a special wave critical level) [*Lott*, 2007]; secondary K-H instability and turbulence can be generated at locally reduced *Ri*. Recently, *Candelier et al.* [2012] found that instability can also occur when the angle between shear and density surfaces resulting from a sloped surface is not zero.

Increasingly, physical and thermodynamic effects of the surface on wave formation have drawn attention of the research community. Topography can impose boundary conditions, which affect wave growth rates and slopes [*Thorpe and Holt*, 1995]. An inflection point in a stably stratified flow is not necessarily required

for wave instability near the surface [e.g., *Chimonas*, 1974]. Radiative cooling of the ground provides ideal stable stratification for wave ducting in the SABL. Heterogeneous land cover and topography may result in formation of cold air pools and density currents, which provides potential disturbances for generation of IGWs and vorticity waves [e.g., *Sun et al.*, 2015].

The surface can provide boundary conditions not only for generating waves but also for simultaneously generating turbulence. Turbulent eddies attached to the surface are generated by shear instability associated with the bulk shear, U/z, which are much more powerful than turbulent eddies that are detached from the surface in the very stable atmosphere [e.g., *Sun et al.*, 2012, 2015] (more in section 3.1.1). Turbulent mixing near the surface also affects mountain waves [*Georgelin et al.*, 1994; *Smith et al.*, 2002; *Jiang et al.*, 2006; *Smith et al.*, 2006; *Smith*, 2007; *Smith et al.*, 2007; *Vosper and Brown*, 2007]. In response to pressure fluctuations induced by mountains, wind changes in the turbulent ABL lead to surface drag and ABL depth changes, reduced IGW amplitudes, and upwind wave phase shifts. The momentum deposited in the ABL can take the form of a turbulent stress. *Smith et al.* [2007] found that the reduction of pressure drag and wave momentum flux in the SABL is most severe for small-scale hills. Turbulence mixing can reduce dynamic impacts of terrain on IGW generation. Influence of the turbulent ABL on mountain waves has been investigated for increasingly complex terrain [*Grubišić and Stiperski*, 2009; *Stiperski and Grubišić*, 2011], various structures of the ABL [*Teixeira et al.*, 2013], and varying thicknesses of the stable layer above the ABL [*Ralph et al.*, 1997].

With a constant horizontal pressure gradient over a sloped surface or forest canopies in the SABL, periodic motions can be generated due to imbalance between the pressure gradient and turbulent stress [e.g., *Pulido and Chimonas*, 2001; *Chimonas*, 2003], which is called the *Jeffreys' mechanism* [*Jeffreys*, 1925]. TFO generation mechanism (sections 2.3 and 3) is analogous to Jeffereys' mechanism. Laboratory experiments have also been used to investigate waves associated with shear instability near the surface and resonant feedback with turbulence [*Dohan and Sutherland*, 2003].

2.3.6. Instability and Critical Richardson Number

In the inviscid linear theory, Ri_{cr} for shear instability is derived for the very specific case of a steady parallel shear flow with no IGWs in a stably stratified medium, for example, by *Miles and Howard* [1964]. Furthermore, they investigated $Ri > Ri_{cr} = 0.25$ as the condition for a stably stratified flow, which has been an assumed corollary in the fluid dynamics that the flow is unstable for $Ri < Ri_{cr}$. The wave-induced velocity in a nonrotating medium causes the parallel shear to oscillate in space and time, which violates the assumption of the parallel ambient wind and likely leads to the Ri_{cr} criterion for wave breaking/turbulence generation to be irrelevant. In addition, wave oscillations modulate the mean shear of the background flow such that the local Ri may be smaller than the Ri averaged over a wavelength [e.g., *Finnigan et al.*, 1984]. In the ABL, Ri_{cr} is often found to be 0.2. *Busch* [1973] pointed out that the Ri_{cr} found in the ABL should not be confused with the $Ri_{cr} = 0.25$ for the transition from laminar to turbulent flows. *Zilitinkevich and Esau* [2007] and *Zilitinkevich et al.* [2008] made the same point. In addition to the above confusion, instead of Ri, the turbulent flux Richardson number, R_f, is often used in boundary layer studies [e.g., *Grachev et al.*, 2013], which can be related to Ri in the surface layer [e.g., *Sorbjan*, 1989]. The close connection between the bulk shear U/z and turbulence strength found by *Sun et al.* [2012] implies that local shear $\partial U/\partial z$ cannot capture variations of turbulence strength except for weak winds. J. Sun et al. (submitted manuscript, 2015) suggested that the gradient Ri may need to be calculated using the length scale of turbulence generation, which is the length scale of the shear instability in a stably stratified flow.

Ri_{cr} plays a significant role in determining the onset of turbulence in many mesoscale models. However, its relevance to turbulence generation has been debated in the literature, and an increasing number of studies question its universality and accuracy in predicting turbulence generation [e.g., *Howard and Maslowe*, 1973; *Thorpe*, 1977; *Abarbanel et al.*, 1984; *Grisogono*, 1994b; *Strang and Fernando*, 2001; *Andreas*, 2002; *Zilitinkevich and Baklanov*, 2002; *Fernando*, 2003; *Troy and Koseff*, 2005; *Achatz*, 2007; *Galperin et al.*, 2007; *Mauritsen and Svensson*, 2007; *Zilitinkevich and Esau*, 2007; *Sun*, 2011; *Sun et al.*, 2012; *Grachev et al.*, 2013]. For example, an IGW may be unstable to PSI regardless of the Ri value [*Drazin*, 1977; *Klostermeyer*, 1991; *Walterscheid et al.*, 2013]. The value of Ri_{cr} depends on whether the transition is from turbulent to laminar flows or the reverse [e.g., *Canuto*, 2002]. *Howard and Maslowe* [1973] pointed out that "... it is misleading to think that the onset of instability in a parallel stratified nonturbulent flow can be characterized in general by any universal critical Richardson number."

As explained in section 2.3.1, stratification and wind shear are connected in a stably stratified shear flow. Because shear generation is the only turbulence generation mechanism in a stably stratified fluid, the

influence of stratification on turbulence strength is suppressive. Stable stratification in the SABL driven by surface cooling reflects the vertical variation of density resulting from turbulent mixing that is generated by shear instability near the surface [*Sun et al.*, 2015]. Increasing turbulent mixing can significantly reduce the vertical temperature gradient near the surface. Without external forcing, turbulence leads to the energy transfer from TKE to TPE in a stably stratified flow, as clearly demonstrated in laboratory experiments [e.g., *Lin and Pao*, 1979]. Increasing stratification in the SABL by cold advection associated with density currents is often related to significant wind changes. Therefore, turbulence generation may not be well correlated with local *Ri* for a range of stability conditions in the atmosphere. As a result of the above mentioned issues, the use of Ri_{cr} is sometimes avoided by using functions fitted from observations, such as the long-tail formula [*Louis*, 1979; *Steeneveld et al.*, 2008], or through consideration of the total turbulence energy balance [e.g., *Mauritsen and Svensson*, 2007], or spectral theories [e.g., *Sukoriansky and Galperin*, 2005; *Sukoriansky et al.*, 2005] (more in 4.2.1).

2.3.7. Numerical Tools for Investigation of Wave-Turbulence Interactions

Numerical simulation has become an important tool to investigate wave-turbulence interactions in the SABL. Both *direct numerical simulation* (DNS), where turbulence can be resolved directly, and *large eddy simulation* (LES), where large turbulence eddies are directly resolved and subgrid turbulence eddies can be parameterized, are increasingly being used as the computer power increases with time. *Fritts et al.* [2009, 2013] demonstrated with DNS that direct coupling between large-scale and small-scale IGWs initiates layered and intermittent turbulence through K-H instability in an otherwise quiescent region, which results in a progressive destruction of a shear layer without any overturning convective instability process. *Almalkie and de Bruyn Kops* [2012] simulated turbulence in stably stratified fluids using a very high DNS model resolution of $4096^2 \times 2048$ and confirmed most of these results. They also examined the energy budget and found upscale energy transfer. In addition, they identified locations of sporadic overturning. Using DNS, *Kimura and Herring* [2012] investigated detailed energy spectra of turbulence in stably stratified flows by decomposing the flow into IGW and vortex modes and found different spectral behaviors in horizontal and vertical directions with varying stability. Recently, *Rorai et al.* [2014] showed that turbulence bursting or intermittency (in the form of non-Gaussian vertical velocity values) increases with stratification when nonlinear steepening occurs in the so-called saturation regime where nonlinear advection and buoyancy approximately balance.

The current limitation of DNS is its inability to simulate flows with $Re > 10^4 - 10^5$. Even considering the rapidly increasing computer power, the relatively low *Re* in DNS compared to its atmospheric value of $Re = 10^7$ precludes its resolving the Ozmidov length scale and entering the strong wave-turbulence interaction regime. Simulating turbulence in very stably stratified flows poses a serious challenge to DNS because the time for waves to interact nonlinearly through, for example, resonances, is relatively long, which translates into long model runs. A compromise solution is to utilize LES to simulate moderately stable flows [*Beare et al.*, 2006]. For example, in the convective daytime ABL, *Sullivan and Patton* [2011] showed that the higher-moment terms such as skewness, variances, and fluxes become grid size independent if the scale separation between the energy-containing eddies and those near filter cutoff eddies is adequate. Such high-resolution LES models with a dynamic subgrid-scale model have been used to simulate atmospheric turbulence and K-H instabilities, for example, in simulating radar backscattering [e.g., *Franke et al.*, 2011].

2.4. Challenging Issues in Wave-Turbulence Interactions

Investigation of waves in complex environments has been conducted increasingly through mathematical and numerical approaches due to increasing computing capabilities. Vorticity waves are commonly assumed once wave unstable modes are found. Progress has been made in understanding the early transition-to-wave stage of channel flows provided that *Re* is not large [e.g., *Vosper et al.*, 1999]. However, only a few studies include effects of turbulence on wave motions. Most vorticity wave investigations are limited to the onset of turbulence, which is assumed to occur if $Ri < Ri_{cr}$ as a result of wave-mean flow or wave-wave interactions. Our understanding of wave development is still limited. Statistical understanding of wave-turbulence interactions using spectral analysis can provide useful information on the general state of mixed wavelike motions and turbulence in the upper atmosphere [e.g., *Cho et al.*, 1999], but the analysis depends on sample conditions, wave states, and locations. Statistical investigations do not provide information on the evolution of the wave-turbulence energy transfer in space and time. Most numerical investigations of wave-turbulence interactions focus mainly on the interior of the flow domain and avoid impacts of the surface on wave-turbulence interactions.

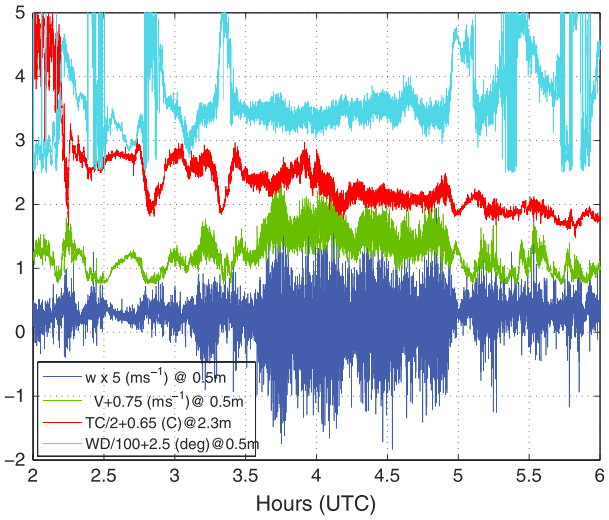

Figure 2. The time series of the "dirty" waves during the night of 20 October 1999 during the field campaign of the Cooperative Atmosphere-Surface Exchange Study in 1999 (CASES-99), which includes the wind speed V, the vertical velocity w, and the wind direction WD at 0.5 m above the surface and the thermocouple temperature TC at 2.3 m. All the variables are scaled as indicated in the figure for easy comparison [after *Sun et al.*, 2012, Figure 12] (©American Meteorological Society, used with permission).

To understand intermittent turbulence in the SABL, we need to understand how wave motions lead to turbulence and how turbulence modifies background flows and characteristics of existing wave motions. The approximate validity of linear theory for prediction of wavelength and wave periods is not fully understood even though the assumption of small amplitudes for linear and weakly nonlinear analysis is clearly not valid in most observed atmospheric wave motions. Basically, most wave investigations concentrate on mathematical solutions of unstable modes and lack physical understanding of wave evolution, which makes understanding impacts of waves on turbulence and wave-turbulence interactions difficult.

Additionally, the atmosphere is full of 3-D vortices of various sizes [*Gibson*, 1999]. Interactions between waves, 3-D background winds, and vortical motions add additional complication to the dynamics of wave-turbulence interactions [*Riley and Lelong*, 2000], which is particularly relevant in the SABL. Including vortices in a stably stratified flow can lead to interactions of wave motions with widely separated scales and complicate energy transfer to both shorter and longer wavelengths. In this light, one can remark that a dual cascade of energy toward both large and small scales has been observed recently in DNS of Boussinesq flows in the presence of rotation and stratification [*Pouquet and Marino*, 2013].

Evolution of wave-turbulence interactions can be an initial value problem as well as a boundary condition problem. Nonstationarity of airflow and spatial inhomogeneity of landscape have not yet been adequately addressed in theoretical and numerical studies. Because of the surface constraint, understanding evolution of wave motions is crucial for understanding spatial and temporal variations of shear instability for generating turbulence near the surface. An investigation requires careful consideration of the conservation of the total energy, momentum, and heat, which is lacking in most theoretical investigations of wave motions and is crucial for wave-turbulence interactions in the SABL [*West*, 1981; *Müller et al.*, 1986; *Durran*, 1995].

3. Observations of Waves and Wave-Turbulence Interactions

Observed waves in geophysical flows especially in the SABL are far more complex than theoretically investigated waves. Signatures that are sinusoidal for just a couple of cycles are often referred to as "waves" due to lack of observations to estimate the special characteristics of waves discussed in the previous section [*Caughey and Readings*, 1975; *de Baas and Driedonks*, 1985; *Einaudi and Finnigan*, 1993; *Lee et al.*, 1997; *Cuxart et al.*, 2002; *Anderson*, 2003; *Meillier et al.*, 2008; *Viana et al.*, 2010, 2012]. Waves with a number of cycles of approximately constant amplitude and period are referred to as clean waves here and have been observed mainly in the middle and upper troposphere [e.g., *Hicks and Angell*, 1968; *Gage and Gossard*, 2003; *Alexander et al.*, 2010], and $z \geq$ O(10 m) in the SABL, where turbulent mixing is often weak and the mean wind varies less compared to the flow near the surface [e.g., *Gossard et al.*, 1970; *Einaudi and Finnigan*, 1993; *Eaton et al.*, 1995]. Time series of wind observations reveal that waves near the surface in the SABL commonly have only a few cycles with varying amplitudes and periods (Figure 2). Complex waves may consist of many wave modes; wave spectra may be spread out in frequency and wave number space [*Tennekes*, 1976]. Some waves have significant asymmetry between wave crests and troughs and may approach ramp-like structures. In this section, we collectively refer to these common approximately periodic motions, such as those in Figure 2, as "dirty waves."

Turbulence obviously contributes to the dirtiness of observed waves, especially over rough and typically heterogeneous surfaces [e.g., *Sun et al.*, 2015]. Even away from the surface influence, coexistence of waves and turbulence is evident in temporal variations of cloud patterns [e.g., *Thorpe*, 2002] and remotely sensed images that rely on spatial gradients of the refractive index for visualization [e.g., *Gage and Gossard*, 2003]. Wave activities associated with fronts have been observed to contain intermittent turbulence [e.g., *Tjernström and Mauritsen*, 2009]. Wave-turbulence interactions are also evident from direct observations of wind speed and indirect observations such as sensible heat fluxes, which is revealed by the observed nonorthogonal phase difference between vertical velocity and temperature oscillations [e.g., *Viana et al.*, 2012]. In contrast to the zero sensible heat transport by a monochromatic buoyancy wave of infinitely small amplitude in an inviscid medium over a wave period based on linear wave theory, the observed sensible heat transport is often not zero. A finite value of the sensible heat transport can result partly from a noninteger number of wave cycles in the averaging time for calculating the wave heat transport and partly from the contribution of the ambient flow. If IGW and turbulence frequencies partially overlap, the wave scalar transport may lead to "random" turbulent flux errors, which could significantly impact the accuracy of the turbulent transport estimated by the widely used eddy covariance method in monitoring the material and energy exchange between the atmosphere and the ecosystem [e.g., *van Gorsel et al.*, 2011]. Because turbulence develops as vorticity waves evolve, sensible heat fluxes are not zero for vorticity waves.

Wave observations face challenges in the SABL partly due to weak vertical wave motions, wave reflection in the strongly stratified and nonstationary ducting zone [*Meillier et al.*, 2008; *Viana et al.*, 2009], and temporal variations of the background flow. In addition, observations of turbulence require research quality measurements, which cannot be obtained through routine observations. Observations of dirty waves are the focus of this section, where we review some observed waves and wave-turbulence interactions, instruments that are suitable for observing wave-turbulence interactions, and methodology for identifying turbulence in waves.

3.1. Observed Wave Generation Mechanisms and Wave-Turbulence Interactions

By applying the methodology developed for theoretical studies of waves, observed waves are often confirmed once unstable modes in the background flow are identified. That is, the initiation and the origin of wave motions are often unknown due to limited observation coverage. Identifying wave generation mechanisms has been attempted when good observation coverage exists for obtaining wave characteristics although accurate determination of wave origins is still challenging even when extensive data sets are available from field campaigns [*Lothon et al.*, 2014; *Román-Cascón et al.*, 2015]. Following the theoretical discussion in the previous section, we organize observed waves into two general categories according to their generation mechanisms: (1) buoyancy waves forced by displacing streamlines and (2) vorticity waves including vortex sheets or rolls initiated by shear instability. Wave-turbulence interactions may also result from local shear instability generated by wave-wave interactions [e.g., *Pavelin and Whiteway*, 2002], which are even more difficult to observe.

3.1.1. Observed Buoyancy Waves and Wave-Turbulence Interactions

Evidence of observed IGWs resulting from streamlines displaced by physical obstacles is abundant. The physical obstacles can be either large-scale obstacles, such as mountains [e.g., *Lenschow et al.*, 1988; *Smith*, 1989; *Lane et al.*, 2009], or small-scale features, such as shallow topography [e.g., *Rees and Mobbs*, 1988; *Rees et al.*, 2000; *Steeneveld et al.*, 2009]. However, physical obstacles may not necessarily generate buoyancy waves if conditions are not right (section 2). Observations of fog by video cameras over small-scale surface obstacles in a strong SABL reveal that air motions often flow around the obstacles (http://www.youtube.com/watch?v=8fu1bvGIF44), which precludes IGW generation. The weak wind and the stable stratification near the surface could prevent any significant displacement in this situation.

Displaced streamlines have also been observed in convergence zones associated with various weather phenomena such as intrusion of convective updrafts from the ABL into the stably stratified free troposphere [*Kuettner et al.*, 1987; *Nastrom et al.*, 1990; *Nastrom and Fritts*, 1992; *Sato et al.*, 1995; *Böhme et al.*, 2004; *Gibert et al.*, 2011; *Melfi and Palm*, 2012; *Petenko et al.*, 2012] and collisions between background flows and density currents from fronts, squall lines, or downdrafts from convective thunderstorms and downslope flows in the ABL [e.g., *Jordan*, 1972; *Curry and Murty*, 1974; *Balachandran*, 1980; *Eckermann and Vincent*, 1993; *Samah and Thorpe*, 1993; *Simpson*, 1997; *Ralph et al.*, 1999; *Soler et al.*, 2002; *Tjernström and Mauritsen*, 2009; *Viana et al.*, 2010; *Udina et al.*, 2013; *Soler et al.*, 2014; *Román-Cascón et al.*, 2015]. The scale of density currents can be as small as microscale such as mini-density currents and microfronts as a result of cold air from cold air pools in small gullies or from relatively colder surfaces due to different cooling rates over heterogeneous surfaces

[e.g., *Balsley et al.*, 2002; *Hohreiter*, 2008; *Mahrt*, 2010a; *Sun et al.*, 2015]. The wind sheltering effect of small valleys also contributes to development of cold air pools and cold air movements [*Vosper and Brown*, 2008; *Zhou and Chow*, 2013]. Alternation between acceleration of a cold drainage flow and its deceleration by adiabatic warming can cause nonpropagating buoyancy oscillations in valleys, leading to IGWs trapped by an overlying critical wave level [e.g., *McNider*, 1982; *Chemel et al.*, 2009]. IGWs have been reported on the top or leading edge of density currents [e.g., *Sun et al.*, 2002; *Viana et al.*, 2010]. IGWs generated by different density currents, for example, from the drainage flows in a valley and its tributaries [*Porch et al.*, 1991], may interact with each other. IGWs may at times appear to be above the SABL but are generated in the deep SABL upstream [e.g., *Mahrt et al.*, 2013]. *Rees et al.* [2000] found that about 10% of the observed IGWs over the Brunt Ice Shelf in Antarctica are strongly controlled by conditions near the top of the SABL. IGWs above the ABL may modulate the wind field of even neutral and convective ABLs through their pressure field and the inversion height.

Recent observations of relationships between the size distribution of turbulent eddies and turbulence generation have led to new understanding of interactions between IGWs and turbulence near the surface. *Sun et al.* [2012] found that strong turbulence near-neutral conditions consists of large turbulent eddies that scale with z and are generated by the bulk shear, U/z. In contrast, relatively weak turbulence is generated by local shear with a length scale less than z. Applying this new concept of the turbulence generation mechanisms, *Sun et al.* [2015] found that oscillations of IGW wind speed lead to differences in turbulence generation at wind speed wave crests and troughs: strong turbulence with large eddies attached to the surface at wave crests and relatively weak and vertically elevated turbulence at wave troughs. The periodically strong mixing at wave crests redistributes heat and momentum vertically over a relatively deep layer, resulting in apparent temperature oscillations in the layer of IGWs near the surface and apparent and temperature oscillations above the layer, i.e., turbulence-forced oscillations. The temperature oscillation in the IGW layer is in phase, instead of 90°out of phase, with wind speed as in the linear IGW, resulting in heat transfer. The wind speed and temperature of the TFOs are 180°out of phase with the original IGW wind speed, leading to countergradient momentum and heat transfer at the IGW frequency. The enhanced local turbulent mixing at wave troughs reduces the wave period of the existing IGWs. Therefore, the different turbulence generation mechanisms lead to wave asymmetry between wave crests and troughs, which is commonly observed.

Observations of solitary waves in the atmosphere have been extensively documented [e.g., *Christie et al.*, 1981; *Doviak and Ge*, 1984; *Lin and Goff*, 1988; *Smith*, 1988; *Jeffrey*, 1989; *Cheung and Little*, 1990; *Rottman and Grimshaw*, 2002; *Anderson*, 2003; *Sun et al.*, 2004]. *Rottman and Grimshaw* [2002] have categorized observed solitary waves as shallow-layer and deep-layer solitary waves depending on whether the solitary waves occupy a shallow layer near the Earth's surface or the entire troposphere. In addition, they concluded that the shallow waves are generated by mesoscale processes such as density currents, and the deep waves are generated by synoptic-scale features such as large-scale convective systems and geostrophic adjustment. Due to limited observation coverages, the generation mechanism of solitary waves is often speculative [*Doviak and Ge*, 1984; *Chimonas and Nappo*, 1987].

Solitary waves in the SABL are often observed with one or several bell-shaped surface pressure perturbations. The amplitude of the pressure perturbation and the ratio of its value to wavelength are significantly larger for solitary waves than those with IGWs [*Hauf et al.*, 1996]. They are often observed to travel long distances without losing their shape even over rough urban surfaces [*Rao et al.*, 2004], suggesting that they are not significantly influenced by local turbulence [*Doviak and Ge*, 1984; *Edwards and Mobbs*, 1997]. In addition, trapping mechanisms, such as weakly stratified layers or wave critical levels over a strongly stratified layer, are frequently observed with solitary waves [*Rottman and Grimshaw*, 2002; *Coleman et al.*, 2009]. *Rees et al.* [1998] found that solitary waves are common within a surface inversion with weak winds over a coastal Antarctic ice shelf and often propagate at speeds of 10–20 m s^{-1} or more. They can be much deeper than a typical observation tower with considerable uncertainty on the upper boundary trapping mechanism. This may be one of the difficulties for theoretical confirmation of solitary waves [*Doviak et al.*, 1991]. Because of their nonlinearity, scalar fluxes, such as sensible heat flux, can be associated with solitary waves [e.g., *Edwards and Mobbs*, 1997; *Sun et al.*, 2004].

3.1.2. Observed Vorticity Waves and Wave-Turbulence Interactions

Observed vorticity waves are often associated with K-H instability [e.g., *Hardy et al.*, 1973; *Busack and Brümmer*, 1988; *de Silva et al.*, 1996; *Lee et al.*, 1997; *Blumen et al.*, 2001; *Fukao et al.*, 2011]. *Fukao et al.* [2011] have conducted an extensive study of K-H billows in the height range of 1.32–20.34 km using a wind radar profiler. They found that K-H billows are not ubiquitous and typically occur when vertical speed shear is about

15–30 m s^{-1} km^{-1}. They also noticed that the depth and the wavelength of K-H billows are smaller in the ABL than in the free atmosphere. *Lyulyukin et al.* [2013] composited shapes and structures of braid patterns of K-H billows in the SABL observed by a sodar and found that they frequently appear during the morning and evening transition hours. *Readings et al.* [1973] summarized scientific issues on formation and breakdown of K-H billows based on atmospheric observations and laboratory results.

Waves generated by shear instability associated with wave critical heights are also frequently observed [*Merrill and Grant*, 1979; *Finnigan et al.*, 1984; *Ralph et al.*, 1993; *Tjernström et al.*, 2009]. *Einaudi and Finnigan* [1993] found that wave critical levels were common above the 300 m tall Boulder Atmospheric Observatory tower in Colorado and atmosphere profiles up to several kilometers above the surface were necessary to obtain K-H modes from the T-G equations.

Vorticity waves associated with inflection points in the wind profile are routinely observed near velocity jets and canopy tops [e.g., *Raupach et al.*, 1996; *Lee*, 1997; *Lee et al.*, 1997; *Lee and Barr*, 1998; *Finnigan*, 2000; *Finnigan et al.*, 2009]. Vorticity waves in a layer of finite depth above plant canopies at night are almost ubiquitous for several reasons [*Fitzjarrald and Moore*, 1990; *Belcher et al.*, 2012]. Interaction between the radiative cooling of the upper canopy after sunset and the different efficiencies of momentum and heat transfer in the layers just above the canopy and the upper canopy ensure the relatively large $Ri \sim O(10)$ in the upper canopy layer and the relatively small $Ri \sim O(0.1)$ above the canopy. Hence, this inflection point instability, which results from a maximum wind shear at the canopy top, keeps generating vorticity waves at the canopy top interface. *Hu et al.* [2002] found that the momentum and heat fluxes of vorticity waves at the canopy top vary with height as a result of turbulent mixing from vortex rolls and are maintained by extracting kinetic energy from the background flow. Therefore, turbulence is periodically generated by nonlinearity of vorticity waves initiated by the inflection point instability, which can effectively transport scalars as well as momentum at both turbulence and wave scales. In contrast to buoyancy waves, they observed that the vorticity waves travel at approximately the background flow speed.

3.2. Wave Observation Methods for Wave-Turbulence Interactions

A variety of wave observation methods and technology has been discussed, for example, in *Lenschow* [1986], *Gage and Gossard* [2003], and *Nappo* [2012]. Here we focus on the suitability of various methods for investigating wave-turbulence interactions in the SABL.

3.2.1. Fixed-Point Measurements

Pressure measurements are frequently used for identifying waves, as vertical motion and temperature of waves are generally weak near the surface, and horizontal velocity components can be strongly influenced by local terrain features and surface heterogeneity. The pressure root-mean-square is much larger for spatially coherent waves than for turbulence; for turbulence over a rough wall, it is $\sim 2.6\ \rho u_*^2$ (u_* is the friction velocity) [e.g., *Elliott*, 1972; *Anderson et al.*, 1992]. Thus, pressure variations induced by waves are less likely contaminated by turbulence. This makes surface microbarographs ideal for detecting waves compared to direct observations of wave motions near the surface. To obtain wave phase speed and direction as well as wave frequency, amplitude, and wavelength, an array of a minimum of three microbarographs is required based on the following assumptions: (1) the wave structure preserves a constant shape while propagating through the network and (2) the wave front is perpendicular to its propagation direction within the observation domain [e.g., *Herron and Tolstoy*, 1969; *Herron et al.*, 1969; *Eom*, 1975; *Hooke and Hardy*, 1975]. Microbarographs have been recently improved in terms of the accuracy and the sampling rate due to advances in counting circuitry and digital signal processing. Current pressure transducers are sufficiently accurate to allow trustworthy measurements of even turbulent pressure fluctuations. Therefore, pressure measurements can now identify turbulent mixing related to wave activities [e.g., *Viana et al.*, 2007].

An objective way to obtain wave parameters from quasi-sinusoidal signals that persist for several cycles at a fixed point is to analyze coherent structures of pressure fluctuations from an array of microbarographs by applying the maximum cross-correlation method [e.g., *Rees and Mobbs*, 1988; *Einaudi et al.*, 1989; *Hauf et al.*, 1996] or the beam steering algorithm [*Denholm-Price and Rees*, 1999]. The maximum cross-correlation method is suitable for waves even under the influence of turbulence if their frequencies are separable. The beam steering algorithm may be able to differentiate wave numbers of multiple waves with the same frequency [*Denholm-Price and Rees*, 1999]. However, the accuracy of the derived wave phase speed may not be as good as $O(10^{-1}$ m $s^{-1})$, which is required for testing some wave theories [e.g., *Chimonas*, 2002]. Wave climatology has been established under various synoptic conditions using surface microbarograph observation networks

[*Gedzelman*, 1983], in the nocturnal SABL in the lee of the Rocky Mountains [*Einaudi et al.*, 1989], over the Brunt Ice Shelf, Antarctica, using both microbarographs and wind observations [*Rees and Mobbs*, 1988; *Rees et al.*, 2000], and for mesoscale wave events within a diameter of about 50 km [*Grivet-Talocia et al.*, 1999].

The limitation of the microbarograph network is, however, the spatial separation of the sensors, which determines the resolved wavelength [*Grivet-Talocia et al.*, 1999]. Most observed waves estimated from a network of microbarographs on scales of O(200 m) have periods of O(1–30 min) and wavelengths of O(1–100 km). The frequency of buoyancy waves is limited by N, which is affected by turbulent mixing and radiative cooling of the ground in the SABL [*Sun et al.*, 2015]. Smaller spacing between microbarographs would allow identifying shorter waves, but the resulting pressure differences for long waves may be difficult to detect. The challenging issue for deploying microbarograph arrays is optimizing the spatial arrangement of a limited number of microbarographs.

As surface pressure measurements reflect vertically integrated density variations over the entire atmosphere above pressure sensors, surface pressure fluctuations may reflect wave disturbances well above the surface, which may or may not be associated with waves in the SABL. *Herron and Tolstoy* [1969] observed wave activities associated with jet streams near the tropopause from the surface pressure signals; however, *Trexler and Koch* [2000] found that microbarographs can detect the existence of waves only in the lowest 2–3 km of the atmosphere. The above studies suggest that the pressure oscillations observed at the surface may be dominated by the contribution from heavier air in the lower atmosphere, while the origin of the waves can be much higher. Turbulent mixing can vertically distribute cold air above microbarographs from the radiatively cooled ground [*Sun et al.*, 2015]. Thus, turbulent mixing near the surface can influence wave pressure signals from ground-based microbarograph networks, which is evident in the observed pressure oscillation differences at different heights by *Viana et al.* [2010]. Large temporal and spatial pressure variations of weather systems may also contribute to the relatively small surface wave pressure amplitudes [e.g., *Sun et al.*, 2013].

Because covariances of wave pressure and vertical velocity are related to wave energy, they may also provide better objective wave signals compared to pressure signals alone [*Woods and Smith*, 2010]. On the other hand, the vertical velocity of waves can be significantly affected by turbulent mixing, which may be undesirable for wave analysis.

Although wave pressure signals are clearly identifiable in the SABL, waves are also identifiable by monitoring time series of temperature oscillations [e.g., *Lee and Barr*, 1998; *Viana et al.*, 2012] and horizontal or vertical wind oscillations from towers [e.g., *Rees and Mobbs*, 1988]. *Sun et al.* [2015] found that the percentage of observed wind speeds that exceed the wind speed required for generation of strong turbulent mixing near the surface decreases with height. Therefore, the chance of observing bulk shear-generated strong turbulence influencing wave temperature and wind signals decreases with height. Thus, the probability of observing relatively clean wind and temperature wave oscillations increases with height. In addition, wave motions near the surface are characterized by small flow angles with respect to a horizontal surface, in which case even small misalignment of the sonic anemometers can lead to large relative errors in vertical wave motions [e.g., *Mahrt*, 2010b]. Similar to using pressure for wave information, using wind and temperature observations for wave phase speed and propagation direction, as well as wave frequencies, requires an array of towers with wind and temperature sensors. To avoid the strong turbulence influence and the small flow angle issue near the surface, these measurements need to be at approximately 10 m or higher depending on the depth of the wave layer. Furthermore, careful removal of the temporal variation of large-scale background flow is also required for this method.

Recently, fast-response fiber optic measurements of temperature fluctuations have been deployed over spatial scales of O(1–100 m) to visualize wave propagation [*Thomas et al.*, 2012]. Its deployment in a 2-D to 3-D formation near the surface could potentially be used for studying wave-turbulence interactions.

3.2.2. Mobile Platform Measurements

Balloon oscillations are another useful method for investigation of waves in the free troposphere [e.g., *Corby*, 1957; *Booker and Cooper*, 1965; *Vergeiner and Lilly*, 1970; *De La Torre and Alexander*, 1995; *Hertzog et al.*, 2008]. However, it is limited for accurately measuring waves in shallow SABLs because of the relatively small vertical velocity near the surface and vertical resolutions of sondes [*Hertzog et al.*, 2008].

Tethered lifting systems, which use either an aerodynamic balloon or a kite that is connected to a tether with instrument packages attached [e.g., *Balsley et al.*, 1998; *Balsley*, 2008], are also useful for observing wave-turbulence interactions. They can carry not only basic meteorological packages but also turbulence

instruments to identify turbulence and waves above a typical tower height [*Frehlich et al.*, 2003; *Fritts et al.*, 2003; *Meillier et al.*, 2008]. However, using tethered lifting systems to measure wave phase speed and propagation direction has not been done.

Small aircraft with sufficient payload to carry sensors and associated systems can measure variables related to both waves and turbulence. Combining inertial reference systems and differential global positioning systems (GPS) with air motion sensors (e.g., differential pressure measurements in a radome) on small aircraft may allow measurements of 3-D wind. Similarly, pressure perturbations can be obtained by combining GPS height with accurate static pressure measurements. Thus, wave energy transfer can be observed directly from aircraft [*Woods and Smith*, 2010; *Bange et al.*, 2013]. A remotely piloted aircraft (RPA) can also provide direct observations of horizontal structures, such as horizontal wavelengths [e.g., *Bonin et al.*, 2013], and repetitive soundings over a relatively deep layer [*Mayer et al.*, 2012a, 2012b; *Reuder et al.*, 2012]. Turbulence measurements start to become available on RPA [e.g., *van den Kroonenberg et al.*, 2008; *Thomas et al.*, 2011; *Reineman et al.*, 2013], which makes RPA a great potential tool for investigating wave-turbulence interactions. The relatively slow flight speed of RPAs can provide relatively high spatial resolution measurements but complicates wave analyses as it cannot capture a "snapshot" of fast-moving waves. Potentially large roll and pitch angles of RPA may challenge correction methods for removing aircraft motions particularly if the aircraft rolling time scale overlaps the time scale of interest. This technology is expected to advance rapidly in the near future.

Recently, *Belušić et al.* [2014] developed an instrument package that has been deployed on a car for mobile turbulence measurements. It can be used to measure spatial variations of turbulence within a few meters of the surface following a terrain slope, which cannot be achieved with aircraft or networks of flux towers. This mobile platform provides another method to investigate wave-turbulence interactions in the SABL.

3.2.3. Remote Sensing

Remote sensors, either on the ground or airborne vehicles, can obtain many observations within a large air volume in a short time, while in situ sensors are limited to sampling a limited number of points. The high temporal and spatial resolutions required for studying wave-turbulence interactions in the SABL may constrain the number of suitable remote sensors. Commonly used active sensors designed for investigation of the ABL are based on radio detection and ranging (radar), sonic detection and ranging (sodar), and light detection and ranging (lidar) [*Lenschow*, 1986; *Wilczak et al.*, 1996; *Emeis*, 2011]. Using radar technology and pointing radar vertically, radar wind profilers, such as Doppler radars at ultrahigh frequency (UHF) of 915 MGz, with a spaced antenna technique can measure wind speed to an accuracy of $\sim$1–2 m s^{-1} with 1–5 min time resolution and 50–60 m altitude resolution at the minimum height of 180 m under clear-sky conditions [e.g., *Ecklund et al.*, 1988; *Carter et al.*, 1995; *Cohn et al.*, 1997, 2001]. This vertical resolution is adequate for investigating convective boundary layers but may miss some of the fine-scale wave-turbulence interactions near the surface in the SABL. The spatial resolution can be improved using multiple-frequency interferometry or range imaging techniques [e.g., *Muschinski et al.*, 2005]. The digital beam-forming phased array radar, i.e., the turbulent eddy profiler with coherent radar imaging, can achieve 30 m spatial resolution and measure the refractive index and 3-D wind [e.g., *Mead et al.*, 1998; *Cheong et al.*, 2008]. Frequency-modulated, continuous-wave (FM-CW) radars can provide vertical profiles of refractive index inhomogeneities with spatial resolution of about 2.5 m and temporal resolution of O(10 s) [e.g., *Gossard et al.*, 1970; *Eaton et al.*, 1995; *İnce et al.*, 2003], which is adequate for detecting wave-turbulence interactions in the SABL.

By measuring backscatter acoustic signal intensity from temperature, velocity, and moisture fluctuations, sodars can be used to monitor wave-turbulence interactions in the SABL at a time resolution of $\sim$10 s and range resolution of $\sim$10 m, which is essentially free of ground clutter on measured signals [e.g., *Brown and Hall*, 1978; *Neff and Coulter*, 1986]. Sodars can be used to measure wind speed, vertical variations of vertical velocity, and sensible heat fluxes in the convective boundary layer through the relationship between the structure function of temperature and sensible heat flux [e.g., *Angevine et al.*, 1993; *Coulter and Kallistratova*, 2004; *Engelbart et al.*, 2007]. Small sensible heat fluxes in the SABL can be challenging for sodar measurements; however, enhanced intermittent sensible heat fluxes resulting from wave-turbulence interactions could be detectable. In addition, including multiple frequencies increases the range gate resolution to 19 m and allows sodar measurements in the vertical range of 10–300 m, which is suitable for investigating the SABL [*Coulter and Martin*, 1986; *Coulter*, 1990; *Hoover et al.*, 2015]. Current efforts to better understand the influence of anisotropy and intermittency of turbulence on acoustic waves may lead to a better understanding of sodar signals and increase their use for SABL research [e.g., *Kallistratova*, 2002].

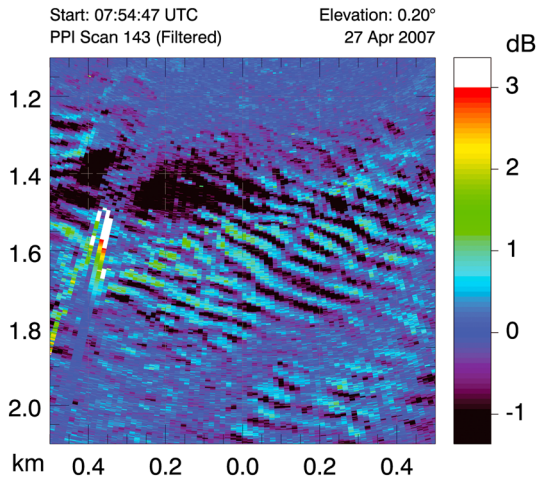

Figure 3. A 1 km^2 section of a single, nearly horizontal, lidar scan through wavy motions on 27 April 2007 at 7:54 UTC during the field campaign of the Canopy Horizontal Array Turbulence Study [*Patton et al.*, 2011]. The wavelength is ~70 m. The range-corrected backscatter intensity was high-pass median filtered to reveal the wave pattern. Brighter colors represent higher backscatter intensity [after *Mayor et al.*, 2012b; *Jachens and Mayor*, 2012].

Radio acoustic sounding system (RASS), which utilizes radio and acoustic sounding systems together, can measure air temperature profiles [*May et al.*, 1990]. With the combination of a sodar system and a Doppler RASS, both temperature and wind can be measured simultaneously at a vertical resolution of 5 m and a minimum height of 10 to 20 m, which may be suitable for SABL [e.g., *Engelbart and Bange*, 2002; *Viana et al.*, 2012].

Significant advancements in lidar technology have made lidar measurements more attractive for extending observations above a typical tower height. Compact Doppler lidars are now commercially available and can provide high-resolution vertical profiles of horizontal winds close to the surface. For example, the Halo Photonics Stream Line Doppler lidar can provide vertical profiles of horizontal winds down to a minimum altitude of 40 m at 8 s time intervals with an altitude resolution of 24 m. Wind profiles can be achieved from conical scanning and fitting trigonometric functions to the resulting radial velocity data if the velocity field is approximately horizontally homogeneous. By pointing a Doppler lidar beam vertically instead of scanning, time-height profiles of vertical velocity can be obtained. With a horizontal scan, Doppler lidars are typically capable of making radial velocity measurements to distances from 1 to 10 km depending on the aerosol backscatter conditions [*Grund et al.*, 2001; *Pearson et al.*, 2009]. Air motions at one point have also been measured by three pulsed coherent Doppler lidars running concurrently to obtain three-dimensional velocities of the fluctuating atmosphere at two samples per second [*Mann et al.*, 2009]. The fast response and small sample volume of this observation technique allow direct measurements of turbulence and waves in a spatial domain that is much larger than typical towers can cover. In addition, it is free of the flow distortion associated with masts and in situ sensors. This technique can potentially measure spatial variations of turbulent winds. By scanning in azimuth or elevation, lidar can also map out the wind field over a 2-D atmosphere, which can capture spatial variations of waves [e.g., *Newsom and Banta*, 2003]. By combining conical azimuth scans and the velocity-azimuth-display technique, temporal variations of wind variance profiles can be derived [e.g., *Banta et al.*, 2006; *Pichugina et al.*, 2008]. Using two conical scanning Doppler lidars, the vertical flux of horizontal momentum can be measured [*Mann et al.*, 2010]. Raman lidars can be used to measure water vapor with the adequate resolution and scanning ability for SABL investigations [e.g., *Whiteman et al.*, 1992; *Froidevaux et al.*, 2013].

Rapid-scanning aerosol lidars, such as the Raman-shifted Eye-safe Aerosol Lidar (REAL) [*Mayor and Spuler*, 2004], can provide time-lapse animations of wave activity within the SABL. This occurs when the waves vertically displace aerosol layers [*Jachens and Mayor*, 2012; *Randall et al.*, 2012]. Images from the REAL have shown canopy wave motions and provide information on wavelength and wave propagation velocity (Figure 3). In addition to spatial information and wave motions, backscattered lidar data from the REAL can be processed with motion estimation algorithms to deduce multicomponent wind fields [*Mayor and Eloranta*, 2001; *Mayor et al.*, 2012a].

Both waves and related turbulence in the SABL have been investigated in the literature with FM-CW radars [e.g., *Atlas et al.*, 1970; *Gossard et al.*, 1970; *Eaton et al.*, 1995], sodars [e.g., *Bean*, 1971; *Culf and McIlveen*, 1993; *Viana et al.*, 2009, 2010], lidars [e.g., *Newsom and Banta*, 2003], and both a radar and a sodar [e.g., *Ottersten et al.*, 1973]. These studies document detailed wave-turbulence interactions in the SABL, as well as the structure of waves, synoptic conditions for wave formation, and investigation of wave instability theories, and development of turbulent mixing through its role in enhancing the refractive index in stably stratified flows.

They documented structures of IGWs, vorticity wave breaking, thin turbulent layers of less than O(10 m), and the relationship between turbulence and collapse of waves in the stably stratified atmosphere.

3.3. Distinguishing Waves From Turbulence

Objective separation of turbulence and waves from limited time series of any meteorological variable regardless of the turbulence intensity is substantially more difficult than recognizing the mere existence of waves or extracting wave characteristics from observations. Separation between waves and turbulence is required when attempting to compute the "true" turbulent fluxes and possible wave fluxes. The methods that may be used to separate relatively clean waves from three-dimensional turbulence are summarized below, which is an extension of a list from *Stewart* [1969]. The first three criteria are for buoyancy waves, such as IGWs, and the last three can be used for all waves.

Criterion 1. Differences in the energy transport speed. Turbulence energy transport follows the background wind speed, while IGW packets and wave energy follow the group velocity. Identifying wave propagation speeds different from wind speeds can be used for separating waves from turbulence. The method may be difficult to apply if the wind is nonstationary. The dispersion relationship derived from linear wave theory can only be used as a guide because most observed IGWs are nonlinear.

Criterion 2. Differences in mixing. Turbulence mixing occurs both along and across surfaces of a constant density, whereas linear IGWs do not mix across density surfaces. Wave breaking into turbulence can be location or wave-phase dependent, which appears to be intermittent spatially and temporally. This criterion may not work if wave and turbulence frequencies overlap (criterion 6).

Criterion 3. Differences in transporting scalars. Linear waves can transport momentum but not heat if covariances between vertical velocity and scalars are averaged over a set of integer wave periods while turbulence can transport both momentum and scalars. Thus, waves can be distinguished by their efficiency in momentum transport relative to scalars [e.g., *Dewan*, 1979; *Yagüe and Cano*, 1994, *Yagüe et al.*, 2001, 2006; *Sukoriansky et al.*, 2009; *Fernando and Weil*, 2010]. However, zero wave heat flux in the SABL near the surface is seldom observed. The phase difference between the vertical velocity and temperature is strongly affected by turbulent mixing, which tends to be 180°at night and 0°during the day, i.e., downward turbulent sensible heat flux at night and upward during the day. Nonlinearity alone can shift the phase difference between wave vertical velocity and temperature, leading to nonzero heat transport [*Burns et al.*, 2012]. In addition, estimating of scalar fluxes on the wave scale in the atmosphere is problematic due to serious flux errors associated with variable wavelengths and the averaging time of a noninteger number of wave periods. This criterion also relies on separation between IGWs and turbulence in frequency or wave number, which can be difficult (criterion 6).

Criterion 4. Differences in correlations between pressure and wind speed fluctuations. Static pressure fluctuations associated with turbulence are related to the square of wind fluctuations, whereas pressure fluctuations associated with waves vary linearly with velocity fluctuations. This criterion requires fast response wind and pressure measurements. Because turbulent mixing often increases with decreasing height in the SABL, the wind wave signal can be significantly affected by turbulent mixing near the surface; this criterion may be difficult to apply near the surface.

Criterion 5. Variations in Rossby-Ertel PV values. Both linear and nonlinear waves have the baroclinic vorticity vector perpendicular to the density gradient vector, i.e., zero PV [e.g., *Riley and Lelong*, 2000], while turbulence is associated with 3-D vortex stretching and bending and has nonzero PV. In a compressible fluid without dissipative forces or fluxes, the PV following fluid parcels should be conserved, i.e., $\mathrm{D(PV)}/\mathrm{D}t = 0$, where $\mathrm{PV} = (1/\rho)\boldsymbol{\xi} \cdot \nabla\theta$ ($\boldsymbol{\xi}$ is the vorticity vector). Because of this conservation law, the scalar PV is a useful indicator for IGW breaking and turbulence generation [e.g., *Haynes and McIntyre*, 1987; *Smith and Smith*, 1995; *Rotunno et al.*, 1999; *Smith*, 2002; *Schneider et al.*, 2003; *Epifanio and Qian*, 2008; *McIntyre*, 2008]. Diagnosing the time variation of PV may be useful for numerical models. However, it cannot be easily applied to field observations due to the limited 3-D spatial coverage.

Criterion 6. Differences in frequencies or wavelengths. Separation between waves and turbulence is possible if spectral gaps between waves and turbulence or phase relationships between wave variables are well defined [*Caughey and Readings*, 1975; *Caughey*, 1977; *Gedzelman*, 1983; *Lu et al.*, 1983; *Hunt et al.*, 1985]. Frequency separation between waves and turbulence is often assumed in data analysis. For example, random features with periods of less than 1 min are often considered as

turbulence and are eliminated by low-pass filters for wave analysis [*Kaimal et al.*, 1972; *Caughey*, 1977; *Gedzelman*, 1983; *Klipp and Mahrt*, 2004; *Grachev et al.*, 2013]. To do so, the subjective low pass must be broad enough to avoid creating waves from noise. For example, the Fourier transforms used in these analyses can introduce spurious wave signatures, e.g., aliasing. By investigating each individual data segment, *Vickers and Mahrt* [2006] used the multiresolution decomposition to separate turbulence from waves. In contrast to traditional filtering methods, empirical orthogonal functions can capture more of the wave amplitudes and require less preconditioning of the time series data [*Fiorino and Correia*, 2002]. Since waves generally occur in local packets, various wavelet techniques appear superior to Fourier spectra for separating wave and turbulence quantities and are increasingly used in wave analyses [*Rees et al.*, 2001; *Terradellas et al.*, 2001; *Cuxart et al.*, 2002; *Terradellas et al.*, 2005; *Viana et al.*, 2009, 2010, 2012]. Waves that interact strongly with turbulence generally have periods that lie in the energy-containing range of the turbulence spectrum. For wavelengths much longer than any turbulent eddies, a spectral gap between waves and turbulence is likely in wave number space instead of in frequency space. Therefore, waves are better examined in space than in time, which requires time series of observations from a spatial network or a moving platform. Separating waves from turbulence in wave number space requires an adequate observation network to capture a variety of wavelengths (section 3.2). The method also relies on the assumption that turbulent mixing does not seriously affect the traveling waves within the network; i.e., the observed waves cannot be too dirty.

3.4. Challenging Observational Issues in Understanding Wave-Turbulence Interactions

Use of existing observational techniques to improve understanding of wave-turbulence interactions in the SABL has not been fully exploited. Most of the observations so far are from ground-based measurements at isolated locations. There have been only a small number of adequate horizontal networks of turbulence measurements and rare research aircraft observations of the SABL [e.g., *Belušić and Mahrt*, 2008].

The wind dispersion relation has not been fully explored due to difficulty in obtaining wave numbers with a limited number of barometers. To capture waves with different wave vectors and wavelengths, an optimal use of a fixed number of microbarographs may involve variable spacing across the network. In addition, long-term measurements (longer than several months) at many levels would provide a better opportunity to partially separate various atmospheric influences on waves in the SABL.

To understand intermittent turbulence associated with wave-turbulence interactions, observations of spatial and temporal variations of turbulence as well as wave motions are needed. Surface networks of sonic anemometers have not been specifically configured to examine wave motions near the surface. Because of the difficulty to obtain high-resolution spatial observations, calculating spatial derivatives of any variable with a fixed-point network is almost impossible. The spatial requirement for observing low-frequency and standing IGWs of 1–30 min periods for several cycles may require a costly extension of the network to larger scales. Major progress toward such understanding requires 3-D observations with a considerable number of sensors or new instrumentation and new network configuration strategies.

Frequent measurements of the vertical atmospheric structure above a typical tower height for identifying characteristics and potential sources of wave motions are important but are generally not available. Theoretically, wave-turbulence interactions may modulate the velocity and density profiles, which influences the production of the TKE and TPE in the SABL. Frequent observations of the atmospheric structure may be useful to detect initiation of wave motions even with the linear theory. Conventional aircraft are generally unable to fly sufficiently low to study the shallow SABL even when there is sufficient light. Remote sensing tools discussed in this section provide valuable information on wave-turbulence interactions spatially and temporally. However, interpretation of remote sensing images requires better understanding of wave evolution, wave-turbulence interactions, and the influence of anisotropic turbulence on remote sensing signals. Therefore, a good colocated in situ and remote sensing 3-D network may be necessary to establish reliable and quantifiable complimentary observations of wave-turbulence interactions.

Overall, turbulence and potential wave generation mechanisms are abundant in the SABL. Wave-turbulence interactions in the SABL provide challenges, but becoming-available new tools provide observational capabilities to probe waves, turbulence, vortices, and their interactions in the SABL, which is relatively easy to access compared to the upper atmosphere and oceans. Thus, the observational investigation in the SABL contributes

to understanding of wave-turbulence interactions in general geophysical flows and provides databases for validating wave and turbulence theories and parameterizations for numerical models.

4. Parameterization of Waves and Wave-Turbulence Interactions

The current literature on parameterization of waves and wave-turbulence interactions in the SABL is sparse. Due to the significant impact of waves in large-scale circulation models, most of the literature on wave parameterizations, particularly for IGWs, focuses on the upper atmosphere, where temporal variations of wind and stability profiles are relatively small. However, many recent investigations have found that IGWs in the free troposphere are influenced by the ABL (section 3); interactions between the ABL and the free troposphere have been demonstrated in a global atmospheric model [*Kim and Hong*, 2009]. A few attempts to devise parameterizations of IGWs in the SABL have been based on linear inviscid IGW theory. *Steeneveld et al.* [2008] explained the ad hoc enhancement of turbulence in current parameterization schemes caused by failing to account for IGWs in the calculations of turbulence fluxes. Thus, accounting for unresolved IGWs and their effects on the SABL in numerical models is still a challenging issue for the community.

Numerical model prediction errors can generally be attributed to deficiencies in model initialization, physics, numerical methods, and grid resolution [e.g., *Stauffer*, 2012]. The same error sources also contribute to the challenges that we are facing for modeling wave-turbulence interactions in the SABL. The model grid spacing decreases as the computer power increases, which means that many previously unresolved phenomena become, in principle, resolvable by numerical models. Although certain submeso motions may be reproducible by models [*Seaman et al.*, 2012; *Suarez and Stauffer*, 2014], recent studies suggest that some important physics may still be missing in models for proper representation of observed irregular wavelike features regardless of the model grid spacing [e.g., *Belušić and Güttler*, 2010; *Güttler and Belušić*, 2012; *Luhar and Hurley*, 2012]. For relatively large terrain slopes and curvatures, the full momentum and scalar flux tensors need to be included in the boundary condition in finite-difference models [*Epifanio*, 2007]. This suggests that proper parameterizations of small-scale nonturbulent variability are needed until well into the future even with increasing development of numerical models and computational resources.

4.1. Wave Parameterization in Numerical Models

Attempts to parameterize waves have been concentrated on a few types of waves mentioned in the previous sections. Wave stress from terrain-induced stationary IGWs has been parameterized based on linear wave theory with the wave saturation in place so that IGWs with finite amplitude can be achieved. *Nappo et al.* [2004] developed a parameterization of IGW stress generated by subgrid-scale topography for single-column models and emphasized the importance of the vertical grid spacing in obtaining wave breaking. *Steeneveld et al.* [2008] developed a formulation for the terrain-induced wave drag in the SABL for large-scale models and applied it to a column model. They found that the wave stress adds to the total drag to the atmosphere. The resulting enhanced drag can prevent the unrealistic runaway cooling in the model without using the long-tail formula in the SABL turbulence parameterization scheme. Furthermore, the availability of fine-spatial-resolution global topography allows for a very detailed subgrid treatment of these terrain-induced waves. Therefore, parameterization of terrain-induced stationary waves in numerical models, although neither fully satisfactorily parameterized nor as yet implemented in any numerical model, seems to be achievable in the near future [e.g., *Nappo and Svensson*, 2008]. The effects of form drag due to unresolved orography have also been parameterized through effective roughness length [*Wood et al.*, 2001].

Most terrain wave drag is effectively obtained by assuming interactions between unidirectional flow and terrain. IGW parameterization over realistic terrain with vertically varying wind direction becomes complex [*Shutts*, 1995]. Wind direction variations with height over realistic terrain may lead to critical level wave absorption at all heights for some portion of the wave spectrum. Numerically resolved wave motions depend on characteristics of terrain and model resolutions.

Observations of canopy waves are relatively well documented [e.g., *Lee et al.*, 1997; *van Gorsel et al.*, 2011], and their generation has been theoretically investigated [e.g., *Pulido and Chimonas*, 2001; *Hu et al.*, 2002]. The parameterization of canopy waves is considered intermediately complex for implementation in numerical models because its theory is not as solid and simple as for the terrain-induced IGWs. In addition, the realistic representation of detailed characteristics of canopy in numerical models is more difficult than that for complex terrain.

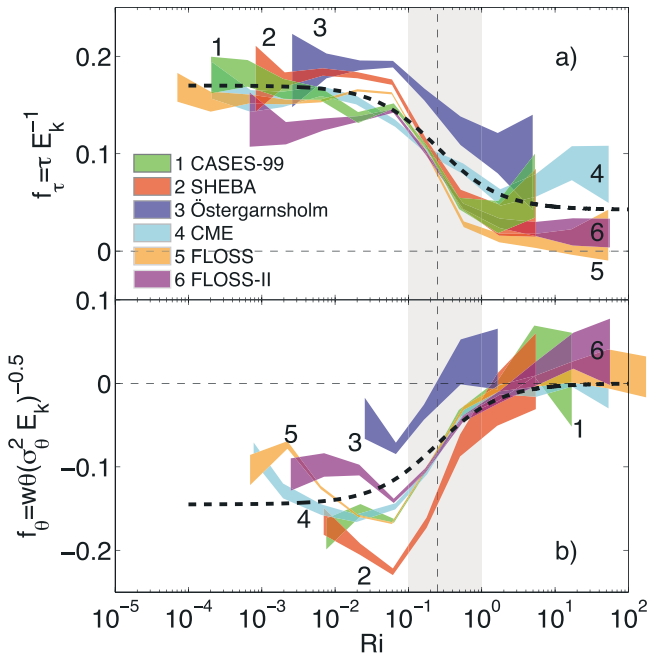

Figure 4. Nondimensionalized fluxes of (a) momentum and (b) heat, as functions of *Ri* for six observational field data sets. The shaded areas show 95% confidence intervals on the binned mean. The thick dash lines are empirical fits. The vertical thin dashed line and the shaded area show $Ri = 0.25$ and the interval $0.1 < Ri < 1$ where the transition between strong and weak turbulent mixing occurs (modified after *Mauritsen and Svensson* [2007, Figure 3] ©American Meteorological Society, used with permission).

Parameterizations of complex but known wave generation mechanisms pose challenges too. Recently observed temperature oscillations in a surface cold pool and surface wind direction shifts as a result of topographic IGWs and a rotor circulation have been reasonably reproduced by using the Weather Research and Forecasting (WRF) model with a fine mesoscale model resolution (444 m horizontal grid spacing and 10 layers in the lowest 50 m ABL) and modifications of the Mellor-Yamada-Janjic turbulence parameterization scheme [*Suarez and Stauffer*, 2014]. The enhanced downward mixing associated with the rotor circulation produced a short-term, local warming within the cold pool, leading to an observed near-surface wind direction shift of almost 180°. Observations and the modified WRF model were used with a variety of atmospheric conditions within a valley and demonstrated that waves above the SABL contribute to the submeso motions in the SABL [*Suarez and Stauffer*, 2014; *Wendoloski et al.*, 2014; *Hoover et al.*, 2015].

4.2. Prospects for Parameterization of Wave-Turbulence Interactions in the SABL

4.2.1. Current Approaches for Parameterization of Wave-Turbulence Interactions in the SABL

Currently, several parameterization schemes for the SABL attempt to include both waves and turbulence. One example is given by *Mauritsen et al.* [2007] based on the idea of the total turbulence energy balance (section 2.3.1). They used surface observations from six field experiments and developed relationships between momentum and heat fluxes as functions of *Ri* (Figure 4), where contribution from both breaking waves and turbulence may be included. In addition, they used LES results to formulate the mixing length beyond the surface layer where Monin-Obukhov similarity theory (MOST) is considered valid. This approach represents improvement in the framework of the Reynolds-averaged Navier-Stokes (RANS) equation.

Another example is a spectral model, which is coined quasi-normal scale elimination (QNSE) [*Sukoriansky and Galperin*, 2005; *Sukoriansky et al.*, 2005, 2006; *Galperin and Sukoriansky*, 2010; *Sukoriansky and Galperin*, 2013]. QNSE is based on solving the nonlinear Navier-Stokes and temperature equations in a stably stratified flow through a stochastic approach. High-frequency velocity and temperature fluctuations resulting from nonlinearity of the momentum and temperature equations are considered as a stochastic process. By systematic ensemble averaging of small shells of high wave number velocity and temperature modes, one eliminates these modes from the governing equations and computes the resulting corrections to the viscosity and diffusivity. One of the main products of the QNSE theory are scale-dependent, horizontal and vertical eddy viscosities and eddy diffusivities. Among other results, the nonhydrostatic theory demonstrates the anisotropization of mixing with increasing stable stratification, the modification of the classical dispersion relation of linear internal waves by turbulence (Figure 5), the stability dependence of the Prandtl number, and the nonexistence of Ri_{cr}. The QNSE-based subgrid-scale parameterization can be used in both LES and RANS.

An example of the direct approach to wave-turbulence interactions is the work of *Zilitinkevich et al.* [2009], where the momentum and heat equations of IGWs are explicitly solved and the contribution of momentum flux from IGWs is explicitly added into the total momentum equation in addition to the turbulence

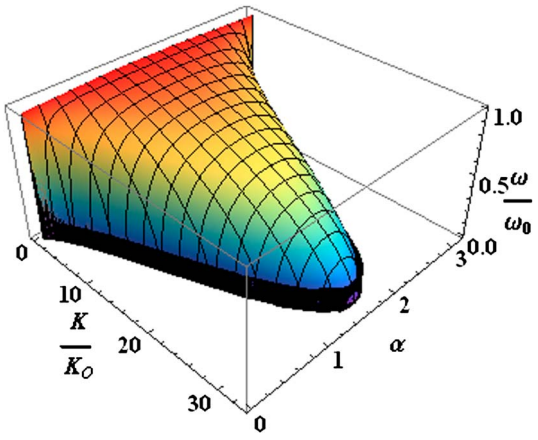

Figure 5. The dispersion relation $\omega(K)$ derived from the QNSE theory. Here $K^2 = k^2 + m^2$, k and m are the horizontal and vertical wave numbers, respectively, K_O is the Ozmidov wave number, $\alpha = \pm\arcsin(m/\sqrt{k^2+m^2})$, $\omega_0 = \pm N\cos\alpha = \pm Nk/\sqrt{k^2+m^2}$ is the classical linear dispersion relation with zero U in (4), and N is the Brunt-Väisälä frequency of the flow. The colors here are for visualization only.

contribution. They also found the flows independent of Ri_{cr} and suggested a contribution of IGWs to momentum fluxes under large Ri conditions.

4.2.2. Improving Higher-Order Turbulence Closure Schemes

There is a need to reinvestigate the higher-order turbulence closure (HOC) parameterization schemes that are typically used nowadays [e.g., *Mellor and Yamada*, 1982]. These HOC schemes, once considered advanced and sophisticated, were developed in the 1970s with the hydrostatic assumption [e.g., *Yamada and Mellor*, 1975; *Yamada*, 1983; *Andrén*, 1990]. The nonhydrostatic effects (besides vertical accelerations), such as vertical variations of the vertical velocity variance, may not be adequately represented by K theory, and yet the first-order closure is not a suitable option in the state-of-the-art nonhydrostatic models [*Yang*, 1991]. Therefore, a nonhydrostatic approach in improving or even redefining HOC schemes and allowing for fully horizontally inhomogeneous flows is necessary to treat inhomogeneous and highly anisotropic turbulent fields in fine-resolution numerical models.

Another problem that goes to the heart of HOC assumptions for refining numerical model resolution is the energy redistribution hypothesis of *Rotta* [1951], which is used in various versions of the Mellor-Yamada schemes [*Mellor and Yamada*, 1982; *Andrén*, 1990]. This assumption pertains to the division of pressure-related terms in the TKE equation into the nonlinear return-to-isotropy part (related to inertial interactions within the turbulence field) and the "rapid" part (due to interactions between turbulence and mean variables). Furthermore, isotropic turbulent eddies at the Kolmogorov scale are assumed to dissipate energy in the HOC schemes so that the TKE dissipation, ϵ, can be parameterized as a function of the ratio between $\mathrm{TKE}^{3/2}$ and a mixing length scale, l. With increasingly refined spatial resolution in numerical models for stratified flows over complex terrain, it is not clear whether such isotropic dissipative eddies exist near the high-frequency end of modeled turbulence spectrum under weak-wind conditions. The Kolmogorov inertial subrange may not be fully realized if the relevant Re is less than 10^4. Nevertheless, *Mellor and Yamada* [1982] claim that the assumptions of the hydrostatic state and the energy redistribution of *Rotta* [1951] are relatively less important for modeling turbulent geophysical flows than defining a suitable, flexible, and robust l. Meanwhile, most l formulations are rather empirical.

4.2.3. Mixing Length Scales

Typically, the height above the surface, z, and l expressed in Obukhov length $L_O = -u_{*0}^3\bar{\theta}_v/(\kappa g\overline{w'\theta'_{v0}})$ (u_{*0} is the surface friction velocity, $\bar{\theta}_v$ is the virtual potential temperature, κ is the Von Karman constant, and $\overline{w'\theta'_{v0}}$ is the surface heat flux) is used for characterizing turbulence near the surface [e.g., *Mahrt et al.*, 2012]. However, often in strongly stratified flows, the turbulent layer near the surface is extremely thin, for example, sometimes it is ≤ 1 m. Under this situation, l is less than z and turbulent eddies are decoupled from the surface. So-called "z-less" formulations for l based on local turbulence rather than surface turbulence have been used. One of these is l_w, which is associated with the Ozmidov length l_O (section 2.3.1). However, σ_w in l_w is not easily obtained from either measurements or benchmark simulations of strongly stratified flows. As a result, σ_w is often parameterized as a function of $\mathrm{TKE}^{1/2}$ in numerical models. Another approach for l in a stably stratified flow is to relate l to σ_θ, where σ_θ is the standard deviation of the potential temperature [*Sorbjan and Balsley*, 2008]. Often, the near-surface turbulence structure is governed by a low-level jet, in which turbulence is transported downward instead of being generated at the surface. In this situation, z or L_O may not be relevant [*van der Avoird and Duynkerke*, 1999]. Introducing σ_θ can incorporate the main effects of the low-level jet and be used to modify L_O [*Grisogono et al.*, 2007]. However, all of the above mentioned approaches for l are designed for specific situations and not for a broad range of stably stratified flows.

Grisogono [2010] attempted to formulate a general l valid for the neutral to stably stratified atmosphere. His proposed l is based on l_w with explicit inclusions of local TKE, wind shear, static stability, turbulent Prandtl number, and Ri. This l, although it has not been thoroughly tested in numerical models, can potentially include wavelike motions. Overall, improvement in formulating a generalized l beyond empirical or dimensional arguments is certainly needed.

4.2.4. Empirical and Stochastic Approaches

To facilitate further understanding of the dynamics, analysis of observations in the literature has concentrated on an ABL that is reasonably well defined in terms of vertical structure and turbulence. Many SABLs include complex interactions between turbulence, short wavelike motions, low-frequency deep waves, and other submeso motions. Waves and other submeso motions may not be separable in many situations.

The submeso motions appear as a stochastic mix, at least with our present understanding and observational techniques. Then stochastic "turbulence" becomes forced by stochastic processes in contrast to stationary SABL processes that obey similarity theory. As examples of stochastic formulation of the forcing, *Farrell and Ioannou* [2008] introduced a stochastic wind field to study the response of sea surface waves, while *Bakas and Ioannou* [2007] examined waves forced by randomly generated temperature and vorticity fluctuations.

Since submeso motions do not seem fully amenable to being obtained deterministically, progress in understanding wave-turbulence interactions could be made through empirical and stochastic parameterizations. For example, the influence of submeso motions on turbulent fluxes could be accounted for when the bulk formula for surface turbulent fluxes is used with a generalized velocity scale, which includes submeso motions [*Mahrt*, 2008]. The drawback of this approach is that the empirical submeso velocity scale does not obey local similarity valid only to equilibrium turbulence and is site dependent and, therefore, may not be universal.

Quantifying model uncertainty related to wave-turbulence interactions in the SABL and applying numerical models to predict atmospheric transport and dispersion of hazardous materials should consider a probabilistic approach using a sufficient number of suitably calibrated ensemble members [e.g., *Kolczynski et al.*, 2009, 2011; *Wendoloski et al.*, 2014]. The ensemble members can be created by varying the model initial conditions, physical parameterizations, and grid resolutions. We should not rely solely on deterministic forecasts for complex interactions between waves and turbulence within the SABL.

4.2.5. Potential Impacts of Parameterized Wave Drags in Large-Scale/Mesoscale Models on Wave-Turbulence Interactions in the SABL

Current wave parameterizations in general circulation models are used to represent the drag produced by unresolved waves at the tropopause and above. These parameterizations are in two categories: one for subgrid-scale orographic IGWs [e.g., *Palmer et al.*, 1986; *McFarlane*, 1987; *Lott and Miller*, 1997] and the other for waves generated by all other sources such as convective and shear instabilities and geostrophic adjustment. The second type is also known as nonorographic wave parameterization [e.g., *Hines*, 1997; *Scinocca*, 2003].

IGWs represented in the nonorographic IGW parameterizations are generally launched between midtroposphere and the tropopause. Therefore, the upward propagating IGWs do not affect the ABL. However, there are two well-known mechanisms that may lead to downward propagating IGWs toward the ABL. One is the reflection of nonhydrostatic waves by the background flow; i.e., reflection of IGWs occurs at a height where $\omega = N + kU$ and $m = 0$. The reflected IGWs were examined by *Scinocca* [2002] using the IGW parameterization developed by *Warner and McIntyre* [1996]. *Scinocca* [2002] found that a significant part of the spectrum is reflected back but he did not explicitly examine the impact of the reflected IGWs on the ABL. Currently, nonorographic wave parameterizations represent only the momentum flux divergence due to wave breaking and its impact on the background flow. However, the effects of wave generation on the background flow may also be important in the ABL. These momentum flux divergences due to wave generation have not been parameterized.

The other mechanism that may lead to downward propagating waves is through the so-called secondary generation, which occurs when an upward propagating primary wave breaks. As the wave breaking produces a sudden localized forcing to the flow, the response of the flow to the wave forcing has two components: a geostrophic mode and inertio-gravity waves [*Scavuzzo et al.*, 1998; *Pulido and Thuburn*, 2005]. These relatively small scale inertio-gravity waves are the so-called secondary waves, which propagate both upward and downward from the forcing region [*Woods and Smith*, 2010]. The importance of these downward propagating secondary waves for the ABL momentum budget is as yet unknown and needs to be further investigated.

Current subgrid-scale orographic parameterizations account for low-level drag [*Lott and Miller*, 1997]. The parameterization, which is operational in the European Centre for Medium-Range Weather Forecasts and the Laboratoire de Météorologie Dynamique Zoom models, represents two drag mechanisms: one is produced by the low-level flow blocked by the subgrid-scale orography and the other is produced by the flow over the subgrid orography, which generates upward propagating IGWs. Comparing the drag resulting from this scheme with the measured pressure drag, *Lott and Miller* [1997] concluded that the form drag contributes significantly to the total mountain drag and improves the overall agreement with the drag obtained from the measurements.

4.2.6. Improving ABL Parameterizations Using Data Assimilation

Current parameterization of the ABL requires a number of parameters that cannot be directly measured, such as Ri_{cr} and eddy diffusivities. Objectively optimizing the values of these unknown parameters from observations may improve the accuracy of the ABL schemes. A recent review of data assimilation techniques for parameter estimation shows that the forecast skill of atmospheric models may be improved by optimizing parameters of the physical schemes [*Ruiz et al.*, 2013].

Hu et al. [2010] applied an ensemble Kalman filter technique to estimate two parameters in the ABL scheme of the asymmetric convective model (version 2), which is implemented in WRF deterministic forecasts. The two parameters—the turbulence eddy diffusivity for the daytime ABL and Ri_{cr} for the nighttime SABL—were chosen as a result of a previous sensitivity study [*Nielsen-Gammon et al.*, 2010] and were updated through assimilation of wind profile observations. *Hu et al.* [2010] showed that the parameter optimization provides more realistic wind profiles as a result of improved momentum mixing in the ABL. *Tandeo et al.* [2015] also applied an ensemble Kalman filter technique to estimate optimal parameters for the subgrid-scale orographic parameterization developed by *Lott and Miller* [1997]. Parameters related to the form drag (at the critical mountain height) and the wave drag (the amplitude factor is related to the mountain sharpness and Ri_{cr}) can be optimized using data assimilation. They also showed that data assimilation techniques are useful to determine which parameters of the subgrid-scale orographic parameterization should be changed when the model or orography resolution is changed.

Data assimilation techniques may also be helpful in determining the model error related to unresolved or underresolved processes in an atmospheric model. *Pulido and Thuburn* [2005, 2008] applied a variational data assimilation technique to determine the missing momentum forcing due to unresolved waves in the stratosphere. Similarly, the missing momentum flux in the ABL due to unresolved or underresolved waves could be estimated using observations and data assimilation techniques. However, to our knowledge, studies for estimating model errors due to unresolved motions and for combining observations and modeling in the ABL through a variational or ensemble-based data assimilation technique have not yet been conducted.

4.3. Challenges for Waves and Wave-Turbulence Parameterizations in the SABL

Increasingly, observations reveal that the prevalence of propagating wavelike structures in the airflow, which is characteristic of only single to several cycles of sinusoidal or irregular shapes, seems to be often associated with wave-turbulence interactions and turbulence intermittency in the SABL [*Mahrt*, 2011]. These motions are the most difficult to parameterize because their sources, lifetimes, and propagation mechanisms are generally unknown and cannot be treated with a deterministic wave theory. It is unclear whether the turbulent mixing associated with the wave motion can be parameterized as extended turbulence using local vertical gradients of mean variables in the current framework of turbulence parameterizations. It is also unclear whether the mixing length scale, which is one of the weakest elements in most turbulence parameterization schemes, could possibly be extended to include some of the wave effects. Very little has been done so far to define a mixing length that includes both turbulence and wave motions in the SABL. Since wave motions are nonlocal, turbulence generated by wave motions is generally nonstationary and cannot be expected to obey similarity theory [*Finnigan*, 1999]. Even if these wave motions can be included in a deterministic part of the mean flow, turbulence generated by such waves is in approximate equilibrium only if the wave period is large compared to the turbulence adjustment time scale.

Unlike research models, the current state-of-the-art operational mesoscale numerical models have grid spacing too large to capture observed waves or submeso motions and their effects on the SABL [*Grisogono*, 2010]. Currently, the National Centers for Environmental Prediction is running the High-Resolution Rapid Refresh model with a 3 km horizontal grid spacing and a ~20 m deep lowest layer. Both growing misgivings in applying MOST to the highly nonstationary SABL and the inadequacy of the target model resolution for future

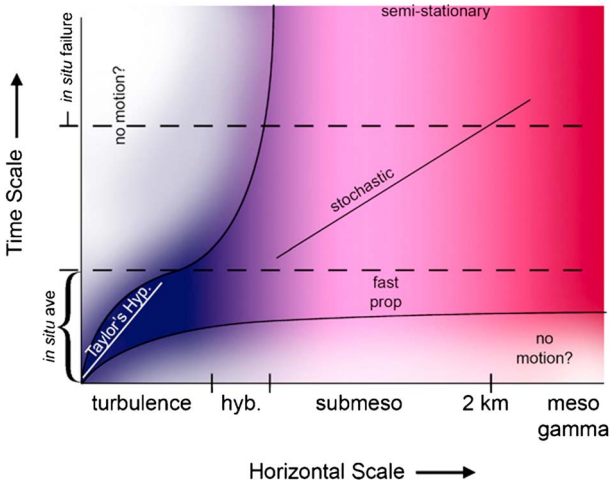

Figure 6. A schematic of the scale regimes for transport near the surface in weak-wind stable conditions. Hybrid motions ("hyb") do not have all the characteristics of turbulence, for example, the initial stage of shear instability or nonlinear wave-wave interactions. "In situ failure" denotes the difficulty of measuring vertical velocity variations on larger time scales. "In situ ave" identifies the range of time scales included in the turbulence flux calculation, which varies substantially between studies. The dark blue color represents the turbulence, while lighter and red colors denote nonturbulent motions. The overlap of color points to the unclear boundary between the turbulence and submeso motions [after *Mahrt*, 2010b] (with permission from Elsevier).

numerical weather prediction and ensemble systems to resolve waves in the SABL imply that the effects of submeso motions and wave-turbulence interactions will need to be parameterized far into the future.

Another important parameterization issue relates to the variable horizontal and vertical resolutions in numerical models. Resolving part of wave motions in high-resolution models introduces different problems compared to climate and other low-resolution models, which rely on a bulk parameterization for the entire ABL [e.g., *Wyngaard*, 2004]. It is not yet clear whether it is better to increase the vertical resolution near the surface for partially resolved small-scale features, such as shallow cold pools in the SABL, or to treat the layer below the lowest model level at a coarse resolution with a bulk parameterization. It has been shown that predicting weak surface winds and shallow drainage flows in the SABL requires much finer resolutions than currently used in operational and research mesoscale models [*Seaman et al.*, 2012; *Hoover et al.*, 2015]. A finer vertical resolution would also be useful throughout, for example, the "regional SABL" of a valley where waves are produced and interact with turbulence. However, it may be very difficult to develop a parameterization when some but not all of the wave submeso motions are actually being resolved in numerical models.

Currently, even exploratory research models provide only limited insights into the characteristics of submeso motions, and major progress in the near future will probably have to rely on field observations [*Hoover et al.*, 2015]. However, the differences between the usual field experiment setup and the nature of numerical models limit the applicability of observational analyses for parameterization development. Measurements of small-scale processes are usually obtained at a single point on a tower, which only represents the land-atmosphere interaction within the footprint of the tower [e.g., *Cai et al.*, 2010], while variables at each model grid point represent volume-averaged quantities. Taylor's hypothesis for interpreting spatial structures from time series is not valid for submeso motions, especially with weak winds [e.g., *Mahrt et al.*, 2009]. The mean wind itself might not be a relevant velocity scale for very weak winds [e.g., *Mahrt*, 2008]. Therefore, relating the observed time series from single-point measurements to the horizontal space scale is generally not achievable in the SABL (Figure 6). It is impossible to quantify the effects of spatial features of subgrid phenomena from single-point measurements because the spatial scale of subgrid features cannot be precisely determined. A lack of spatial observations limits our current ability to parameterize subgrid submeso phenomena. New model verification methods for submeso motions are also needed [e.g., *Belušić and Güttler*, 2010; *Suarez et al.*, 2014].

Various nonorographic wave parameterization schemes have been developed for the free atmosphere above the ABL. Similar wave generation mechanisms are abundant in the SABL, but their parameterization is lacking. *Hasha et al.* [2008] demonstrated the importance of horizontally inhomogeneous effects of waves on the ambient flow, suggesting that parameterization of waves based on a single-column approach may not be good enough for large-scale circulation models. To investigate intermittent turbulence, spatial and temporal variations of wave motions are particularly important; therefore, parameterization of spatially varying waves in the SABL is a further challenge.

5. Summary

We have reviewed theories, observations, and numerical parameterizations that are relevant to wave-turbulence interactions in stably stratified flows with a focus on the SABL. There is still a lack of understanding of the evolution of wave dynamics in geophysical flows, partly due to inadequacy of existing observations. Although wave motions may not be the only submeso motions that impact intermittent turbulence in the SABL, considering the favorable conditions for wave motions in the SABL and a large body of wave theories, understanding wave-turbulence interactions can lead us to improve our understanding of turbulence intermittency in the SABL.

Theoretical wave studies have progressed significantly from the linear inviscid wave theories of the 1970s. Increasingly, theoretical wave studies include nonlinearity and interactions among turbulence, waves, and background flows. However, physical understanding of wave generation and evolution in the turbulent atmosphere beyond mathematical modes is still lacking. Part of the issue is the lack of understanding of generation of turbulence and 3-D vortical motions of various scales under stably stratified conditions. In reality, waves, turbulence, and 3-D vortical motions are closely related. Applying conservation laws such as energy and momentum balances would add constraints in such a complex environment. Generation processes for waves, turbulence, and possibly vortical motions in the stably stratified environment are related. Improved understanding of their interactions is critical for weather and environmental forecasts.

Limited observations suggest that turbulent mixing occurs in spatially and temporally localized intermittent patches and waves are common in the SABL. Due to a lack of theoretical guidance for wave motions in a turbulent environment, most observations are compared to linear inviscid wave theory even though assumptions used in the linear derivations are not valid in nature. Furthermore, observational investigations of wave-turbulence interactions are currently constrained by limited spatial coverage of observations, which hampers our investigation of wave number-frequency relationships of wave motions in the atmosphere. To investigate wave-turbulence interactions, a large number of affordable instruments are required for adequate temporal and spatial coverages, preferably in three dimensions. Future observations should consider networks of measurements on spatial scales suitable for studying wave motions and possible vortices and on time scales suitable for studying the role of turbulence in wave-turbulence interactions. Observations of vertical structure of wave motions and turbulence above a typical tower height could also provide important information for understanding generation of waves and turbulence and their interactions and yet are often not available, especially for the vertical structure of turbulence. With improved technology, spatial and temporal observation networks need to take advantage of both ground and airborne platforms and both in situ and remote sensing techniques.

Increasing computing power leads to higher-resolution numerical studies of wave motions and wave-turbulence interactions. However, most nonlinear numerical simulations focus on turbulence generation in the interior of the fluid without considering significant impacts of boundaries on wave-turbulence interactions, which is unique for the SABL. The surface provides constraints in the momentum transfer, wave dynamics, and thermodynamics. Currently, numerical models have difficulty simulating SABLs with strong stable stratification partly due to subgrid parameterization. Even the highest-resolution DNS, for which subgrid parameterization is not needed, cannot simulate the SABL due to its low *Re* number compared to the atmosphere. Using state-of-the-art models, careful comparison between observations and numerical model results would extend our understanding of important physical processes of wave-turbulence interactions. Including the effects of submeso motions such as wave motions on turbulence may improve numerical parameterization of intermittent turbulence in the SABL.

Overall, understanding wave-turbulence interactions and intermittent turbulence largely relies on observations for validation. A focused field experiment to investigate wave-turbulence interactions in the SABL should be doable and is crucial for advancing our understanding of waves, turbulence, and vortices in geophysical flows. Observations of wave formation and propagation and wave-turbulence interactions can also inspire more refined theoretical wave studies with more realistic conditions. With better understanding of wave-turbulence interactions, improving subgrid parameterization is possible. Due to the need for more complete spatial and temporal coverage for the required observations, collaborative efforts to aggregate resources and instruments may be necessary. Progress in wave-turbulence interactions in the SABL may also shed light on better understanding of the upper atmosphere and oceans, where observations are less accessible.

Acknowledgments
The workshop, WINABL, was sponsored by the National Center for Atmospheric Research (NCAR), Geophysical Turbulence Program (GTP). We would like to thank Andreas Muschinski, William Brown, Steve Cohn, Donald Lenschow, Sergej Zilintinkevich, and two reviewers for their helpful comments on this review. The University Corporation for Atmospheric Research manages NCAR under sponsorship by the National Science Foundation. Any opinions, findings and conclusions, or recommendations expressed in this publication are those of the authors and do not necessarily reflect the views of the NSF.

The Editor for this paper was Alan Robock. He thanks Sergei Zilitinkevich and two anonymous reviewers for their review assistance with this manuscript.

References

Abarbanel, H., D. Holm, J. Marsden, and T. Ratiu (1984), Richardson number criterion for the nonlinear stability of three-dimensional stratified flow, *Phys. Rev. Lett.*, *52*, 2352–2355.
Achatz, U. (2007), Gravity-wave breaking: Linear and primary nonlinear dynamics, *Adv. Space Res.*, *40*, 719–733.
Alexander, M. J., et al. (2010), Recent developments in gravity-wave effects in climate models and the global distribution of gravity-wave momentum flux from observations and models, *Q. J. R. Meteorol. Soc.*, *136*, 1103–1124.
Almalkie, S., and S. de Bruyn Kops (2012), Kinetic energy dynamics in forced, homogeneous, and axisymmetric stably stratified turbulence, *J. Turbulence*, *13*, N29, doi:10.1080/14685248.2012.702909.
Anderson, P. (2003), Fine-scale structure observed in a stable atmospheric boundary layer by sodar and kite-borne tethersonde, *Boundary Layer Meteorol.*, *107*, 323–351.
Anderson, P. S., J. C. K. S. D. Mobbs, I. McConnell, and J. M. Rees (1992), A microbarograph for internal gravity wave studies in Antarctica, *Antarctica Sci.*, *4*(2), 241–248.
Andreas, E. L. (2002), Parameterizing scalar transfer over snow and ice: A review, *J. Hydrol.*, *3*, 417–432.
Andrén, A. (1990), Evaluation of a turbulence closure scheme suitable for air-pollution applications, *J. Appl. Meteorol.*, *29*, 224–239.
Angevine, W. M., S. Avery, and G. Kok (1993), Virtual heat flux measurements from a boundary-layer profiler-RASS compared to aircraft measurements, *J. Appl. Meteorol.*, *32*(12), 1901–1907.
Atlas, D., J. Metcalf, J. Richter, and E. Gossard (1970), The birth of "CAT" and microscale turbulence, *J. Atmos. Sci.*, *27*, 903–913.
Baines, P. G. (1995), *Topographic Effects in Stratified Flows*, 482 pp., Cambridge Univ. Press, New York.
Bakas, N. A., and P. J. Ioannou (2007), Momentum and energy transport by gravity waves in stochastically driven stratified flows. Part I: Radiation of gravity waves from a shear layer, *J. Atmos. Sci.*, *64*, 1509–1529.
Baklanov, A., B. Grisogono, R. Bornstein, L. Mahrt, S. Zilitinkevich, P. Taylor, S. Larsen, M. Rotach, and H. Fernando (2011), The nature, theory and modeling of atmospheric planetary boundary layers, *Bull. Am. Meteorol. Soc.*, *92*, 123–128.
Balachandran, N. K. (1980), Gravity waves from thunderstorms, *Mon. Weather Rev.*, *108*, 804–816.
Balsley, B., D. Fritts, R. Frehlich, M. Jones, S. Vadas, and R. Coulter (2002), Up-gully flow in the Great Plains region: A mechanism for perturbing the nighttime lower atmosphere, *Geophys. Res. Lett.*, *29*, 1931, doi:10.1029/2002GL015435.
Balsley, B. B. (2008), The CIRES Tethered Lifting System: A survey of the system, past results and future capabilities, *Acta Geophys.*, *56*(1), 21–57.
Balsley, B. B., M. L. Jensen, and R. G. Frehlich (1998), The use of state-of-the-art kites for profiling the lower atmosphere, *Boundary Layer Meteorol.*, *87*(1), 1–25.
Bange, J., et al. (2013), Measurement of aircraft state and thermodynamic and dynamic variables, in *Airborne Measurements for Environmental Research: Methods and Instruments*, edited by M. Wendisch and J.-L. Brenguier, pp. 7–75, John Wiley, Weinheim, Germany.
Banta, R., Y. Pichugina, and W. Brewer (2006), Turbulent velocity-variance profiles in the stable boundary layer generated by a nocturnal low-level jet, *J. Atmos. Sci.*, *63*, 2700–2719.
Bean, B. R. (1971), Comparisons of remote and in situ measurements of meteorological parameters and processes, in *Statistical Methods and Instrumentation in Geophysics*, edited by A. G. Kjelaas, pp. 181–196, Teknologisk Forlag, Oslo.
Beare, R., et al. (2006), An intercomparison of large-eddy simulations of the stable boundary layer, *Boundary Layer Meteorol.*, *118*, 247–272.
Belcher, S. E., I. N. Harman, and J. J. Finnigan (2012), The wind in the willows: Flows in forest canopies in complex terrain, *Annu. Rev. Fluid Mech.*, *44*, 479–504.
Beljaars, A. (2011), The stable boundary layer in the ECMWF model, in *ECMWF GABLES Workshop on Diurnal Cycles and the Stable Boundary Layer*, pp. 1–10, ECMWF, Shinfield Park, Reading, Berks, U. K.
Belušić, D., and I. Güttler (2010), Can mesoscale models reproduce meandering motions?, *Q. J. R. Meteorol. Soc.*, *136*, 553–565.
Belušić, D., and L. Mahrt (2008), Estimation of length scales from mesoscale networks, *Tellus*, *60a*, 706–715.
Belušić, D., and L. Mahrt (2012), Is geometry more universal than physics in atmospheric boundary layer flow?, *J. Geophys. Res.*, *117*, D09115, doi:10.1029/2011JD016987.
Belušić, D., D. Lenschow, and N. Tapper (2014), Performance of a mobile car platform for mean wind and turbulence measurements, *Atmos. Meas. Tech.*, *7*(6), 1825–1837.
Billant, P., and J.-M. Chomaz (2000), Experimental evidence for a new instability of a vertical columnar vortex pair in a strongly stratified fluid, *J. Fluid Mech.*, *418*, 167–188.
Billant, P., and J.-M. Chomaz (2001), Self-similarity of strongly stratified inviscid flows, *Phys. Fluids*, *13*, 1645–1651.
Billant, P., A. Deloncle, J.-M. Chomaz, and P. Otheguy (2010), Zigzag instability of vortex pairs in stratified and rotating fluids. Part 2: Analytical and numerical analyses, *J. Fluid Mech.*, *660*, 396–429.
Blumen, W. (1972), Geostrophic adjustment, *Rev. Geophys. Space Phys.*, *10*, 485–528.
Blumen, W., R. Banta, S. Burns, D. Fritts, R. Newsom, G. Poulos, and J. Sun (2001), Turbulence statistics of a Kelvin-Helmholtz billow event observed in the nighttime boundary layer during the Cooperative Atmospheric-Surface Exchange Study field program, *Dynam. Atmos. Oceans*, *34*, 189–204.
Böhme, T., T. Hauf, and V. Lehmann (2004), Investigation of short-period gravity waves with the Lindenberg 482 MHz tropospheric wind profiler, *Q. J. R. Meteorol. Soc.*, *130*, 2933–2952.
Bonin, T., P. Chilson, B. Zielke, and E. Fedorovich (2013), Observations of the early evening boundary-layer transition using a small unmanned aerial system, *Boundary Layer Meteorol.*, *146*, 119–132.
Booker, D. R., and L. W. Cooper (1965), Superpressure balloons for weather research, *J. Appl. Meteorol.*, *4*, 122–129.
Booker, J. R., and F. P. Bretherton (1967), The critical layer for internal gravity waves in a shear flow, *J. Fluid Mech.*, *27*(3), 513–539.
Bretherton, F. (1966), The propagation of groups of internal gravity waves in a shear flow, *Q. J. R. Meteorol. Soc.*, *92*(394), 466–480.
Brown, A. R., M. Athanassiadou, and N. Wood (2003), Topographically induced waves within the stable boundary layer, *Q. J. R. Meteorol. Soc.*, *129*, 3357–3370.
Brown, E. H., and F. F. Hall (1978), Advances in atmospheric acoustics, *Rev. Geophys.*, *16*(1), 47–110.
Brown, R. (1972), On the inflection point instability of a stratified Ekman boundary layer, *J. Atmos. Sci.*, *29*, 850–859.
Bühler, O. (2009), *Waves and Mean Flows*, 341 pp., Cambridge Univ. Press, New York.
Bühler, O. (2010), Wave-vortex interactions in fluids and superfluids, *Annu. Rev. Fluid Mech.*, *42*, 205–228.
Bulatov, V. V., and Y. V. Vladimirov (2010), Estimate of the applicability limits of a linear theory of internal waves, *Fluid Dyn.*, *45*(5), 787–792.
Burns, S. P., T. W. Horst, L. Jacobsen, P. D. Blanken, and R. K. Monson (2012), Using sonic anemometer temperature to measure sensible heat flux in strong winds, *Atmos. Meas. Tech.*, *5*, 2095–2011.
Busack, B., and B. Brümmer (1988), A case study of Kelvin-Helmholtz waves within an off-shore stable boundary layer: Observations and linear model, *Boundary Layer Meteorol.*, *44*, 105–135.

Busch, N. E. (1973), The surface boundary layer, *Boundary Layer Meteorol.*, *4*(1–4), 213–240.
Cai, X., J. Chen, and R. L. Desjardins (2010), Flux footprints in the convective boundary layer: Large-eddy simulation and Lagrangian stochastic modelling, *Boundary Layer Meteorol.*, *137*, 31–47.
Candelier, J., et al. (2012), Inviscid instability of a stably stratified compressible boundary layer on an inclined surface, *J. Fluid Mech.*, *694*, 524–539.
Canuto, V. M. (2002), Critical Richardson numbers and gravity waves, *Astron. Astrophys.*, *384*, 1119–1123.
Carpenter, J. R., E. W. Tedford, E. Heifetz, and G. A. Lawrence (2013), Instability in stratified shear flow: Review of a physical interpretation based on interacting waves, *Appl. Mech. Rev.*, *64*, 60,801.
Carter, D., K. Gage, W. Ecklund, W. Angevine, P. Johnston, A. Riddle, J. Wilson, and C. Williams (1995), Developments in UHF lower tropospheric wind profiling at NOAA's Aeronomy Laboratory, *Radio Sci.*, *30*(4), 977–1001.
Case, K. M. (1960a), Stability of inviscid plane Couette flow, *Phys. Fluids*, *3*, 143–148.
Case, K. M. (1960b), Stability of an idealized atmosphere: I. Discussion of results, *Phys. Fluids*, *3*, 149–154, doi:10.1063/1.1706011.
Caughey, S. (1977), Boundary-layer turbulence spectra in stable conditions, *Boundary Layer Meteorol.*, *11*, 3–14.
Caughey, S., and C. Readings (1975), An observation of waves and turbulence in the Earth's boundary layer, *Boundary Layer Meteorol.*, *9*, 279–296.
Chemel, C., C. Staquet, and Y. Largeron (2009), Generation of internal gravity waves by a katabatic wind in an idealized alpine valley, *Meteorol. Atmos. Phys.*, *103*, 187–194.
Cheong, B., R. Palmer, T. Yu, K. Yang, M. Hoffman, S. Frasier, and F. Lopez-Dekker (2008), Effects of wind field inhomogeneities on Doppler beam swinging revealed by an imaging radar, *J. Atmos. Oceanic Tech.*, *25*(8), 1414–1422.
Cheung, T. K., and C. G. Little (1990), Meteorological tower, microbarograph array, and sodar observations of solitary-like waves in the nocturnal boundary layer, *J. Atmos. Sci.*, *47*, 2516–2536.
Chimonas, G. (1972), The stability of a coupled wave-turbulence system in a parallel shear flow, *Boundary Layer Meteorol.*, *2*, 444–452.
Chimonas, G. (1974), Considerations of the stability of certain heterogeneous shear flows including some inflexion-free profiles, *J. Fluid Mech.*, *65*(1), 65–69.
Chimonas, G. (2002), On internal gravity waves associated with the stable boundary layer, *Boundary Layer Meteorol.*, *102*, 139–155.
Chimonas, G. (2003), Pressure gradient amplification of shear instabilities in the boundary layer, *Dyn. Atmos. Oceans*, *37*, 131–145.
Chimonas, G., and J. R. Grant (1984), Shear excitation of gravity waves. Part I: Modes of a two-scale atmosphere, *J. Atmos. Sci.*, *41*, 2269–2277.
Chimonas, G., and C. Hines (1986), Doppler ducting of atmospheric gravity waves, *J. Atmos. Sci.*, *91*(D1), 1219–1230.
Chimonas, G., and C. J. Nappo (1987), A thunderstorm bow wave, *J. Atmos. Sci.*, *44*, 533–541.
Cho, J. Y. N., R. E. Newell, and J. D. Barrick (1999), Horizontal wavenumber spectra of winds, temperature, and trace gases during the Pacific Exploratory Mission: 2. Gravity waves, quasi-two-dimensional turbulence, and vortical modes, *J. Geophys. Res.*, *104*(D13), 16,297–16,308.
Christie, D. R. (1989), Long nonlinear waves in the lower atmosphere, *J. Atmos. Sci.*, *46*, 1462–1491.
Christie, D. R., K. J. Muirhead, and A. L. Hales (1978), On solitary waves in the atmosphere, *J. Atmos. Sci.*, *35*, 805–825.
Christie, D. R., K. J. Muirhead, and R. H. Clarke (1981), Solitary waves in the lower atmosphere, *Nature*, *293*, 46–49.
Churilov, S. (2005), Stability analysis of stratified shear flows with a monotonic velocity profile without inflection points, *J. Fluid Mech.*, *539*, 25–55.
Churilov, S. (2008), Stability analysis of stratified shear flows with a monotonic velocity profile without inflection points. Part 2: Continuous density variation, *J. Fluid Mech.*, *617*, 301–326.
Churilov, S. M., and I. G. Shukhman (1996), The nonlinear critical layer resulting from the spatial or temporal evolution of weakly unstable disturbances in shear flows, *J. Fluid Mech.*, *318*, 189–221.
Clark, H. A., and B. R. Sutherland (2010), Generation, propagation, and breaking of an internal wave beam, *Phys. Fluids*, *22*, 076601. doi:10.1063/1.3455432.
Cohn, S. A., C. L. Holloway, S. P. Oncley, R. J. Doviak, and R. J. Lataitis (1997), Validation of a UHF spaced antenna wind profiler for high-resolution boundary layer observations, *Radio Sci.*, *32*(3), 1279–1296.
Cohn, S. A., W. Brown, C. Martin, M. Susedik, G. Maclean, and D. Parsons (2001), Clear air boundary layer spaced antenna wind measurement with the Multiple Antenna Profiler (MAPR), *Ann. Geophys.*, *19*(8), 845–854.
Coleman, T. A., K. R. Knupp, and D. Herzmann (2009), The spectacular undular bore in Iowa on 2 October 2007, *Mon. Weather Rev.*, *137*, 495–503.
Corby, G. A. (1957), A preliminary study of atmospheric waves using radiosonde data, *Q. J. R. Meteorol. Soc.*, *83*(355), 49–60.
Coulter, R. (1990), A case study of turbulence in the stable nocturnal boundary layer, *Boundary Layer Meteorol.*, *52*, 75–91.
Coulter, R., and M. Kallistratova (2004), Two decades of progress in SODAR techniques: A review of 11 ISARS proceedings, *Meteorol. Atmos. Phys.*, *85*(1–3), 3–19.
Coulter, R., and T. Martin (1986), Results from a high-power, high-frequency sodar, *Atmos. Res.*, *20*(2), 257–269.
Culf, A. D., and J. F. R. McIlveen (1993), Acoustic observation of the peripheral Antarctic boundary layer, in *Waves and Turbulence in Stably Stratified Flows*, edited by S. D. Mobbs and J. C. King, pp. 139–154, Clarendon Press, Oxford, U. K.
Curry, M. J., and R. C. Murty (1974), Thunderstorm-generated gravity waves, *J. Atmos. Sci.*, *31*, 1402–1408.
Cuxart, J., G. Morales, E. Terradellas, and C. Yagüe (2002), Study of coherent structures and estimation of the pressure transport terms for the nocturnal boundary layer, *Boundary Layer Meteorol.*, *105*, 305–328.
Cuxart, J., M. Jiménez, and D. Martínez (2007), Nocturnal meso-beta basin and katabatic flows on a midlatitude island, *Mon. Weather Rev.*, *135*, 918–932.
Davis, P., and W. Peltier (1976), Resonant parallel shear instability in the stably stratified planetary boundary layer, *J. Atmos. Sci.*, *33*(7), 1287–1300.
de Baas, A. F., and A. G. M. Driedonks (1985), Internal gravity waves in a stably-stratified boundary layer, *Boundary Layer Meteorol.*, *31*, 303–323.
De La Torre, A., and P. Alexander (1995), The interpretation of wavelengths and periods as measured from atmospheric balloons, *J. Appl. Meteorol. Clim.*, *34*, 2747–2754.
de Silva, I., H. Fernando, F. Eaton, and D. Hebert (1996), Evolution of Kelvin-Helmholtz billows in nature and laboratory, *Earth Planetary Sci. Lett.*, *143*, 217–231.
Deng, A., N. Seaman, G. Hunter, and D. Stauffer (2004), Evaluation of interregional transport using the MM5-SCIPUFF system, *J. Appl. Meteorol.*, *43*, 1864–1886.
Denholm-Price, J. C. W., and J. M. Rees (1999), Detecting waves using an array of sensors, *Mon. Weather Rev.*, *127*, 57–69.
Dewan, E. M. (1979), Stratospheric wave spectra resembling turbulence, *Science*, *204*(4395), 832–835.

Ditlevsen, P. (2004), *Turbulence and Climate Dynamics*, 349 pp., KøbenhavnsUniversitetKøbenhavns Universitet, Det Natur-og Biovidenskabelige FakultetFaculty of Science, Niels Bohr InstitutetThe Niels Bohr Institute, Is og klimalce and Climate, Copenhagen.
Dohan, K., and B. Sutherland (2003), Internal waves generated from a turbulent mixed region, *Phys. Fluids*, *15*, 488, doi:10.1063/1.1530159.
Dörnbrack, A., and C. J. Nappo (1997), A note on the application of linear wave theory at a critical level, *Boundary Layer Meteorol.*, *82*, 399–416.
Doviak, R. J., and R. Ge (1984), An atmospheric solitary gust observed with a Doppler radar, a tall tower and a surface network, *J. Atmos. Sci.*, *41*, 2559–2573.
Doviak, R. J., S. S. Chen, and D. R. Christie (1991), A thunderstorm-generated solitary wave observation compared with theory for nonlinear waves in sheared atmosphere, *J. Atmos. Sci.*, *48*(1), 87–111.
Doyle, J. D., and Q. Jiang (2006), Observations and numerical simulations of mountain waves in the presence of directional wind shear, *Q. J. R. Meteorol. Soc.*, *132*, 1877–1905.
Drazin, P. G. (1977), On the instability of internal gravity wave, *Proc. R. Soc. London, Ser. A*, *356*, 411–432.
Drazin, P. G. (2002), *Introduction to Hydrodynamic Stability*, 258 pp., Cambridge Univ., New York.
Durran, D. R. (1995), Do breaking mountain waves decelerate the local mean flow?, *J. Atmos. Sci.*, *52*, 4010–4040.
Eaton, F. D., S. A. McLaughlin, and J. R. Hines (1995), A new frequency-modulated continuous wave radar for studying planetary boundary layer morphology, *Radio Sci.*, *30*(1), 75–88.
Eckermann, S. D., and R. A. Vincent (1993), VHF radar observations of gravity-wave production by cold fronts over Southern Australia, *J. Atmos. Sci.*, *50*(6), 786–806.
Ecklund, W. L., D. A. Carter, and B. B. Balsley (1988), A UHF wind profiler for the boundary layer: Brief description and initial results, *J. Atmos. Oceanic Tech.*, *5*(3), 432–441.
Edwards, N. R., and S. D. Mobbs (1997), Observations of isolated wave-turbulence interactions in the stable atmospheric boundary layer, *Q. J. R. Meteorol. Soc.*, *123*, 561–584.
Einaudi, F., and J. J. Finnigan (1993), Wave-turbulence dynamics in the stably stratified boundary layer, *J. Atmos. Sci.*, *50*, 1842–1864.
Einaudi, F., D. Lalas, and G. Perona (1978), The role of gravity waves in tropospheric processes, *Pure Appl. Geophys.*, *117*(4), 627–663.
Einaudi, F., J. Finnigan, and D. Fua (1984), Gravity wave turbulence interaction in the presence of a critical level, *J. Atmos. Sci.*, *41*, 661–667.
Einaudi, F., A. J. Bedard, and J. J. Finnigan (1989), A climatology of gravity waves and other coherent disturbances at the Boulder Atmospheric Observatory during March–April 1984, *J. Atmos. Sci.*, *46*, 303–329.
Eliassen, A., and E. Palm (1960), On the transfer of energy in stationary mountain waves, *Geofysiske Publikasjoner*, *22*, 1–23.
Elliott, J. A. (1972), Microscale pressure fluctuations measured within the lower atmospheric boundary layer, *J. Fluid Mech.*, *53*, 351–383.
Emeis, S. (2011), *Surface-Based Remote Sensing of the Atmospheric Boundary Layer*, 174 pp., Springer, Netherlands.
Engelbart, D., and J. Bange (2002), Determination of boundary-layer parameters using wind profiler/RASS and sodar/RASS in the frame of the LITFASS project, *Theor. Appl. Climatol.*, *73*(1–2), 53–65.
Engelbart, D. A., M. Kallistratova, and R. Kouznetsov (2007), Determination of the turbulent fluxes of heat and momentum in the ABL by ground-based remote-sensing techniques (a review), *Meteorol. Z.*, *16*(4), 325–335.
Eom, J. K. (1975), Analysis of the internal gravity wave occurrence of 19 April 1970 in the Midwest, *Mon. Weather Rev.*, *103*, 217–226.
Epifanio, C. C. (2007), A method for imposing surface stress and heat flux conditions in finite-difference models with steep terrain, *Mon. Weather Rev.*, *135*(3), 906–917.
Epifanio, C. C., and T. Qian (2008), Wave-turbulence interactions in a breaking mountain wave, *J. Atmos. Sci.*, *65*(10), 3139–3158.
Etling, D. (1993), Turbulence collapse in stably stratified flows: Application to the atmosphere, in *Waves and Turbulence in Stably Stratified Flows*, edited by S. D. Mobbs and J. C. King, pp. 1–21, Clarendon Press, Oxford, U. K.
Farrell, B. F., and P. J. Ioannou (2008), The stochastic parametric mechanism for growth of wind-driven surface water waves, *J. Phys. Oceanogr.*, *38*, 862–879.
Fernando, H. (2003), Turbulence patches in a stratified shear flow, *Phys. Fluids*, *15*(10), 3164–3169.
Fernando, H., and J. Hunt (1996), Some aspects of turbulence and mixing in stably stratified layers, *Dyn. Atmos. Oceans*, *23*(1), 35–62.
Fernando, H., and J. C. Weil (2010), Whither the stable boundary layer?—A shift in the research agenda, *Bull. Amer. Meteor. Soc.*, *91*(11), 1475–1484.
Finnigan, J. (1988), Kinetic energy transfer between internal gravity waves and turbulence, *J. Atmos. Sci.*, *45*, 486–505.
Finnigan, J. (1999), A note on wave-turbulence interaction and the possibility of scaling the very stable boundary layer, *Boundary Layer Meteorol.*, *90*, 529–539.
Finnigan, J. (2000), Turbulence in plant canopies, *Agric. For. Meteorol.*, *32*, 519–571.
Finnigan, J., and R. Shaw (2008), Double-averaging methodology and its application to turbulent flow in and above vegetation canopies, *Acta Geophys.*, *56*, 534–561.
Finnigan, J., F. Einaudi, and D. Fua (1984), The interaction between an internal gravity wave and turbulence in the stably-stratified nocturnal boundary layer, *J. Atmos. Sci.*, *41*, 2409–2436.
Finnigan, J. J., R. H. Shaw, and E. G. Patton (2009), Turbulence structure above a vegetation canopy, *J. Fluid Mech*, *637*, 387–424.
Fiorino, S. T., and J. Correia Jr. (2002), Analysis of a mesoscale gravity wave event using empirical orthogonal functions, *Earth Interact.*, *6*(1), 1–19.
Fitzjarrald, D. R., and K. E. Moore (1990), Mechanisms of nocturnal exchange between the rain forest and the atmosphere, *J. Geophys. Res.*, *95*(D10), 16,839–16,850.
Franke, P. M., S. Mahmoud, K. Raizada, K. Wan, D. C. Fritts, T. Lund, and J. Werne (2011), Computation of clear-air radar backscatter from numerical simulations of turbulence: 1. Numerical methods and evaluation of biases, *J. Geophys. Res.*, *116*, D21101, doi:10.1029/2011JD015895.
Frehlich, R., Y. Meillier, M. L. Jensen, and B. Balsley (2003), Turbulence measurements with the CIRES tethered lifting system during CASES-99: Calibration and spectral analysis of temperature and velocity, *J. Atmos. Sci.*, *60*(20), 2487–2495.
Frisch, U. (1995), *Turbulence: The Legacy of A. N. Kolmogorov*, 296 pp., Cambridge Univ. Press, New York.
Fritts, D., T. Palmer, o. Andereassen, and I. Lie (1996), Evolution and breakdown of Kelvin-Helmholtz billows in stratified compressible flows. Part I: Comparison of two- and three-dimensional flows, *J. Atmos. Sci.*, *53*, 3173–3212.
Fritts, D., L. Wang, and J. Werne (2009), Gravity wave-fine structure interactions: A reservoir of small-scale and large-scale turbulence energy, *Geophys. Res. Lett.*, *36*, L19805, doi:10.1029/2009GL039501.
Fritts, D. C. (1979), The excitation of radiating waves and Kelvin-Helmholtz instabilities by the gravity wave-critical level interaction, *J. Atmos. Sci.*, *36*, 12–23.
Fritts, D. C. (1989), A review of gravity wave saturation processes, effects, and variability in the middle atmosphere, *Pure Appl. Geophys.*, *130*(2–3), 343–371.

Fritts, D. C., and M. J. Alexander (2003), Gravity wave dynamics and effects in the middle atmosphere, *Rev. Geophys.*, *41*(1), 1003, doi:10.1029/2001RG000106.
Fritts, D. C., and M. A. Geller (1976), Viscous stabilization of gravity wave critical level flows, *J. Atmos. Sci.*, *33*, 2276–2284.
Fritts, D. C., and Z. Luo (1992), Gravity wave excitation by geostrophic adjustment of the jet stream. Part I: Two-dimensional forcing, *J. Atmos. Sci.*, *49*(8), 681–697.
Fritts, D. C., C. Bizon, J. A. Werne, and C. K. Meyer (2003), Layering accompanying turbulence generation due to shear instability and gravity-wave breaking, *J. Geophys. Res.*, *108*(D8), 8452, doi:10.1029/2002JD002406.
Fritts, D. C., P. M. Franke, K. Wan, T. Lund, and J. Werne (2011), Computation of clear-air radar backscatter from numerical simulations of turbulence: 2. Backscatter moments throughout the lifecycle of a Kelvin-Helmholtz instability, *J. Geophys. Res.*, *116*, D11105, doi:10.1029/2011JD015895.
Fritts, D. C., K. Wan, P. M. Franke, and T. Lund (2012), Computation of clear-air radar backscatter from numerical simulations of turbulence: 3. Off-zenith measurements and biases throughout the lifecycle of a Kelvin-Helmholtz instability, *J. Geophys. Res.*, *117*, D17101, doi:10.1029/2011JD017179.
Fritts, D. C., L. Wang, and J. A. Werne (2013), Gravity wave-fine structure interactions. Part 1: Influences of fine-structure form and orientation on flow evolution and instability, *J. Atmos. Sci.*, *70*, 3710–3734.
Froidevaux, M., C. W. Higgins, V. Simeonov, P. Ristori, E. Pardyjak, I. Serikov, R. Calhoun, H. v. d. Bergh, and M. B. Parlange (2013), A Raman lidar to measure water vapor in the atmospheric boundary layer, *Adv. Water Resour.*, *51*, 345–356.
Fua, D., and F. Einaudi (1984), On the effects of dissipation on shear instabilities in the stable atmospheric boundary layer, *J. Atmos. Sci.*, *41*, 888–900.
Fua, D., F. Einaudi, and D. P. Lalas (1976), The stability analysis of an inflexion-free velocity profile and its application to the night-time boundary layer in the atmosphere, *Boundary Layer Meteorol.*, *10*, 35–54.
Fua, D., G. Chimonas, F. Einaudi, and O. Zeman (1982), An analysis of wave-turbulence interaction, *J. Atmos. Sci.*, *39*, 2450–2463.
Fukao, S., H. Luce, T. Mega, and M. K. Yamamoto (2011), Extensive studies of large-amplitude Kelvin-Helmholtz billows in the lower atmosphere with VHF middle and upper atmosphere radar, *Q. J. R. Meteorol. Soc.*, *137*(657), 1019–1041.
Gage, K. S., and E. E. Gossard (2003), Recent developments in observation, modeling, and understanding atmospheric turbulence and waves, in *Radar and Atmospheric Science: A Collection of Essays in Honor of David Atlas, Meteorol. Monogr.*, vol. 52, edited by R. M. Wakimoto and R. Srivastava, pp. 139–174, Am. Meteorol. Soc., Boston, Mass.
Galperin, B., and S. Sukoriansky (2010), Geophysical flows with anisotropic turbulence and dispersive waves: Flows with stable stratification, *Ocean Dyn.*, *8*, 65–84.
Galperin, B., S. Sukoriansky, and P. Anderson (2007), On the critical Richardson number in stably stratified turbulence, *Atmos. Sci. Let.*, *8*, 65–69.
Garratt, J. (1992), *The Atmospheric Boundary Layer*, 316 pp., Cambridge Univ. Press, Cambridge, U. K.
Gedzelman, S. D. (1983), Short-period atmospheric gravity waves: A study of their statistical properties and source mechanisms, *Mon. Weather Rev.*, *118*, 1293–1299.
Geller, M. A., H. Tanaka, and D. C. Fritts (1975), Production of turbulence in the vicinity of critical levels for internal gravity waves, *J. Atmos. Sci.*, *32*, 2125–2135.
Georgelin, M., E. Richard, M. Petitdidier, and A. Druilhet (1994), Impact of subgride-scale orography parameterization on the simulation of orographic flows, *Mon. Weather Rev.*, *122*(7), 1509–1522.
Gibert, F., N. Arnault, J. Cuesta, R. Plougonven, and P. Flammant (2011), Internal gravity waves convectively forced in the atmospheric residual layer during the morning transition, *Q. J. R. Meteorol. Soc.*, *137*, 1610–1624.
Gibson, C. H. (1991), Kolmogorov similarity hypotheses for scalar fields: Sampling intermittent turbulent mixing in the ocean and galaxy, *Proc. R. Soc. A*, *434*(1890), 149–164.
Gibson, C. H. (1999), Fossil turbulence revisited, *J. Marine Syst.*, *21*, 147–167.
Gill, A. E. (1982), *Atmosphere-Ocean Dynamics*, 662 pp., Acad. Press, New York.
Gossard, E. E., and W. H. Hooke (1975), *Waves in the Atmosphere: Atmospheric Infrasound and Gravity Waves—Their Generation and Propagation*, 456 pp., Elsevier Sci. Publ. Comp., Univ. of Michigan.
Gossard, E. E., J. H. Richter, and D. Atlas (1970), Internal waves in the atmosphere from high-resolution radar measurements, *J. Geophys. Res.*, *75*(18), 3523–3536.
Grachev, A. A., E. L. Andreas, C. W. Fairall, P. S. Guest, and P. O. G. Persson (2013), The critical Richardson number and limits of applicability of local similarity theory in the stable boundary layer, *Boundary Layer Meteorol.*, *147*(1), 51–82.
Greene, G., and W. Hooke (1979), Scales of gravity waves generated by instability in tropospheric shear flows, *J. Geophys. Res.*, *84*(C10), 6362–6364.
Grisogono, B. (1994a), Dissipation of wave drag in the atmospheric boundary layer, *J. Atmos. Sci.*, *51*(10), 1237–1243.
Grisogono, B. (1994b), A curvature effect on the critical Richardson number, *Croatian Meteorol. J.*, *29*, 43–46.
Grisogono, B. (1995), Wave drag effects in a mesoscale model with a higher-order closure turbulence scheme, *J. Appl. Meteor.*, *34*(4), 941–954.
Grisogono, B. (2010), Generalizing z-less mixing length for stable boundary layers, *Q. J. R. Meteorol. Soc.*, *136*, 213–221.
Grisogono, B., L. Kraljević, and J. Jeričević (2007), The low-level katabatic jet height versus Monin-Obukhov height, *Q. J. R. Meteorol. Soc.*, *133*, 2133–2136.
Grivet-Talocia, S., F. Einaudi, W. L. Clark, R. D. Dennett, G. D. Nastrom, and T. E. VanZandt (1999), A 4-yr climatology of pressure disturbances using a barometer network in Central Illinois, *Mon. Weather Rev.*, *127*, 1613–1629.
Grubišić, V., and I. Stiperski (2009), Lee-wave resonances over double bell-shaped obstacles, *J. Atmos. Sci.*, *66*, 1205–1228.
Grund, C. J., R. M. Banta, J. L. George, J. N. Howell, M. J. Post, R. A. Richter, and A. M. Weickman (2001), High-resolution Doppler lidar for boundary layer and cloud research, *J. Atmos. Oceanic Tech.*, *18*, 376–393.
Güttler, I., and D. Belušić (2012), The nature of small-scale non-turbulent variability in a mesoscale model, *Atmos. Sci. Let.*, *13*, 169–173.
Haberman, R. (1973), Wave-induced distortions of a slightly stratified shear flow: A nonlinear critical-layer effect, *J. Fluid Mech.*, *58*(4), 727–735.
Hardy, K. R., R. J. Reed, and G. K. Mather (1973), Observation of Kelvin-Helmholtz billows and their mesoscale environment by radar, instrumented aircraft, and a dense radiosonde network, *Q. J. R. Meteorol. Soc.*, *99*, 279–293.
Hasha, A., O. Bühler, and J. Scinocca (2008), Gravity wave refraction by three-dimensionally varying winds and the global transport of angular momentum, *J. Atmos. Sci.*, *65*, 2892–2906.
Hauf, T., U. Finke, J. Neisser, G. Bull, and J. -G. Stangenberg (1996), A ground-based network for atmospheric pressure fluctuations, *J. Atmos. Oceanic Tech.*, *13*, 1001–1023.

Haynes, P., and M. McIntyre (1987), On the evolution of vorticity and potential vorticity in the presence of diabatic heating and frictional or other forces, *J. Atmos. Sci.*, *44*(5), 828–841.
Haynes, P., and M. McIntyre (1990), On the conservation and impermeability theorems for potential vorticity, *J. Atmos. Sci.*, *47*(16), 2021–2031.
Hazel, P. (1967), The effect of viscosity and heat conduction on internal gravity waves at a critical level, *J. Fluid Mech.*, *30*(4), 775–783.
Helfrich, K. R., and W. K. Melville (2006), Long nonlinear internal waves, *Annu. Rev. Fluid Mech.*, *38*, 395–425.
Herring, J. R., and O. Métais (1989), Numerical experiments in forced stably stratified turbulence, *J. Fluid Mech.*, *202*, 97–115.
Herron, T. J., and I. Tolstoy (1969), Tracking jet stream winds from ground level pressure signals, *J. Atmos. Sci.*, *26*, 266–269.
Herron, T. J., I. Tolstoy, and D. W. Kraft (1969), Atmospheric pressure background fluctuations in the mesoscale range, *J. Geophys. Res.*, *74*, 1321–1329.
Hertzog, A., G. Boccara, R. Vincent, F. Vial, and P. Cocquerez (2008), Estimation of gravity wave momentum flux and phase speeds from quasi-Lagrangian stratospheric balloon flights. Part II: Results from the Vorcore campaign in Antarctica, *J. Atmos. Sci.*, *65*, 3056–3070.
Hicks, J. J., and J. K. Angell (1968), Radar observations of breaking gravitational waves in the visually clear atmosphere, *J. Appl. Meteorol.*, *7*, 114–121.
Hines, C. O. (1988), Generation of turbulence by atmospheric gravity waves, *J. Atmos. Sci.*, *45*(7), 1269–1247.
Hines, C. O. (1997), Doppler-spread parameterization of gravity-wave momentum deposition in the middle atmosphere. Part 1: Basic formulation, *J. Atmos. Sol. Terr. Phys.*, *59*, 371–386.
Hirt, C. W. (1981), A numerical study of critical layer absorption, in *Nonlinear Properties of Internal Waves*, edited by B. J. West, pp. 141–157, Am. Inst. of Phys., New York.
Hohreiter, V. (2008), Finescale structure and dynamics of an atmospheric temperature interface, *J. Atmos. Sci.*, *65*, 1701–1710.
Holtslag, A. A. M., et al. (2013), Stable atmospheric boundary layers and diurnal cycles—Challenges for weather and climate models, *Bull. Amer. Meteorol. Soc.*, *94*, 1691–1706.
Hooke, W. H., and K. R. Hardy (1975), Further study of the atmospheric gravity waves over the eastern seaboard on 18 March 1969, *J. Appl. Meteorol.*, *65*, 31–38.
Hoover, J. D., D. R. Stauffer, S. J. Richardson, L. Mahrt, B. J. Gaudet, and A. Suarez (2015), Submeso motions within the stable boundary layer and their relationships to local indicators and synoptic regime in moderately complex terrain, *J. Appl. Meteorol. Clim.*, *54*, 352–369, doi:10.1175/JAMC-D-14-0128.1.
Hopfinger, E. J. (1987), Turbulence in stratified fluids: A review, *J. Geophys. Res.*, *92*, 5287–5303.
Howard, L. N., and S. A. Maslowe (1973), Stability of stratified shear flows, *Boundary Layer Meteorol.*, *4*, 511–523.
Hu, X., X. Lee, D. Stevens, and R. Smith (2002), A numerical study of nocturnal wavelike motion in forests, *Boundary Layer Meteorol.*, *102*, 199–223.
Hu, X., F. Zhang, and J. Nielsen-Gammon (2010), Ensemble-based simultaneous state and parameter estimation for treatment of mesoscale model error: A real-data study, *Geophys. Res. Lett.*, *37*, L08802, doi:10.1029/2010GL043017.
Hunt, J., J. Kaimal, and J. Gaynor (1985), Some observations of turbulence structure in stable layers, *Q. J. R. Meteorol. Soc.*, *111*, 793–815.
İnce, T., S. J. Frasier, A. Muschinski, and A. L. Pazmany (2003), An S-band frequency-modulated continuous-wave boundary layer profiler: Description and initial results, *Radio Sci.*, *38*(4), 1072, doi:10.1029/2002RS002753.
Jachens, E. R., and S. D. Mayor (2012), Lidar observations of fine-scale atmospheric gravity waves in the nocturnal boundary layer above an orchard canopy, paper presented at Poster Presentation S8P-05 at the 26th International Laser Radar Conference, International Coordination-Group for Laser Atmospheric Studies (ICLAS) and the International Radiation Commission (IRC), Porto Heli, Greece, 25–29 June.
Jeffrey, A. (1989), A brief history of solitons, in *Waves and Stability in Continuous Media*, edited by S. Rionero, pp. 204–218, World Scientific.
Jeffreys, H. (1925), The flow of water in an inclined channel of rectangular section, *Phi. Mag.*, *49*, 793–807.
Jiang, Q., J. D. Doyle, and R. B. Smith (2006), Interaction between trapped waves and boundary layers, *J. Atmos. Sci.*, *63*, 617–633.
Jimenez, P., J. Dudhia, J. Gonzalez-Rouco, J. Navarro, J. Montavez, and E. Garcia-Bustamante (2012), A revised scheme for the WRF surface layer formulation, *Mon. Weather Rev.*, *140*, 898–918.
Jones, W. L. (1968), Reflexion and stability of waves in stably stratified fluids with shear flow: A numerical study, *J. Fluid Mech.*, *34*, 609–624.
Jones, W. L., and D. D. Houghton (1971), The coupling of momentum between internal gravity waves and mean flow: A numerical study, *J. Atmos. Sci.*, *28*, 604–608.
Jordan, A. R. (1972), Atmospheric gravity waves from winds and storms, *J. Atmos. Sci.*, *29*, 445–456.
Joubaud, S., J. Munroe, and P. Odier (2012), Experimental parametric subharmonic instability in stratified fluids, *Phys. Fluids*, *24*, 41,703, doi:10.1063/1.4706183.
Kaimal, J. C., J. Wyngaard, Y. Izumi, and O. R. Cote (1972), Spectral characteristics of surface-layer turbulence, *Q. J. R. Meteorol. Soc.*, *98*, 563–589.
Kallistratova, M. A. (2002), Acoustic waves in the turbulent atmosphere: A review, *J. Atmos. Sci.*, *19*, 1139–1150.
Kang, Y., D. Belušic, and K. Smith-Miles (2014), Detecting and classifying events in noisy time series, *J. Atmos. Sci.*, *71*, 1090–1104.
Kim, Y.-J., and S.-Y. Hong (2009), Interaction between the orography-induced gravity wave drag and boundary layer processes in a global atmospheric model, *Geophys. Res. Lett.*, *36*, L12809, doi:10.1029/2008GL037146.
Kimura, Y., and J. R. Herring (2012), Energy spectra of stably stratified turbulence, *J. Fluid Mech.*, *698*, 19–50.
Klemp, J. B., and D. K. Lilly (1975), The dynamics of wave-induced downslope winds, *J. Atmos. Sci.*, *32*, 320–339.
Klemp, J. B., and D. K. Lilly (1978), Numerical simulation of hydrostatic mountain waves, *J. Atmos. Sci.*, *35*, 78–106.
Klipp, C., and L. Mahrt (2004), Flux-gradient relationship, self-correlation and intermittency in the stable boundary layer, *Q. J. R. Meteorol. Soc.*, *130*, 2087–2104.
Klostermeyer, J. (1991), Two- and three-dimensional parametric instabilities in finite-amplitude internal gravity waves, *Geophys. Astrophys. Fluid Dyn.*, *61*(1–4), 1–25.
Koch, S. E., B. D. Jamison, C. Lu, T. L. Smith, E. I. Tollerud, C. Girz, N. Wang, T. P. Lane, M. Shapiro, D. D. Parrish, and O. R. Cooper (2005), Turbulence and gravity waves within an upper-level front, *J. Atmos. Sci.*, *62*, 3885–3908.
Koch, S. E., W. Feltz, F. Fabry, M. Pagowski, B. Geerts, C. Bedka, D. Miller, and J. Wilson (2008), Turbulent mixing processes in bores and solitary waves deduced from profiling systems and numerical simulation, *Mon. Weather Rev.*, *136*, 1373–1400.
Kolczynski, W. C., Jr., D. Stauffer, S. Haupt, and A. Deng (2009), Ensemble variance calibration for representing meteorological uncertainty for atmospheric transport and dispersion modeling, *J. Appl. Meteorol.*, *48*, 2001–2021.
Kolczynski, W. C., Jr., D. Stauffer, S. Haupt, N. Altman, and A. Deng (2011), Investigation of ensemble variance as a measure of true forecast variance, *Mon. Weather Rev.*, *139*, 3954–3963.

Koudella, C. R., and C. Staquet (2006), Instability mechanism of two-dimensional progressive internal gravity wave, *J. Fluid Mech.*, *548*, 165–196.
Kuettner, J., P. Hildebrand, and T. Clark (1987), Convection waves: Observations of gravity wave systems over convectively active boundary layers, *Q. J. R. Meteorol. Soc.*, *113*, 445–467.
Lalas, D. P., and F. Einaudi (1976), On the characteristics of gravity waves generated by atmospheric shear layers, *J. Atmos. Sci.*, *33*, 1248–1259.
Lalas, D. P., F. Einaudi, and D. Fua (1976), The destabilizing effect of the ground on Kelvin-Helmholtz waves in the atmosphere, *J. Atmos. Sci.*, *33*, 59–69.
Lane, T. P., and R. D. Sharman (2008), Some influences of background flow conditions on the generation of turbulence due to gravity wave breaking above deep convection, *J. Appl. Meteorol. Clim.*, *47*, 2777–2796.
Lane, T. P., J. D. Doyle, R. D. Sherman, M. A. Shapiro, and C. D. Watson (2009), Statistics and dynamics of aircraft encounters of turbulence over Greenland, *Mon. Weather Rev.*, *137*, 2687–2702.
Largeron, Y., C. Staquet, and C. Chemel (2013), Characterization of oscillatory motions in the stable atmosphere of a deep valley, *Boundary Layer Meteorol.*, *148*, 439–454.
Larraza, A. (1993), Physical applications of wave turbulence: Wind waves and classical collective modes, in *Nonlinear Waves and Weak Turbulence With Applications in Oceanography and Condensed Matter Physics*, edited by N. Fitzmaurice et al., pp. 83–95, Birkhäuser, Boston, Mass.
Lee, X. (1997), Gravity waves in a forest: A linear analysis, *J. Atmos. Sci.*, *54*, 2574–2585.
Lee, X., and A. Barr (1998), Climatology of gravity waves in a forest, *Q. J. R. Meteorol. Soc.*, *124*, 1403–1419.
Lee, X., H. Neuman, G. den Hartog, J. Fuentes, T. Black, R. Mickle, P. Yang, and P. Blanken (1997), Observations of gravity waves in a boreal forest, *Boundary Layer Meteorol.*, *84*, 383–398.
Lelong, M.-P., and J. J. Riley (1991), Internal wave-vortical mode interactions in strongly stratified flows, *J. Fluid Mech.*, *232*, 1–19.
Lenschow, D. H. (Ed.) (1986), *Probing the Atmospheric Boundary Layer*, 269 pp., Am. Meteorol. Soc., Boston, Mass.
Lenschow, D. H., X. Li, C. Zhu, and B. Stankov (1988), The stably stratified boundary layer over the Great Plains: I. Mean and turbulence structure, *Boundary Layer Meteorol.*, *42*, 95–121.
Lighthill, J. (1978), *Waves in Fluids*, 504 pp., Cambridge Univ. Press, Cambridge, U. K.
Lilly, D. K., and P. F. Lester (1974), Wave and turbulence in the stratosphere, *J. Atmos. Sci.*, *31*, 800–812.
Lin, J.-T., and Y.-H. Pao (1979), Wakes in stratified fluids, *Annu. Rev. Fluid Mech.*, *11*, 317–338.
Lin, Y.-L., and R. C. Goff (1988), A study of a mesoscale solitary wave in the atmosphere originating near a region of deep convection, *J. Atmos. Sci.*, *45*(2), 194–205.
Lindborg, E. (2006), The energy cascade in a strongly stratified fluid, *J. Fluid Mech.*, *550*, 207–242.
Lindzen, R. S., and A. J. Rosenthal (1976), On the instability of Helmholtz velocity profiles in stably stratified fluids when a lower boundary is present, *J. Geophys. Res.*, *81*(9), 1561–1571.
Lindzen, R. S., and A. J. Rosenthal (1983), Instabilities in a stratified fluid having one critical level. Part III: Kelvin-Helmholtz instabilities as overreflected waves, *J. Atmos. Sci.*, *40*, 530–542.
Lindzen, R. S., and K.-K. Tung (1976), Banded convective activity and ducted gravity waves, *Mon. Weather Rev.*, *104*, 1602–1617.
Liu, Z., S. A. Thorpe, and W. D. Smyth (2012), Instability and hydraulics of turbulent stratified shear flows, *J. Fluid Mech.*, *695*, 235–256.
Long, R. R. (1953), Some aspects of the flow of stratified fluids. I: A theoretical investigation, *Tellus*, *5*, 42–58.
Lothon, M., et al. (2014), The BLLAST field experiment: Boundary-layer late afternoon and sunset turbulence, *Atmos. Chem. Phys.*, *14*(7), 10,789–10,852.
Lott, F. (2007), The reflection of a stationary gravity wave by a viscous boundary layer, *J. Atmos. Sci.*, *64*, 3363–3371.
Lott, F., and M. Miller (1997), A new subgrid-scale orographic drag parameterization: Its formulation and testing, *Q. J. R. Meteorol. Soc.*, *123*, 101–127.
Louis, J.-F. (1979), A parametric model of vertical eddy fluxes in the atmosphere, *Boundary Layer Meteorol.*, *17*, 187–202.
Lu, N. P., W. D. Neff, and J. C. Kaimal (1983), Wave and turbulence structure in a disturbed nocturnal inversion, *Boundary Layer Meteorol.*, *26*, 141–155.
Luhar, A., and P. J. Hurley (2012), Application of a coupled prognostic model to turbulence and dispersion in light-wind stable conditions with an analytical correction to vertically resolve concentrations near the surface, *Atmos. Environ.*, *51*, 56–66.
Lyulyukin, V., R. Kouznetsov, and M. Kallistratova (2013), The composite shape and structure of braid patterns in Kelvin-Helmholtz billows observed with a sodar, *J. Atmos. Oceanic Tech.*, *30*(12), 2704–2711.
MacKinnon, J. A., M. H. Alford, O. Sun, R. Pinkel, Z. Zhao, and J. Klymak (2013), Parametric subharmonic instability of the internal tide at 29°N, *J. Phys. Oceanogr.*, *43*, 17–28.
Mahrt, L. (1989), Intermittency of atmospheric turbulence, *J. Atmos. Sci.*, *46*, 79–95.
Mahrt, L. (2008), The influence of transient flow distortion on turbulence in stable weak-wind conditions, *Boundary Layer Meteorol.*, *127*, 1–16.
Mahrt, L. (2009), Characteristics of submeso winds in the stable boundary layer, *Boundary Layer Meteorol.*, *130*, 1–14.
Mahrt, L. (2010a), Common microfronts and other solitary events in the nocturnal boundary layer, *Q. J. R. Meteorol. Soc.*, *136*, 1712–1722.
Mahrt, L. (2010b), Computing turbulent fluxes near the surface: Needed improvements, *Agric. Forest Meteorol.*, *150*, 501–509.
Mahrt, L. (2011), Surface wind direction variability, *J. Appl. Meteorol. Clim.*, *50*, 144–152.
Mahrt, L., and D. Vickers (2006), Extremely weak mixing in stable conditions, *Boundary Layer Meteorol.*, *119*, 19–39.
Mahrt, L., C. Thomas, and J. Preuger (2009), Space-time structure of mesoscale modes in the stable boundary layer, *Q. J. R. Meteorol. Soc.*, *135*, 67–75.
Mahrt, L., S. Richardson, N. Seaman, and D. Stauffer (2012), Turbulence in the nocturnal boundary layer with light and variable winds, *Q. J. R. Meteorol. Soc.*, *138*, 1430–1439.
Mahrt, L., C. Thomas, S. Richardson, N. Seaman, D. Stauffer, and M. Zeeman (2013), Non-stationary generation of weak turbulence for very stable and weak-wind conditions, *Boundary Layer Meteorol.*, *147*, 179–199.
Mann, J., J.-P. Cariou, M. S. Courtney, R. Parmentier, T. Mikkelsen, R. Wagner, P. Lindelöw, M. Sjöholm, and K. Enevoldsen (2009), Comparison of 3D turbulence measurements using three staring wind lidars and a sonic anemometer, *Meteorol. Z.*, *18*(2), 135–140.
Mann, J., A. P. na, F. Bingol, R. Wagner, and M. S. Courtney (2010), Lidar scanning of momentum flux in and above the atmospheric surface layer, *J. Atmos. Oceanic Tech.*, *27*, 959–976.
Mashayek, A., and W. Peltier (2012), The zoo of secondary instabilities precursory to stratified shear flow transition. Part 1: Shear aligned convection, pairing, and braid instabilities, *J. Fluid Mech.*, *708*, 45–70.
Mastrantonio, G., F. Einaudi, and D. Fua (1976), Generation of gravity waves by jet streams in the atmosphere, *J. Atmos. Sci.*, *33*, 1730–1738.

Mauritsen, T., and G. Svensson (2007), Observations of stably stratified shear-driven atmospheric turbulence at low and high Richardson numbers, *J. Atmos. Sci.*, *64*, 645–655.
Mauritsen, T., G. Svensson, S. Zilitinkevich, I. Esau, L. Enger, and B. Grisogono (2007), A total turbulent energy closure model for neutral and stably stratified atmospheric boundary layers, *J. Atmos. Sci.*, *64*, 4113–4126.
May, P. T., R. G. Strauch, K. P. Moran, and W. L. Ecklund (1990), Temperature sounding by RASS with wind profiler radars: A preliminary study, *IEEE Trans. Geosci. Remote Sens.*, *28*(1), 19–28.
Mayer, S., A. Sandvik, M. Jonassen, and J. Reuder (2012a), Atmospheric profiling with the UAS SUMO: A new perspective for the evaluation of fine-scale atmospheric models, *Meteorol. Atmos. Phys.*, *116*, 15–26.
Mayer, S., M. O. Jonassen, A. Sandvik, and J. Reuder (2012b), Profiling the Arctic stable boundary layer in Advent Valley, Svalbard: Measurements and simulations, *Boundary Layer Meteorol.*, *143*, 507–526.
Mayor, S. D., and E. W. Eloranta (2001), Two-dimensional vector wind fields from volume imaging lidar data, *J. Appl. Meteorol.*, *40*, 1331–1346.
Mayor, S. D., and S. M. Spuler (2004), Raman-shifted eye-safe aerosol lidar, *Atmos. Ocean. Phys.*, *43*, 3915–3924.
Mayor, S. D., J. P. Lowe, and C. F. Mauzey (2012a), Two-component horizontal aerosol motion vectors in the atmospheric surface layer from a cross-correlation algorithm applied to elastic backscatter lidar data, *J. Atmos. Oceanic Tech.*, *29*, 1585–1602.
Mayor, S. D., E. R. Jachens, and T. N. Randall (2012b), Lidar observations of fine-scale gravity waves in the nocturnal boundary layer above an orchard canopy, paper presented 16th International Symposium for the Advancement of Boundary-Layer Remote Sensing (ISARS), CIRES, Univ. of Colo., and NOAA Earth System Res. Lab., Boulder, 5–8 June.
McComas, C. H., and F. P. Bretherton (1977), Resonant interaction of oceanic internal waves, *J. Geophys. Res.*, *82*(9), 1397–1412.
McFarlane, N. (1987), The effect of orographically excited gravity wave drag on the general circulation of the lower stratosphere and troposphere, *J. Atmos. Sci.*, *44*, 1775–1800.
McIntyre, M. E. (1981), On the "wave momentum" myth, *J. Fluid Mech.*, *106*, 331–347.
McIntyre, M. E. (2008), Potential-vorticity inversion and the wave-turbulence jigsaw: Some recent clarifications, *Adv. Geophys.*, *15*(15), 47–56.
McIntyre, M. E., and W. A. Norton (1990), Dissipative wave-mean interactions and the transport of vorticity or potential vorticity, *J. Fluid Mech.*, *212*, 403–435.
McNider, R. T. (1982), A note on velocity fluctuations in drainage flows, *J. Atmos. Sci.*, *39*, 1658–1660.
Mead, J. B., G. Hopcraft, S. J. Frasier, B. D. Pollard, C. D. Cherry, D. H. Schaubert, and R. E. McIntosh (1998), A volume-imaging radar wind profiler for atmospheric boundary layer turbulence studies, *J. Atmos. Oceanic Tech.*, *15*, 849–859.
Meillier, Y., R. G. Frehlich, R. M. Jones, and B. B. Balsley (2008), Modulation of small-scale turbulence by ducted gravity waves in the nocturnal boundary layer, *J. Atmos. Sci.*, *65*, 1414–1427.
Melfi, S., and S. P. Palm (2012), Estimating the orientation and spacing of midlatitude linear convective boundary layer features: Cloud streets, *J. Atmos. Sci.*, *69*(1), 352–364.
Mellor, G. L., and T. Yamada (1982), Development of a turbulence closure model for geophysical fluid problems, *Rev. Geophys.*, *20*, 851–875.
Merrill, J. T., and J. R. Grant (1979), A gravity-wave critical level encounter observed in the atmosphere, *J. Geophys. Res.*, *84*(C10), 6315–6320.
Mied, R. P. (1976), The occurrence of parametric instabilities in finite-amplitude internal gravity waves, *J. Fluid Mech.*, *78*(04), 763–784.
Miles, J. W., and L. N. Howard (1964), Note on a heterogeneous shear flow, *J. Fluid Mech.*, *20*, 331–336.
Miropol'sky, Y. Z. (2001), *Dynamics of Internal Gravity Waves in the Ocean*, 406 pp., Springer Science and Business Media, Dordrecht, Netherlands.
Monserrat, S., and A. J. Thorpe (1996), Use of ducting theory in an observed case of gravity waves, *J. Atmos. Sci.*, *53*, 1724–1736.
Moustaoui, M., B. Joseph, and H. Teitelbaum (2004), Mixing layer formation near the tropopause due to gravity wave critical level interactions in a cloud-resolving model, *J. Atmos. Sci.*, *61*, 3112–3124.
Müller, P., G. Holloway, F. Henyey, and N. Pomphrey (1986), Nonlinear interactions among internal gravity waves, *Rev. Geophys.*, *24*(3), 493–536.
Munk, W. (1981), Internal waves and small-scale processes, in *Evolution of Physical Oceanography*, edited by B. Warren and C. Wunsch, pp. 264–291, MIT Press, Cambridge, Mass.
Muschinski, A., V. Lehmann, L. Justen, and G. Teschke (2005), Advanced radar wind profiling, *Meteorol. Z.*, *14*(5), 609–625.
Nappo, C., and G. Chimonas (1992), Wave exchange between the ground surface and a boundary-layer critical level, *J. Atmos. Sci.*, *49*, 1075–1091.
Nappo, C., J. Sun, L. Mahrt, and D. Belušić (2014), Determining wave-turbulence interactions in the stable boundary layer, *Bull. Am. Meteorol. Soc.*, *95*, ES11–ES13.
Nappo, C. J. (2012), *An Introduction to Atmospheric Gravity Waves*, 2nd ed., 400 pp., Acad. Press.
Nappo, C. J., and G. Svensson (2008), A parameterization with wave saturation adjustment of subgrid-scale average wave stress over three-dimensional topography, in *18th Symposium on Boundary Layer and Turbulence*, p. 6A.2, Am. Meteorol. Soc., Stockholm, Sweden.
Nappo, C. J., H. Y. Chun, and H. J. Lee (2004), A parameterization of wave stress in the planetary boundary layer for use in mesoscale models, *Atmos. Environ.*, *38*, 2665–2675.
Nastrom, G. D., and F. D. Eaton (1993), The coupling of gravity waves and turbulence at White Sands, New Mexico, from VHF radar observations, *J. Appl. Meteorol.*, *32*(1), 81–87.
Nastrom, G. D., and D. C. Fritts (1992), Sources of mesoscale variability of gravity waves. Part I: Topographic excitation, *J. Atmos. Sci.*, *49*(2), 101–110.
Nastrom, G. D., M. R. Peterson, J. L. Green, K. S. Gage, and T. E. VanZandt (1990), Sources of gravity wave activity seen in the vertical velocities observed by the Flatland VHF radar, *J. Appl. Meteorol.*, *29*, 783–792.
Nazarenko, S. (2011), *Wave Turbulence*, 279 pp., Springer, Berlin.
Neff, W., and R. Coulter (1986), Acoustic remote sensing, in *Probing the Atmospheric Boundary Layer*, edited by Donald H. Lenschow, pp. 201–239, Am. Meteorol. Soc., Boston, Mass.
Newsom, R., and R. Banta (2003), Shear-flow instability in the stable nocturnal boundary layer as observed by Doppler lidar during CASES-99, *J. Atmos. Sci.*, *60*, 16–33.
Nielsen-Gammon, J. W., X. Hu, F. Zhang, and J. E. Pleim (2010), Evaluation of planetary boundary layer scheme sensitivities for the purpose of parameter estimation, *Mon. Weather Rev.*, *138*, 3400–3417.
Ostrovsky, L., and Y. I. Troitskaya (1987), A model of turbulent transfer and dynamics of turbulence in a stratified shear-flow, *Izvestiya Akademii Nauk Sssr Fizika Atmosfery I Okeana*, *23*(10), 1031–1040.
Ostrovsky, L. A., V. I. Kazakov, P. A. Matusov, and D. V. Zaborskikh (1996), Experimental study of the internal wave damping on small-scale turbulence, *J. Phys. Oceanogr.*, *26*, 398–405.

Ottersten, H., K. R. Hardy, and C. G. Little (1973), Radar and sodar probing of waves and turbulence in statically stable clear-air layers, *Boundary Layer Meteorol.*, *4*, 47–89.
Pagel, C., and A. Balogh (2001), A study of magnetic fluctuations and their anomalous scaling in the solar wind: The Ulysses fast-latitude scan, *Nonlinear Proc. Geophy.*, *8*(4/5), 313–330.
Pairaud, I., C. Staquet, J. Sommeria, and M. M. Mahdizadeh (2010), Generation of harmonics and sub-harmonics from an internal tide in a uniformly stratified fluid: Numerical and laboratory experiments, in *IUTAM Symposium on Turbulence in the Atmosphere and Oceans*, pp. 51–62, Springer, Netherlands.
Palmer, T. N., G. J. Shutts, and R. Swinbank (1986), Alleviation of a systematic westerly bias in general circulation and numerical weather prediction models through an orographic gravity wave drag parametrization, *Q. J. R. Meteorol. Soc.*, *112*, 1001–1039.
Patton, E. G., et al. (2011), The Canopy Horizontal Array Turbulence Study (CHATS), *Bull. Am. Meteorol. Soc.*, *92*, 593–611.
Pavelin, E., and J. A. Whiteway (2002), Gravity wave interactions around the jet stream, *Geophys. Res. Lett.*, *29*(21), 2024, doi:10.1029/2002GL015783.
Pearson, G., F. Davies, and C. Collier (2009), An analysis of the performance of the UFAM pulsed Doppler lidar for observing the boundary layer, *J. Atmos. Oceanic Tech.*, *26*, 240–250.
Petenko, I., G. Mastrantonio, A. Viola, S. Argentini, and I. Pietroni (2012), Wavy vertical motions in the ABL observed by sodar, *Boundary Layer Meteorol.*, *143*, 125–141.
Pichugina, Y. L., R. M. Banta, N. D. Kelley, B. J. Jonkman, S. C. Tucker, R. K. Newsom, and W. A. Brewer (2008), Horizontal-velocity and variance measurements in the stable boundary layer using Doppler lidar: Sensitivity to averaging procedures, *J. Atmos. Ocean. Technol.*, *25*, 1307–1327.
Plougonven, R., and F. Zhang (2014), Internal gravity waves from atmospheric jets and fronts, *Rev. Geophys.*, *52*, 33–76, doi:10.1002/2012RG000419.
Porch, W., W. Clements, and R. Coulter (1991), Nighttime valley waves, *J. Appl. Meteorol.*, *30*, 145–156.
Poulin, F. J., G. R. Flierl, and J. Pedlosky (2003), Parametric instability in oscillatory shear flows, *J. Fluid Mech.*, *481*, 329–353.
Pouquet, A., and R. Marino (2013), Geophysical turbulence and the duality of the energy flow across scales, *Phys. Rev. Lett.*, *111*, 234501, doi:10.1103/PhysRevLett.111.234501.
Pulido, M., and G. Chimonas (2001), Forest canopy waves: The long-wavelength component, *Boundary Layer Meteorol.*, *100*, 209–224.
Pulido, M., and C. Rodas (2008), Do transient gravity waves in a shear flow break?, *Q. J. R. Meteorol. Soc.*, *134*, 1083–1094.
Pulido, M., and J. Thuburn (2005), Gravity wave drag estimation from global analyses using variational data assimilation principles. I: Theory and implementation, *Q. J. R. Meteorol. Soc.*, *131*, 1821–1840.
Pulido, M., and J. Thuburn (2008), The seasonal cycle of gravity wave drag in the middle atmosphere, *J. Clim.*, *21*, 4664–4679.
Ralph, F. M., M. Crochet, and S. V. Venkateswaran (1993), Observations of a mesoscale ducted gravity wave, *J. Atmos. Sci.*, *50*(19), 3277–3291.
Ralph, F. M., P. J. Neiman, T. L. Keller, D. Levinson, and L. Fedor (1997), Observations, simulations, and analysis of nonstationary trapped lee waves, *J. Atmos. Sci.*, *54*(10), 1308–1333.
Ralph, F. M., P. J. Neiman, and T. L. Keller (1999), Deep-tropospheric gravity waves created by lee side cold fronts, *J. Atmos. Sci.*, *56*, 2986–3009.
Randall, T. N., E. R. Jachens, and S. D. Mayor (2012), Lidar observations of fine-scale atmospheric gravity waves in the nocturnal boundary layer above an orchard canopy, in *20th Symposium on Boundary Layers and Turbulence*, p. 33, Am. Meteor. Soc., Boston, Mass.
Rao, M., P. Castracane, D. Fua, and G. Fiocco (2004), Observations of atmospheric solitary waves in the urban boundary layer, *Boundary Layer Meteorol.*, *111*, 85–108.
Raupach, M. R., J. J. Finnigan, and Y. Brunet (1996), Coherent eddies and turbulence in vegetation canopies: The mixing-layer analogy, *Boundary Layer Meteorol.*, *78*, 351–382.
Rayleigh, J. W. S. (1945), *The Theory of Sound*, vol. 2, Dover, New York.
Readings, C., D. Atlas, C. EmManuel, Y. -H. Pao, and S. Thorpe (1973), The formation and breakdown of Kelvin-Helmholtz billows, *Boundary Layer Meteorol.*, *5*(1), 233–240.
Rees, J. M., and S. D. Mobbs (1988), Studies of internal gravity waves at Halley Base, Antarctica, using wind observations, *Q. J. R. Meteorol. Soc.*, *114*, 939–966.
Rees, J. M., and J. W. Rottman (1994), Analysis of solitary disturbances over an Antarctic ice shelf, *Boundary Layer Meteorol.*, *69*, 285–310.
Rees, J. M., P. Anderson, and J. King (1998), Observations of solitary waves in the stable atmospheric boundary layer, *Boundary Layer Meteorol.*, *86*, 47–61.
Rees, J. M., J. Denholm-Price, J. King, and P. Anderson (2000), A climatological study of internal gravity waves in the atmospheric boundary layer overlying the Brunt Ice Shelf, Antarctica, *J. Atmos. Sci.*, *57*, 511–526.
Rees, J. M., W. J. Staszewski, and J. R. Winkler (2001), Case study of a wave event in the stable atmospheric boundary layer overlying an Antarctic Ice Shelf using the orthogonal wavelet transform, *Dyn. Atmos. Oceans*, *34*, 245–261.
Rehmann, C. R., and J. R. Koseff (2004), Mean potential energy change in stratified grid turbulence, *Dyn. Atmos. Oceans*, *37*, 271–294.
Reineman, B. D., L. Lenain, N. M. Statom, and W. K. Melville (2013), Development and testing of instrumentation for UAV-based flux measurements within terrestrial and marine atmospheric boundary layers, *J. Atmos. Oceanic Tech.*, *30*(7), 1295–1319.
Renfrew, I. A. (2004), The dynamics of idealized katabatic flow over a moderate slope and ice shelf, *Q. J. R. Meteorol. Soc.*, *130*(598), 1023–1045.
Reuder, J., M. Jonassen, and H. Olafsson (2012), The small unmanned meteorological observer SUMO: Recent developments and applications of a micro-UAS for atmospheric boundary layer research, *Acta Geophys.*, *60*, 1454–1473.
Riley, J. J., and M. -P. Lelong (2000), Fluid motions in the presence of strong stable stratification, *Annu. Rev. Fluid Mech.*, *32*, 613–657.
Riley, J. J., and E. Lindborg (2008), Stratified turbulence: A possible interpretation of some geophysical turbulence measurements, *J. Atmos. Sci.*, *65*, 2416–2424.
Román-Cascón, C., C. Yagüe, S. Viana, M. Sastre, G. Maqueda, M. Lothon, and I. Gómara (2015), Near-monochromatic ducted gravity waves associated with a convective system close to the Pyrenees, *Q. J. R. Meteorol. Soc.*, *141*, 1320–1332, doi:10.1002/qj.2441.
Romanova, N., and I. Yakushkin (1995), Internal gravity waves in the lower atmosphere and sources of their generation (review), *Atmos. Ocean. Phys.*, *31*, 151–172.
Rorai, C., P. Mininni, and A. Pouquet (2014), Turbulence comes in bursts in stably stratified flows, *Phys. Rev. E*, *89*, 043002.
Rosenthal, A., and R. Lindzen (1983a), Instabilities in a stratified fluid having one critical level. Part I: Results, *J. Atmos. Sci.*, *40*(3), 509–520.
Rosenthal, A., and R. Lindzen (1983b), Instabilities in a stratified fluid having one critical level. Part II: Explanation of gravity wave instabilities using the concept of overreflection, *J. Atmos. Sci.*, *40*(3), 521–529.
Rotta, J. (1951), Statistische theorie nichthomogener turbulenz, *Z. für Physik*, *129*, 547–572.
Rottman, J. W., and F. Einaudi (1993), Solitary waves in the atmosphere, *J. Atmos. Sci.*, *50*, 2116–2136.

Rottman, J. W., and R. Grimshaw (2002), Atmospheric internal solitary waves, in *Environmental Stratified Flows, Environ. Fluid Mech.*, edited by R. Grimshaw, chap. 3, pp. 61–88, Springer, New York.
Rotunno, R., V. Grubišic, and P. Smolarkiewicz (1999), Vorticity and potential vorticity in mountain wakes, *J. Atmos. Sci.*, *56*(16), 2796–2810.
Ruiz, J., M. Pulido, and T. Miyoshi (2013), Estimating model parameters with ensemble-based data assimilation: A review, *J. Meteorol. Soc. Jpn.*, *91*, 79–99.
Ruzmaikin, A., J. Feynman, B. Goldstein, E. Smith, and A. Balogh (1995), Intermittent turbulence in solar wind from the south polar hole, *J. Geophys. Res.*, *100*(A3), 3395–3403.
Samah, A. A., and A. J. Thorpe (1993), Gravity wave propagation in a frontal environment, in *Waves and Turbulence in Stably Stratified Flows*, edited by S. D. Mobbs and and J. C. King, pp. 185–212, Clarendon Press, Oxford Univ. Press, U. K.
Sato, K., H. Hashiguchi, and S. Fukao (1995), Gravity waves and turbulence associated with cumulus convection observed with the UHF/VHF clear-air Doppler radars, *J. Geophys. Res.*, *11*(D4), 7111–7119.
Scavuzzo, C., M. Lamfri, H. Teitelbaum, and F. Lott (1998), A study of the low-frequency inertio-gravity waves observed during Pyrénées Experiment, *J. Geophys. Res.*, *103*, 1747–1758.
Schneider, T., I. M. Held, and S. T. Garner (2003), Boundary effects in potential vorticity dynamics, *J. Atmos. Sci.*, *60*(8), 1024–1040.
Scinocca, J. F. (2002), The effect of back-reflection in the parameterization of non-orographic gravity-wave drag, *J. Meteorol. Soc. Jpn.*, *80*(4B), 939–962.
Scinocca, J. F. (2003), An accurate spectral nonorographic gravity wave drag parameterization for general circulation models, *J. Atmos. Sci.*, *60*, 667–682.
Seaman, N. I., B. J. Gaudet, D. R. Stauffer, L. Mahrt, S. J. Richardson, J. Zielonka, and J. C. Wyngaard (2012), Numerical prediction of submesoscale flow in the nocturnal stable boundary layer over complex terrain, *Mon. Weather Rev.*, *140*, 956–977.
Seuront, L., et al. (1996), Multifractal intermittency of Eulerian and Lagrangian turbulence of ocean temperature and plankton fields, *Nonlinear Processes Geophys.*, *3*(4), 236–246.
Shutts, G. J. (1998), Stationary gravity-wave structure in flows with directional wind shear, *Q. J. R. Meteorol. Soc.*, *124*, 1421–1442.
Shutts, J. G. (1995), Gravity-wave drag parameterization over complex terrain: The effects of critical-level absorption in directional wind shear, *Q. J. R. Meteorol. Soc.*, *121*, 1005–1021.
Siebert, H., R. Shaw, and Z. Warhaft (2010), Statistics of small-scale velocity fluctuations and internal intermittency in marine stratocumulus clouds, *J. Atmos. Sci.*, *67*(1), 262–273.
Simpson, J. E. (1997), *Gravity Currents in the Environment and the Laboratory*, 244 pp., Cambridge Univ. Press, New York.
Smith, R. B. (1976), The generation of lee waves by the Blue Ridge, *J. Atmos. Sci.*, *33*, 507–519.
Smith, R. B. (1989), Hydrostatic airflow over mountains, *Adv. Geophys.*, *31*, 1–41.
Smith, R. B. (2002), Stratified flow over topography, in *Environmental Stratified Flows*, edited by R. Grimshaw, chap. 5, pp. 119–159, Kluwer, Netherlands.
Smith, R. B. (2007), Interacting mountain waves and boundary layers, *J. Atmos. Sci.*, *64*, 594–607.
Smith, R. B., and D. F. Smith (1995), Pseudoinviscid wake formation by mountains in shallow-water flow with a drifting vortex, *J. Atmos. Sci.*, *52*(4), 436–454.
Smith, R. B., S. Skubis, J. D. Doyle, A. S. Broad, C. Kiemle, and H. Volkert (2002), Mountain waves over Mont Blanc: Influence of a stagnant boundary layer, *J. Atmos. Sci.*, *59*, 2073–2092.
Smith, R. B., Q. Jiang, and J. D. Doyle (2006), A theory of gravity wave absorption by a boundary layer, *J. Atmos. Sci.*, *63*, 774–781.
Smith, R. B., J. Doyle, Q. Jiang, and S. Smith (2007), Alpine gravity waves: Lessons from MAP regarding mountain wave generation and breaking, *Q. J. R. Meteorol. Soc.*, *133*, 917–936.
Smith, R. K. (1988), Traveling waves and bores in the lower atmosphere: The "morning glory" and related phenomena, *Earth-Sci. Rev.*, *25*, 267–290.
Smyth, W. D., and W. R. Peltier (1991), Instability and transition in finite-amplitude Kelvin-Helmholtz and Holmboe waves, *J. Fluid Mech.*, *228*, 387–415.
Soler, M., C. Infante, P. Buenestado, and L. Mahrt (2002), Observations of nocturnal drainage flow, *Boundary Layer Meteorol.*, *105*, 253–273.
Soler, M., M. Udina, and E. Ferreres (2014), Observational and numerical simulation study of a sequence of eight atmospheric density currents in Northern Spain, *Boundary Layer Meteorol.*, *153*, 1–22.
Sorbjan, Z. (1989), *Structure of the Atmospheric Boundary Layer*, 317 pp., Prentice Hall, Englewood Cliffs, N. J.
Sorbjan, Z., and B. Balsley (2008), Microstructure of turbulence in the stably stratified boundary layer, *Boundary Layer Meteorol.*, *129*, 191–210.
Sorriso-Valvo, L., V. Carbone, P. Veltri, G. Consolini, and R. Bruno (1999), Intermittency in the solar wind turbulence through probability distribution functions of fluctuations, *Geophys. Res. Lett.*, *26*(13), 1801–1804.
Staquet, C. (2004), Gravity and inertia-gravity internal waves: Breaking processes and induced mixing, *Surv. Geophys.*, *25*, 281–314.
Staquet, C., and J. Sommeria (2002), Internal gravity waves: From instabilities to turbulence, *Annu. Rev. Fluid Mech.*, *34*, 559–593.
Stauffer, D. R. (2012), Uncertainty in environmental NWP modeling, in *Handbook of Environmental Fluid Dynamics, Volume Two: Systems, Pollution, Modeling, and Measurements*, edited by H. J. S. Fernando, pp. 411–426, CRC Press.
Stauffer, D. R., B. Gaudet, N. Seaman, L. M. J. C. Wyngaard, and S. Richardson (2009), Sub-kilometer numerical predictions in the nocturnal stable boundary layer, *paper presented at 23rd Conference on Weather Analysis and Forecasting/19th Conference on Numerical Weather Prediction*, Am. Meteorol. Soc., Omaha, Nebr., 1–5 June.
Steeneveld, G., A. Holtslag, C. Nappo, B. van de Weil, and L. Mahrt (2008), Exploring the possible role of small-scale terrain drag on stable boundary layers over land, *J. Appl. Meteorol. Clim.*, *47*, 2518–2530.
Steeneveld, G.-J., C. J. Nappo, and A. A. M. Holtslag (2009), Estimation of orographically induced wave drag in the stable boundary layer during the CASES-99 experimental campaign, *Acta Geophys.*, *57*(4), 857–881.
Stewart, R. W. (1969), Turbulence and waves in a stratified atmosphere, *Radio Sci.*, *4*, 1269–1278.
Stiperski, I., and V. Grubišić (2011), Trapped lee wave interference in the presence of surface friction, *J. Atmos. Sci.*, *68*, 918–936.
Strang, E. J., and H. J. S. Fernando (2001), Entrainment and mixing in stratified shear flows, *J. Fluid Mech.*, *428*, 349–386.
Strumik, M., and W. Macek (2008), Statistical analysis of transfer of fluctuations in solar wind turbulence, *Nonlinear Processes Geophys.*, *15*(4), 607–613.
Suarez, A., and D. Stauffer (2014), Effects of nonstationary wave structures on rotor development and evolution, paper presented at 16th Annual Conference on Mountain Meteorology, Am. Meteorol. Soc., San Diego, Calif., 18–22 Aug.
Suarez, A., D. Stauffer, and B. Gaudet (2014), Forecast sensitivity of waves and submeso motions to initialization strategy and PBL physics in the stable boundary layer, paper presented at 16th Annual Conference on Mountain Meteorology, Am. Meteorol. Soc., San Diego, Calif., 18–22 Aug.

Sukoriansky, S., and B. Galperin (2005), A spectral closure model for turbulent flows with stable stratification, in *Marine Turbulence: Theories, Observations, and Models. Results of the CARTUM Project*, edited by H. Z. Baumert, J. H. Simpson, and J. Sündermann, chap. 6, pp. 53–65, Cambridge Univ. Press, Cambridge, U. K.

Sukoriansky, S., and B. Galperin (2013), An analytical theory of the buoyancy-Kolmogorov subrange transition in turbulent flows with stable stratification, *Philos. Trans. R. Soc. A*, *371*, 20120212, doi:10.1098/rsta.2012.0212.

Sukoriansky, S., B. Galperin, and I. Staroselsky (2005), A quasinormal scale elimination model of turbulent flows with stable stratification, *Phys. Fluids*, *17*, 085107, doi:10.1063/1.2009010.

Sukoriansky, S., et al. (2006), A quasi-normal scale elimination model of turbulence and its application to stably stratified flows, *Nonlinear Processes Geophys.*, *13*(1), 9–22.

Sukoriansky, S., N. Dikovskaya, and B. Galperin (2009), Transport of momentum and scalar in turbulent flows with anisotropic dispersive waves, *Geophys. Res. Lett.*, *36*, L14609, doi:10.1029/2009GL038632.

Sullivan, P., and N. Patton (2011), The effect of mesh resolution on convective boundary layer statistics and structures generated by large-eddy simulation, *J. Atmos. Sci.*, *68*, 2396–2415.

Sun, J. (2011), Vertical variations of the mixing lengths during CASES-99, *J. Appl. Meteorol. Clim.*, *50*, 2030–2041.

Sun, J., et al. (2002), Intermittent turbulence associated with a density current passage in the stable boundary layer, *Boundary Layer Meteorol.*, *105*, 199–219.

Sun, J., et al. (2004), Atmospheric disturbances that generate intermittent turbulence in nocturnal boundary layers, *Boundary Layer Meteorol.*, *110*, 255–279.

Sun, J., L. Mahrt, R. M. Banta, and Y. L. Pichugina (2012), Turbulence regimes and turbulence intermittency in the stable boundary layer during CASES-99, *J. Atmos. Sci.*, *69*, 338–351.

Sun, J., D. H. L. L. Mahrt, and C. Nappo (2013), The relationships among wind, horizontal pressure gradient, and turbulent momentum transport during CASES-99, *J. Atmos. Sci.*, *70*, 3397–3414.

Sun, J., L. Mahrt, C. Nappo, and D. H. Lenschow (2015), Wind and temperature oscillations generated by wave-turbulence interactions in the stably stratified boundary layer, *J. Atmos. Sci.*, *72*, 1484–1503, doi:10.1175/JAS-D-14-0129.1.

Sutherland, B. R. (2010), *Internal Gravity Waves*, 377 pp., Cambridge Univ. Press, Cambridge, U. K.

Sutherland, B. R., C. P. Caulfield, and W. R. Peltier (1994), Internal gravity wave generation and hydrodynamic instability, *J. Atmos. Sci.*, *51*, 3261–3280.

Svensson, G., et al. (2011), Evaluation of the diurnal cycle in the atmospheric boundary layer over land as represented by a variety of single-column models: The second GABLS experiment, *Boundary Layer Meteorol.*, *140*, 177–206.

Tandeo, P., M. Pulido, and F. Lott (2015), Offline parameter estimation using EnKF and maximum likelihood error covariance estimates: Application to a subgrid-scale orography parameterization, *Q. J. R. Meteorol. Soc.*, *141*, 383–395.

Teixeira, M. A. C., and P. M. A. Miranda (2009), On the momentum fluxes associated with mountain waves in directionally sheared flows, *J. Atmos. Sci.*, *66*, 3419–3433.

Teixeira, M. A. C., P. M. A. Miranda, and J. L. Argain (2008), Mountain waves in two-layer sheared flows: Critical-level effects, wave reflection, and drag enhancement, *J. Atmos. Sci.*, *65*, 1912–1926.

Teixeira, M. A. C., J. L. Argaín, and P. M. A. Miranda (2013), Drag produced by trapped lee waves and propagating mountain waves in a two-layer atmosphere, *Q. J. R. Meteorol. Soc.*, *139*, 946–981.

Tennekes, H. (1976), Fourier-transform ambiguity in turbulence dynamics, *J. Atmos. Sci.*, *32*, 1660–1663.

Terradellas, E., G. Morales, J. Cuxart, and C. Yagüe (2001), Wavelet methods: Application to the study of the stable atmospheric boundary layer, *Dyn. Atmos. Oceans*, *34*, 225–244.

Terradellas, E., M. Soler, E. Ferreres, and M. Bravo (2005), Analysis of oscillations in the stable boundary layer using wavelet methods, *Boundary Layer Meteorol.*, *114*, 489–518.

Thomas, C., A. Kennedy, J. Selker, A. Moretti, M. Schroth, A. Smoot, and N. Tufillaro (2012), High-resolution fibre-optic temperature sensing: A new tool to study the two-dimensional structure of atmospheric surface-layer flow, *Boundary Layer Meteorol.*, *142*, 177–192.

Thomas, R. M., K. Lehmann, H. Nguyen, D. L. Jackson, D. Wolfe, and V. Ramanathan (2011), Measurement of turbulent water vapor fluxes using a lightweight unmanned aerial vehicle system, *Atmos. Meas. Tech. Discuss*, *4*, 5529–5568.

Thorpe, S. A. (1977), Turbulence and mixing in a Scottish loch, *Philos. Trans. R. Soc. A*, *286*, 125–181.

Thorpe, S. A. (1987), Transitional phenomena and the development of turbulence in stratified fluids: A review, *J. Geophys. Res.*, *92*(C5), 5231–5248.

Thorpe, S. A. (2002), The axial coherence of Kelvin-Helmholtz billows, *Q. J. R. Meteorol. Soc.*, *128*, 1529–1542.

Thorpe, S. A., and J. T. Holt (1995), The effects of laterally sloping upper and lower boundaries on waves and instability in stratified shear flows, *J. Fluid Mech.*, *286*(1), 49–65.

Tjernström, M., and T. Mauritsen (2009), Mesoscale variability in the summer Arctic boundary layer, *Boundary Layer Meteorol.*, *130*, 383–406.

Tjernström, M., B. B. Balsley, G. Svensson, and C. Nappo (2009), The effects of critical layers on residual layer turbulence, *J. Atmos. Sci.*, *66*, 468–480.

Trexler, C. M., and S. E. Koch (2000), The life cycle of a mesoscale gravity wave as observed by a network of Doppler wind profilers, *Mon. Weather Rev.*, *128*, 2423–2446.

Troy, C. D., and J. R. Koseff (2005), The instability and breaking of long internal waves, *J. Fluid Mech.*, *543*, 107–136.

Turner, J. S. (1973), *Buoyancy Effects in Fluids*, Cambridge Univ. Press, London, U. K.

Udina, M., M. R. Soler, S. Viana, and C. Yagüe (2013), Model simulation of gravity waves triggered by a density current, *Q. J. R. Meteorol. Soc.*, *139*, 701–714.

van den Kroonenberg, A., T. Martin, M. Buschmann, J. Bange, and P. Vörsmann (2008), Measuring the wind vector using the autonomous mini aerial vehicle M^2AV, *J. Atmos. Oceanic Tech.*, *25*, 1969–1982.

van der Avoird, E., and P. Duynkerke (1999), Turbulence in katabatic flow. Does it resemble turbulence in stable boundary layers over flat surfaces?, *Boundary Layer Meteorol.*, *92*, 39–66.

van Gorsel, E., I. N. Harman, J. J. Finnigan, and R. Leuning (2011), Decoupling of air flow above and in plant canopies and gravity waves affect micrometeorological estimates of net scalar exchange, *Agric. For. Meteorol.*, *151*, 927–933.

Vanneste, J. (2013), Balance and spontaneous wave generation in geophysical flows, *Annu. Rev. Fluid Mech.*, *45*, 147–172.

Vergeiner, I., and D. K. Lilly (1970), The dynamic structure of lee wave flow as obtained from balloon and airplane observations, *Mon. Weather Rev.*, *78*(3), 220–232.

Viana, S., G. M. C. Yagüe, and G. Morales (2007), Study of the surface pressure fluctuations generated by waves and turbulence in the nocturnal boundary layer during SABLES2006 field campaign, *Fisica de la Tierra*, *19*, 55–71.

Viana, S., C. Yagüe, and G. Maqueda (2009), Propagation and effects of a mesoscale gravity-wave over a weakly-stratified stable boundary layer during SABLES2006 field campaign, *Boundary Layer Meteorol.*, *133*, 165–188.
Viana, S., S. Terradellas, and C. Yagüe (2010), Analysis of gravity waves generated at the top of a drainage flow, *J. Atmos. Sci.*, *67*, 3949–3966.
Viana, S., C. Yagüe, and G. Maqueda (2012), Vertical structure of the stable boundary layer detected by RASS-SODAR and in-situ measurements in the SABLES 2006 field campaign, *Acta Geophys.*, *60*, 1261–1286.
Vickers, D., and L. Mahrt (2006), A solution for flux contamination by mesoscale motions with very weak turbulence, *Boundary Layer Meteorol.*, *118*, 431–447.
Vindel, J., C. Yagüe, and J. Redondo (2008), Structure function analysis and intermittency in the atmospheric boundary layer, *Nonlinear Proc. Geophys.*, *15*, 915–929.
Vosper, S. B., and A. R. Brown (2007), The effect of small-scale hills on orographic drag, *Q. J. R. Meteorol. Soc.*, *133*, 1345–1352.
Vosper, S. B., and A. R. Brown (2008), Numerical simulations of sheltering in valleys: The formation of nighttime cold-air pools, *Boundary Layer Meteorol.*, *127*, 429–448.
Vosper, S. B., I. P. Castro, W. H. Snyder, and S. D. Mobbs (1999), Experimental studies of strongly stratified flow past three-dimensional orography, *J. Fluid Mech.*, *390*, 223–249.
Waite, M., and P. Smolarkiewicz (2008), Instability and breakdown of a vertical vortex pair in a strongly stratified fluid, *J. Fluid Mech.*, *606*, 239–273.
Walterscheid, R. L., and G. Schubert (1990), Nonlinear evolution of an upward propagating gravity wave: Overturning, convection, transience and turbulence, *J. Atmos. Sci.*, *47*(1), 101–124.
Walterscheid, R. L., L. Gelinas, J. Hecht, and A. Liu (2013), Instability structures during periods of large Richardson number (Ri > 1/4): Evidence of parametric instability, *J. Geophys. Res. Atmos.*, *118*, 6929–6939.
Warner, C. D., and M. E. McIntyre (1996), On the propagation and dissipation of gravity wave spectra through a realistic middle atmosphere, *J. Atmos. Sci.*, *53*(22), 3213–3235.
Weinstock, J. (1982), Nonlinear theory of gravity waves: Momentum deposition, generalized Rayleigh friction, and diffusion, *J. Atmos. Sci.*, *39*, 1698–1710.
Weinstock, J. (1990), Saturated and unsaturated spectra of gravity waves and scale-dependent diffusion, *J. Atmos. Sci.*, *47*(18), 2211–2225.
Wendoloski, E., D. Stauffer, A. Suarez, and G. Hunter (2014), A sub-km-grid ensemble for representing meso-gamma hazard-prediction uncertainty in complex terrain, in *16th Annual Conference on Mountain Meteorology*, p. 9, Am. Meteorol. Soc., San Diego, Calif.
West, B. J. (1981), Overview of workshop, in *Nonlinear Properties of Internal Waves*, edited by B. J. West, pp. 1–10, Am. Inst. of Phys., New York.
Whiteman, D., S. Melfi, and R. Ferrare (1992), Raman lidar system for the measurement of water vapor and aerosols in the Earth's atmosphere, *Atmos. Optics*, *31*(16), 3068–3082.
Whitham, G. B. (1974), *Linear and Nonlinear Waves*, 636 pp., John Wiley Inc., Univ. of Calif.
Wilczak, J., E. Gossard, W. Neff, and W. Eberhard (1996), Ground-based remote sensing of the atmospheric boundary layer: 25 years of progress, *Boundary Layer Meteorol.*, *78*(3–4), 321–349.
Winters, K. B., and E. A. D'Asaro (1994), Three-dimensional wave instability near a critical level, *J. Fluid Mech.*, *272*, 255–284.
Wood, N., A. R. Brown, and F. E. Hewer (2001), Parameterizing the effects of orography on the boundary layer: An alternative to effective roughness lengths, *Q. J. R. Meteorol. Soc.*, *127*, 759–777.
Woods, J., and R. B. Smith (2010), Energy flux and wavelet diagnostics of secondary mountain waves, *J. Atmos. Sci.*, *67*, 3721–3738.
Wyngaard, J. C. (2004), Toward numerical modeling in the "terra incognita", *J. Atmos. Sci.*, *61*, 1816–1826.
Yagüe, C., and J. Cano (1994), The influence of stratification on heat and momentum turbulent transfer in Antarctica, *Boundary Layer Meteorol.*, *69*, 123–136.
Yagüe, C., G. Maqueda, and J. Rees (2001), Characteristics of turbulence in the lower atmosphere at Halley IV station, Antarctica, *Dyn. Atmos. Oceans*, *34*, 205–223.
Yagüe, C., S. Viana, G. Maqueda, and J. M. Redondo (2006), Influence of stability on the flux-profile relationships for wind speed, ϕ_m and temperature, ϕ_h, for the stable atmospheric boundary layer, *Nonlinear Processes Geophys.*, *13*, 185–203.
Yamada, T. (1983), Simulations of nocturnal flows by a q^2l turbulence closure model, *J. Atmos. Sci.*, *40*, 91–106.
Yamada, T., and G. Mellor (1975), A simulation of the Wangara atmospheric boundary layer data, *J. Atmos. Sci.*, *32*, 2309–2329.
Yang, X. (1991), A study of nonhydrostatic effects in idealized sea breeze systems, *Boundary Layer Meteorol.*, *54*, 195–210.
Yanowitch, M. (1967), Effect of viscosity on vertical oscillations of an isothermal atmosphere, *Can. J. Phys.*, *45*(6), 2003–2008.
Zakharov, V., V. S. L'vov, and G. Falkovich (1992), *Kolmogorov Spectra of Turbulence. I: Wave Turbulence*, 264 pp., Springer, Berlin.
Zhou, B., and F. K. Chow (2013), Nested large-eddy simulations of the intermittently turbulent stable atmospheric boundary layer over real terrain, *J. Atmos. Sci.*, *70*, 3262–3276.
Zilitinkevich, S., and A. Baklanov (2002), Calculation of the height of the stable boundary layer in practical applications, *Boundary Layer Meteorol.*, *105*, 389–409.
Zilitinkevich, S., and I. Esau (2007), Similarity theory and calculation of turbulent fluxes at the surface for stably stratified atmospheric boundary layers, *Boundary Layer Meteorol.*, *125*, 193–205.
Zilitinkevich, S., T. Elperin, N. Kleeorin, and I. Rogachevskii (2007), Energy-and flux-budget (EFB) turbulence closure model for stably stratified flows. Part I: Steady state homogeneous regimes, *Boundary Layer Meteorol.*, *125*, 167–191.
Zilitinkevich, S., T. Elperin, N. Kleeorin, I. Rogachevskii, I. Esau, T. Mauritsen, and M. Miles (2008), Turbulence energetics in stably stratified geophysical flows: Strong and weak mixing regimes, *Q. J. R. Meteorol. Soc.*, *134*(633), 793–799.
Zilitinkevich, S., T. Elperin, N. Kleeorin, V. L'vov, and I. Rogachevskii (2009), Energy- and flux-budget turbulence closure model for stably stratified flows. Part II: The role of internal gravity waves, *Boundary Layer Meteorol.*, *133*, 139–164.
Zilitinkevich, S. S., T. Elperin, N. Kleeorin, I. Rogachevskii, and I. Esau (2013), A hierarchy of energy- and flux-budget (EFB) turbulence closure models for stably stratified geophysical flows, *Boundary Layer Meteorol.*, *146*, 341–373.